Topical Report

Optimized Reservoir History Matching Simulation of Canyon Formation, SACROC Unit, Permian Basin

Performed by:
Karine Schepers, Reinaldo J. González, and
Scott R. Reeves

Advanced Resources International, Inc.
11490 Westheimer Rd., Suite 520
Houston, TX 77077

November 9, 2007

Advanced Resources
International, Inc.

Disclaimers

U.S. Department of Energy

This report was prepared as an account of work sponsored by an agency of the United States Government. Neither the United States Government nor any agency thereof, nor any of their employees, makes any warranty, express or implied, or assumes any legal liability or responsibility for the accuracy, completeness, or usefulness of any information, apparatus, product, or process disclosed, or represents that its use would not infringe privately owned rights. Reference herein to any specific commercial product, process, or service by trade name, trademark, manufacturer, or otherwise does not necessarily constitute or imply its endorsement, recommendation, or favoring by the United States Government or any agency thereof. The views and opinions of authors expressed herein do not necessarily state or reflect those of the United States Government or any agency thereof.

Advanced Resources International, Inc.

The material in this Report is intended for general information only. Any use of this material in relation to any specific application should be based on independent examination and verification of its unrestricted applicability for such use and on a determination of suitability for the application by professionally qualified personnel. No license under any Advanced Resources International, Inc., patents or other proprietary interest is implied by the publication of this Report. Those making use of or relying upon the material assume all risks and liability arising from such use or reliance.

Executive Summary

Accurate, high-resolution, three-dimensional (3D) reservoir characterization can provide substantial benefits for effective oilfield management. By doing so, the predictive reliability of reservoir flow models, which are routinely used as the basis for significant investment decisions designed to recover millions of barrels of oil, can be substantially improved. This is particularly true when Secondary Oil Recovery (SOR) or Enhanced Oil Recovery (EOR) operations are planned. If injectants such as water, hydrocarbon gasses, steam, CO_2, etc. are to be used; an understanding of fluid migration paths can mean the difference between economic success and failure. SOR/EOR projects will increasingly take place in heterogeneous reservoirs where interwell complexity is high and difficult to understand. The industry therefore needs improved reservoir characterization approaches that are quicker, more accurate, and less expensive than today's standard methods.

To achieve this objective, the Department of Energy (DOE) has been promoting some studies with the goal of evaluating whether robust relationships between data at vastly different scales of measurement could be established using advanced pattern recognition (soft computing) methods. Advanced Resources International (ARI) has performed two of these projects with encouraging results showing the feasibility of establishing critical relationships between data at different measurement scales to create high-resolution reservoir characterization.

In this third study performed by ARI and also funded by the DOE, a model-based, probabilistic clustering analysis procedure is successfully applied to generate a high-resolution reservoir characterization outcome. The approach was applied in the Pennsylvanian-Permian reef carbonates (Cisco and Canyon Formations) of a subregion of the SACROC Unit, Horseshoe Atoll, Permian Basin, Texas, and acknowledged as a highly complex carbonate reservoir.

A selected area within the SACROC Unit platform was used for this study. In the first stage of this project, a two-step "soft-computing" procedure was developed for efficiently generating core-scale porosity and permeability values (as well as rock types geologically consistent) at well locations where only gamma ray (GR) and neutron porosity logs (NPHI) were available. In this way, "core" parameter profiles, with high vertical resolution, could be generated for many wells which permitted to populate any well location with core-scale estimates of porosity and permeability (P&P) and rock types facilitating direct application of geostatistical methods to build 3D reservoir models. This process provided a data set considered sufficient to characterize directly the reservoir representations of P&P. Next, in the second stage of the project, stochastic simulation algorithms were utilized to construct high resolution characterizations of P&P in the selected study region.

The models developed in this study successfully captured the nature of lithofacies distributions and depositional environments, providing genuine representations of P&P in concordance with the selected grid resolution for characterizing the studied region. In the final stage of this project, validation of the porosity and permeability representations was done by a computer-assisted reservoir simulation history-match of prior production, which was achieved without

SACROC Simulation KS080807

significant changes to the original characterization of the studied region. For these purposes, a black-oil model was utilized, and this report focuses on the reservoir modeling and history matching of 57 years of production data for 19 producing wells included in the study area. As a consequence, the validation result of the reservoir characterization methodology is presented.

An assisted history match was achieved using a global optimization method (evolutionary algorithms). This history match, in which several results were produced, was based on the matching of oil, gas and water production rates, and the average reservoir pressure. The match was accomplished by manipulating 13 uncertain design parameters which included two formation properties, other ten variables related with the corresponding relative permeability curves, and one variable linked to the reservoir production. Evolutionary algorithms can handle a large amount of input design parameters. And, in this work, they were successfully applied for history matching complex reservoir performance drivers thanks to their capabilities to explore an enormous range of parameter combinations and produce lots of results related to the reservoir performance.

History match results confirmed that the 3D reservoir models of P&P constructed applying the combined reservoir characterization approach (advanced pattern recognition techniques and geostatistical algorithms) were legitimate representations of the spatial distribution of these parameters. In addition, they confirmed initial assumptions that the developed porosity model was highly trustworthy, whereas the permeability model, despite of capturing correctly geological trends and heterogeneities of Canyon Reef reservoir (SACROC field) presented slightly underestimated values.

The modeling efforts resulted in a very good history match for the center wells in the study area. A good match was also achieved for the outer producing wells and the average reservoir pressure. These achievements were thanks to the setting up of proper boundary conditions that described the flow behavior at the boundary of the analyzed region. Overall, the match of liquid production rate was very well achieved. Matches of oil, gas and water production rates were from satisfactory to very good. The average reservoir pressure match was also of good quality although slightly high between years 1972 and 1988.

The simple black oil model developed here was sufficient to capture the reservoir behavior of SACROC Unit, Canyon Reef Formation since simulated oil-water relative permeability curves match perfectly actual core measurement, and a recovery factor equal to 46% (a maximum of 39% was reported in literature) was obtained from the simulated reservoir model. This factor was probably overestimated due to the injection of miscible gas in our black-oil model, when immiscibility injection should have occurred.

The addition of optimization methods (for assisted history matching) to the combined soft-computing/geostatistical approach (utilized for reservoir characterization purposes) constituted a powerful triad of mathematical techniques ideally suited for addressing reservoir integrated studies, with the capacity of facing these complex tasks more rapidly and efficiently than using traditional methodologies.

Advanced Resources International, Inc.

SACROC Simulation KS080807

Table of Contents

List of Tables

List of Figures

Advanced Resources International, Inc.

SACROC Simulation KS080807

1.0   Introduction

Accurate, high-resolution, three-dimensional (3D) reservoir characterization can provide substantial benefits for effective oilfield management. Even a small improvement in incremental oil recovery for high-value assets can result in important contributions to bottom-line profitability.

This is particularly true when Secondary Oil Recovery (SOR) or Enhanced Oil Recovery (EOR) operations are planned. If water, hydrocarbon gasses, steam or CO_2 are to be used, an understanding of fluid migration paths can mean the difference between economic success or failure. In these types of projects, injectant costs can be a significant part of operating expenses, and hence their optimized utility is critical.

Although reasonable reservoir characterization information often exists at the wellbore, the only economical way to sample the interwell region is with seismic methods. Surface reflection seismic has relatively low cost per unit volume of reservoir investigated, but the resolution of surface seismic data available today, particularly in the vertical dimension, is not sufficient to produce the kind of detailed reservoir description necessary for effective SOR/EOR optimization and planning.

Today's standard practice for developing a 3D reservoir description is to use seismic inversion techniques. These techniques make use of rock physics concepts to solve the inverse problem, i.e., to iteratively construct a likely geologic model and then upscale and compare its acoustic response to that actually observed in the field. This method suffers from the fact that rock physics relationships are not well understood, and the need to rely on porosity-permeability transforms to estimate permeability from porosity. Further, these methods require considerable resources to perform, and thus it is applied to only a small percentage of oil and gas producing assets.

Since the majority of fields do not utilize these technologies currently, many fields are sub-optimally developed. The industry therefore needs an improved reservoir characterization approach that is quicker, more accurate, and less expensive than today's standard methods. This will permit more reservoirs to be better characterized, allowing recoveries to be optimized and significantly adding to recoverable reserves.

A new approach to achieve this objective was first examined in a Department of Energy (DOE) study performed by Advanced Resources International (ARI) in 2000/2001[1]. The goal of that study was to evaluate whether robust relationships between data at vastly different scales of measurement could be established using virtual intelligence (VI) methods. The proposed workflow required that three specific relationships be established through use of data-driven modeling methods, in that case Artificial Neural Networks (ANN's): core-to-log, log-to-

crosswell seismic and crosswell-to-surface seismic. A key attribute of this approach is the inclusion of borehole seismic (such as crosswell and/or vertical seismic profiling – VSP) in the data collection scheme. Borehole seismic fills a critical gap in the resolution spectrum of reservoir measurements between the well log and surface seismic scales, thus establishing important constraints on characterization outcomes.

The results of the initial study showed that it is, in fact, feasible to establish the three critical relationships required, and that use of data at different scales of measurement to create high-resolution reservoir characterization is possible. The study showed sufficient promise in the utility of soft-computing methods for reservoir characterization that further refinement of the process was undertaken.

In this study, performed by ARI and funded by the DOE, the same approach was again utilized to generate a high-resolution reservoir characterization outcome as a first stage in an integrated clustering/geostatistical approach for 3D reservoir characterization. The entire study, subject of previous reports[2,3], was performed at the SACROC Unit, operated by Kinder Morgan CO_2 Co., L.P ($KMCO_2$), in the Permian basin of West Texas.

The SACROC Unit was formed in 1952 to facilitate coordinated water flooding operations in the field, which began in 1954. CO_2-EOR began in 1972 originally using anthropogenic CO_2, and in recent years has primarily been focused in the Central Plain area of the unit where reservoir architecture is more horizontal and therefore amenable to pattern flooding.

The decade of the 1990's found operations at a critical juncture in the field. Production had been dropping more than 20% per year from a peak of 210,000 barrels of oil per day (BOPD) in the mid-1970's to only 9,000 BOPD in 1995. The field was considered to be very mature by the mid-1990s, and the estimated economic limit was rapidly approaching. The Unit owners were faced with a significant abandonment effort including negative cash flow and abandonment liability. However, under the leadership of a new operator (Pennzoil), a long-term plan was implemented to arrest the production decline, reduce expenditures, and ultimately restore the economic viability of the Unit.

Since acquiring SACROC in 2000, $KMCO_2$ has succeeded in reducing costs and has almost tripled production via a more focused and aggressive CO_2 injection program, as well as better well pattern management. $KMCO_2$ has increased oil production to 23,000 BOPD, and is now considering production operation options for the 1-3 billion barrel (OOIP) Northern Platform portion of the field. The area appears to have the necessary reservoir characteristics for hosting a gravity-stable flood in some regions. However, reservoir pressure may be below the minimum miscibility pressure (MMP) since operations have been nominal since the 1990's. Therefore, aggressive CO_2 injection and pressure control efforts will be needed.

2

A better understanding of the reservoir properties could make the difference between economic success or failure in future development of the field. Developing legitimate models of the porosity and permeability distributions in a selected study area of SACROC was the goal of this project. The models developed in this study successfully captured the nature of lithofacies distributions and depositional environments, providing genuine representations of permeability and porosity in concordance with the selected grid resolution for characterizing the studied region.

Validation of the representations was done by history matching using porosity and permeability characterizations, production data, and reservoir simulation. A black-oil model was then built.

This report focuses on the reservoir modeling and history matching of 57 years of production data for 19 producing wells included in the study area.

The specific objectives of this study were:
- To create a reservoir simulation model using the reservoir characterization generated in previous stages of the project (see topical reports[2, 3]).
- To match the individual production of each well included in the study area
- To match reservoir pressure as well
- To be able to understand the fundamentals of the reservoir performance using a simple black oil reservoir model
- To use the model as a base for an eventual more-advanced compositional model, covering a larger area of the Northern platform.

The methodology employed to achieve the project objective was as follow:
- Create a simple black oil model covering the study area and including the geostatistical porosity and permeability characterizations previously generated
- Estimate proper boundary conditions around the model using several different techniques
- Implement pseudo wells to reproduce proper flux at the edge of the model
- History match the production history of each individual producing well inside the study area

This report presents the results of the validation of the reservoir characterization and the history matching of 19 producing wells and the reservoir pressure.

SACROC Simulation KS080807

3.0   Methodology

The reservoir model built in this study covers an area selected jointly with the operator KMCO$_2$. The area was chosen based on the existence of a completely cored well (well 37-11), a planned crosswell seismic survey inside the area, and a future CO$_2$ injection procedure to be implemented to improve the production levels. Porosity and permeability distributions were defined using geostatistical characterizations extensively described in previous topical reports[2, 3]. KMCO$_2$ provided production and injection data, and PVT and formation data came from published literature. A black oil model of more than 65,000 grid-blocks was build which included the 19 producing wells and 3 injecting wells.

The ability to reproduce proper boundary conditions at the edge of the model was critical to achieve a good match. Boundary conditions at the edge of the models were calculated using several different methods (simple large scale reservoir model, differential water volume calculations, and material balance). Pseudo wells were incorporated at the edge of the modeled area to reproduce water fluxes. However, some uncertainties remained because the different methods gave different answers. Therefore, a factor controlling water fluxes at the edge of the model was used, and was optimized during the history matching process.

For each individual producing well included in the study area, liquid, water and gas production rates were history matched. We were confident in the upscaling of porosity; hence, original porosity realization was used as-is in the reservoir model. However, it was anticipated that upscaled permeability would probably underestimate actual permeability. To preserve geological trends and heterogeneities, the original permeability characterization was used but was multiplied by a factor between 1 and 5 that needed to be optimized during the history matching process.

The final objective was to understand and to reproduce the reservoir performance of Canyon Reef formation in the Kelly-Snyder field using a simple but accurate black-oil model. The history matching would be achieved by using an automated optimization process.

Advanced Resources International, Inc.

SACROC Simulation KS080807

4.0 Field and Reservoir Description and Development

4.1 Field Description

The SACROC Unit occupies most of Kelly-Snyder field and portions of Diamond "M" field (Figure 1). The Kelly-Snyder field is the major unitized field of four contiguous fields aligned along the 35 miles Canyon Reef formation[4]. It is the largest of 15 fields that lie along the eastern flank of the giant Horseshoe Atoll, which accumulated during Pennsylvanian time[5]. The study area within SACROC unit was selected jointly with $KMCO_2$, and is shown in Figure 2.
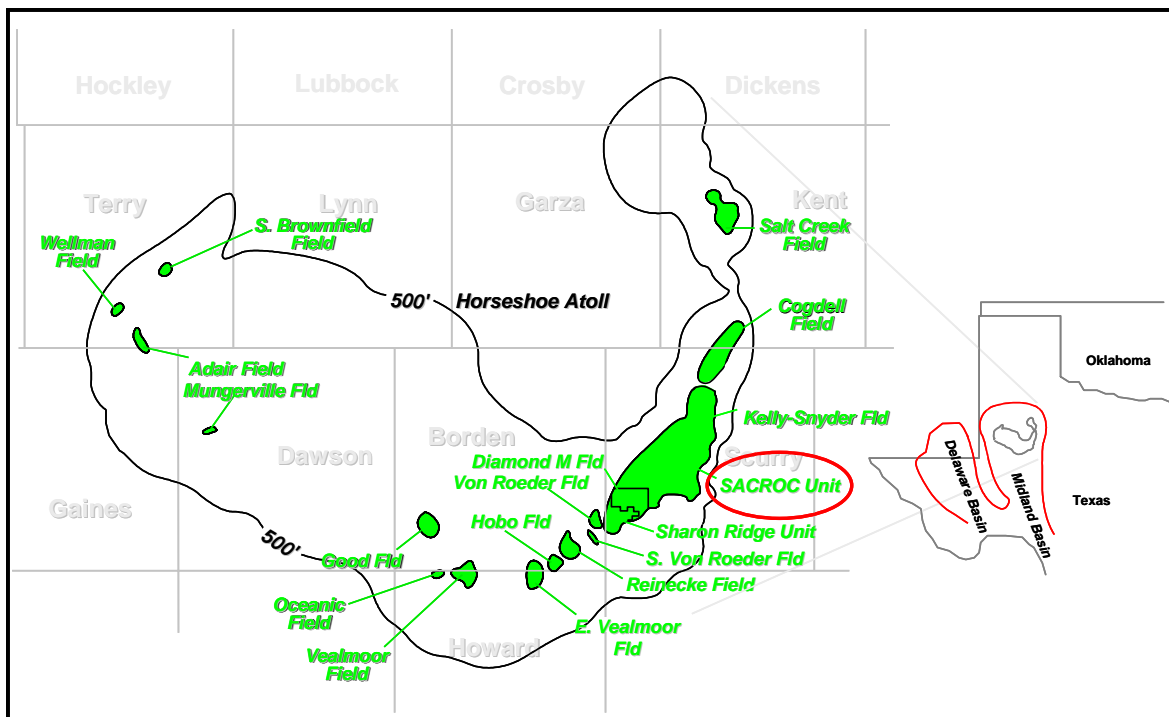
Figure 1: Location of Kelly Snyder Field, SACROC Unit[2]

SACROC Simulation KS080807
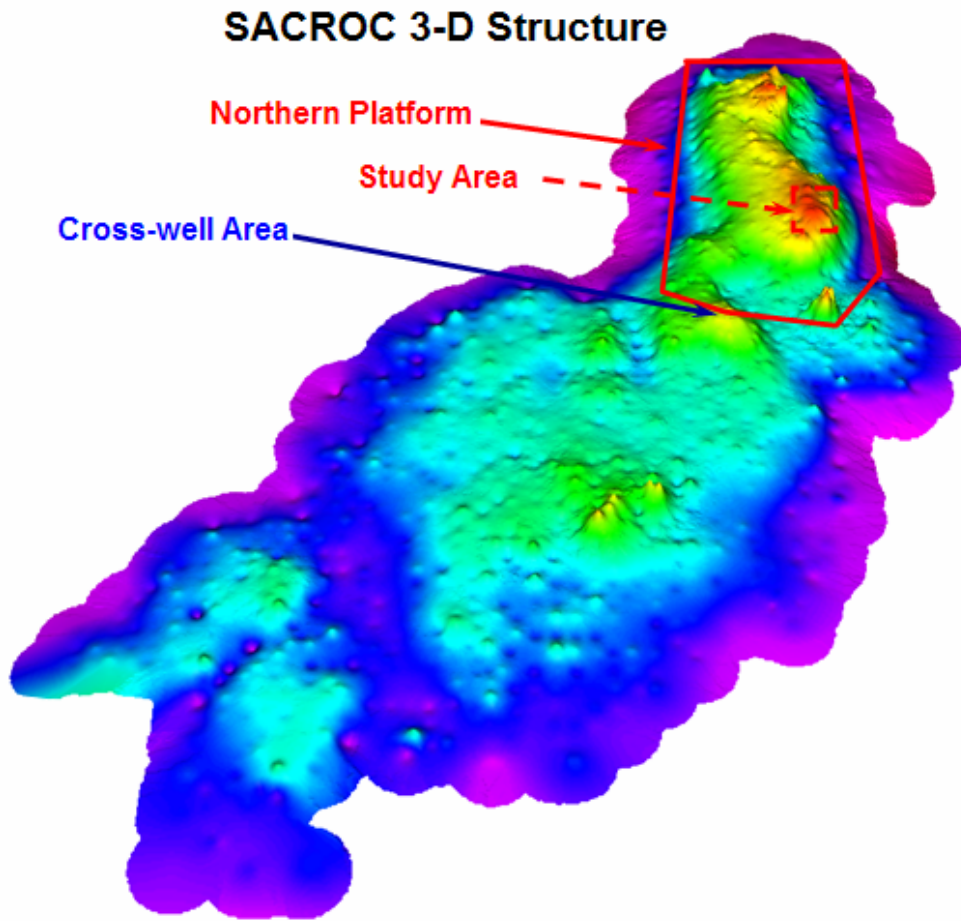
Figure 2: Location of Study Area, Kelly Snyder Field[2]

The target reservoir is a limestone occurring at an average depth of 6,700 ft and is a northeast-southwest trending massive reef build-up with gently slopping flanks. Formation thickness varies from an average of 900 ft on the crest of the structure to less than 50 ft on the flanks and averages 213 ft over all[4]. A stratigraphic column[6], and a type log[7] are presented in Figure 3. A simplified cross section is also presented in Figure 4.
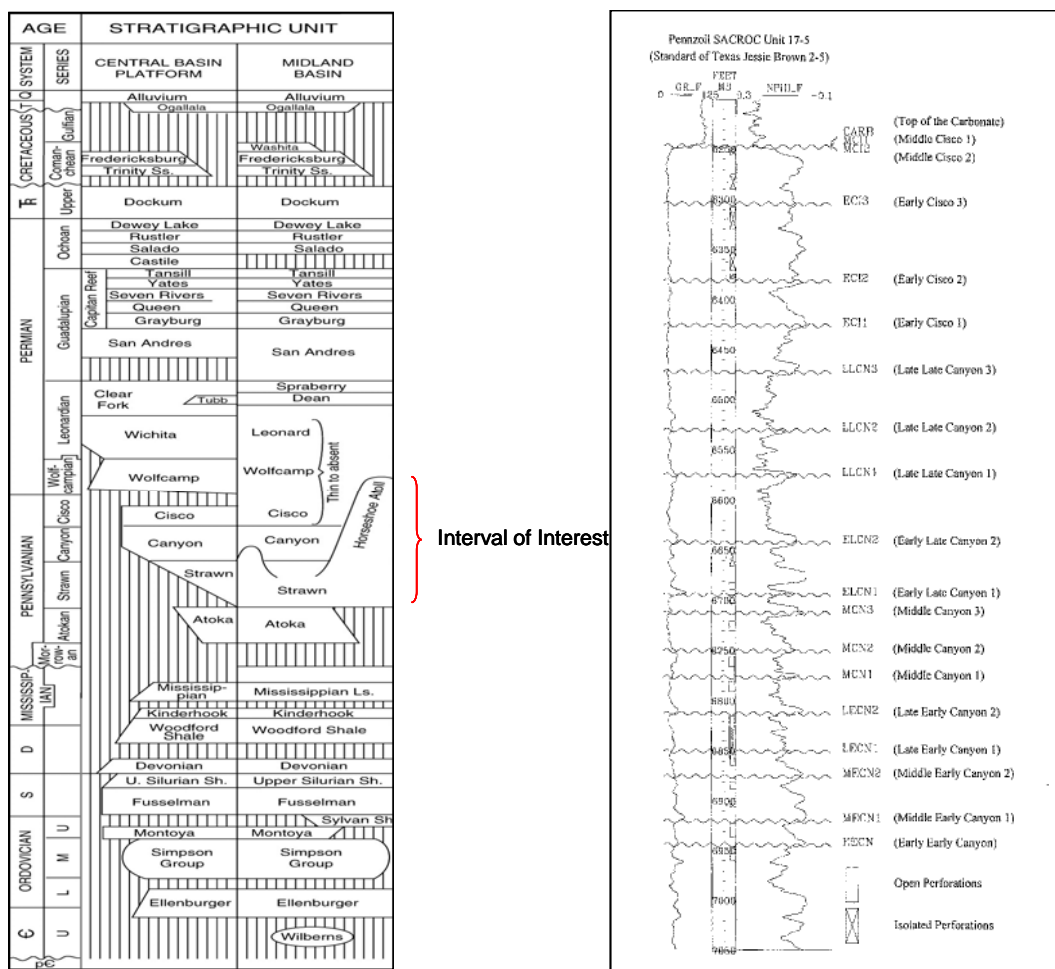
Figure 3: Stratigraphic Column and Type-Log of Permian Basin, SACROC Unit[6, 7]
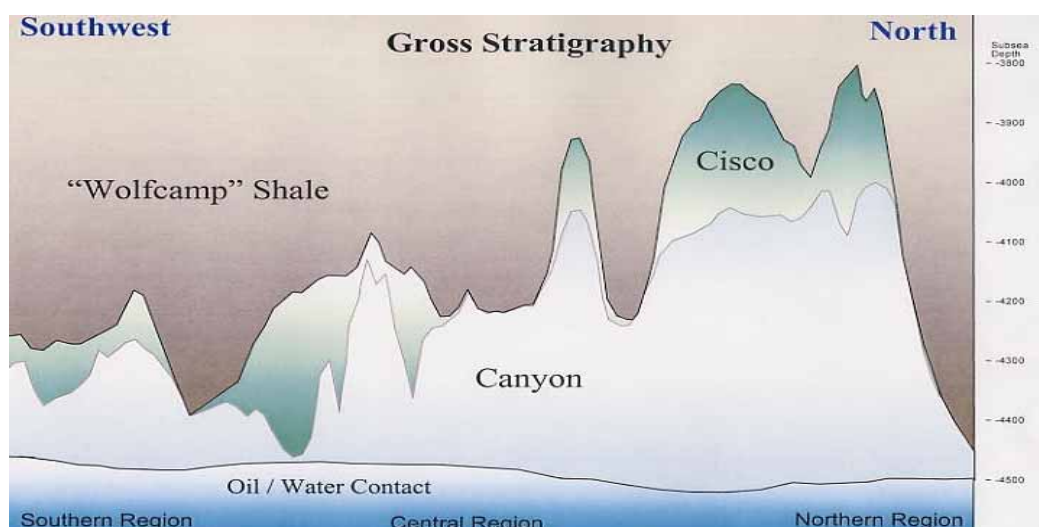
Figure 4: Canyon Reef Formation – Cross Section[2]

SACROC Simulation KS080807

The reservoir was discovered in November 1948 when Chevron Oil Co. completed the first well at a depth interval of 6,334 to 6,414 ft. This discovery was named the Kelly-Snyder field. Soon afterward, other operators discovered the Diamond "M" and Sharon Ridge Canyon fields to the south. Eventually, production revealed that the three fields merged to form one continuous reservoir. Subsequent development was rapid and essentially complete by November 1951 when 1617 producing wells had been drilled by 88 different operators[5]. By that time, reservoir pressure had declined by 50 percent after producing only 5% of the oil in place, and it was estimated that only 19% of the original oil in place would be recovered by primary depletion[5]. This indicated that solution gas drive was the primary producing mechanism and it was recognized that a pressure-maintenance program would be required to improve the recovery:.

In 1953, the Texas Railroad Commission approved formation of the SACROC (Scurry Area Canyon Reef Operators Committee) Unit, which includes about 98 percent of Kelly-Snyder field, to facilitate coordinated water flooding operations. Water injection started in SACROC in September 1954 into 53 wells located along the longitudinal axis of the crest of the reef. This pattern is often referred as the "center-line" water flood in SACROC[5].

The center-line water flood proved to be efficient because several independent reservoir studies showed that it ultimately would recover more than 50% of the oil in place. However, although the performance of the water injection was very promising, technical experts recommended that a water-driven slug of carbon dioxide should be used to miscibly displace oil in the non-water invaded portion of the reservoir, and that a pattern injection program be developed. CO_2-EOR began in 1972 originally using anthropogenic CO_2, and in recent years has primarily been focused in the Central Plain portion of the field where reservoir is more amenable for pattern flooding. The 57-year performance history of Kelly-Snyder field is shown in Figure 5 and Figure 6.
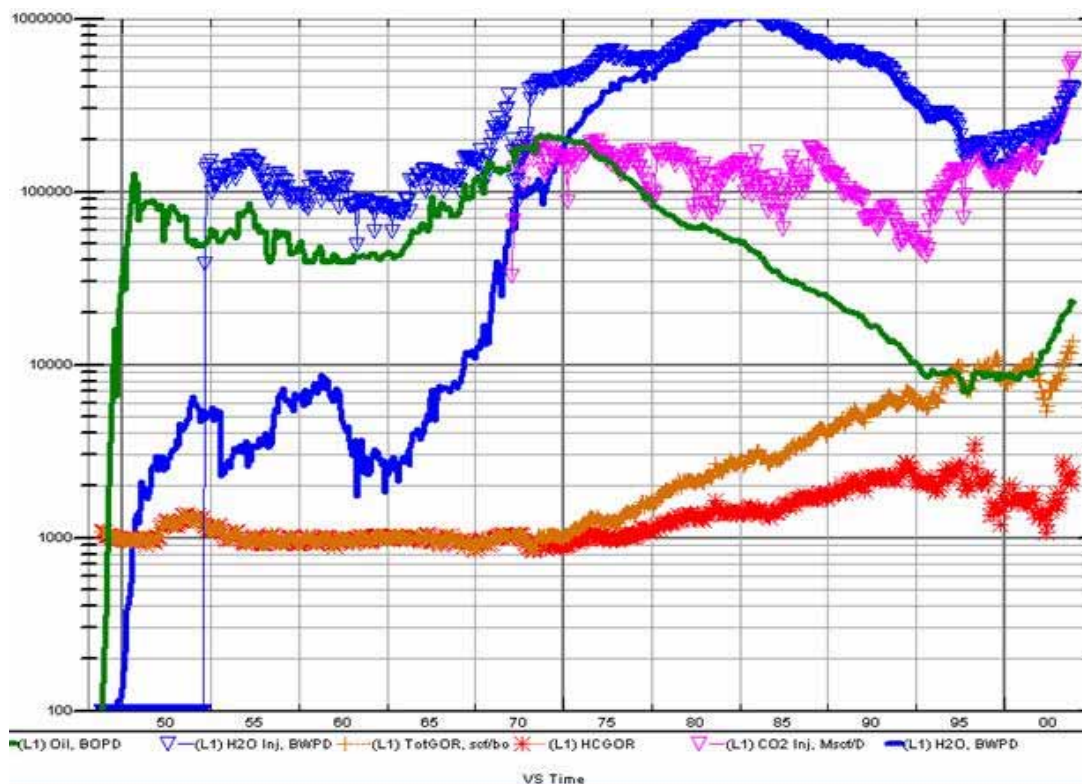
Figure 5: Kelly-Snyder Field Performance History[6]
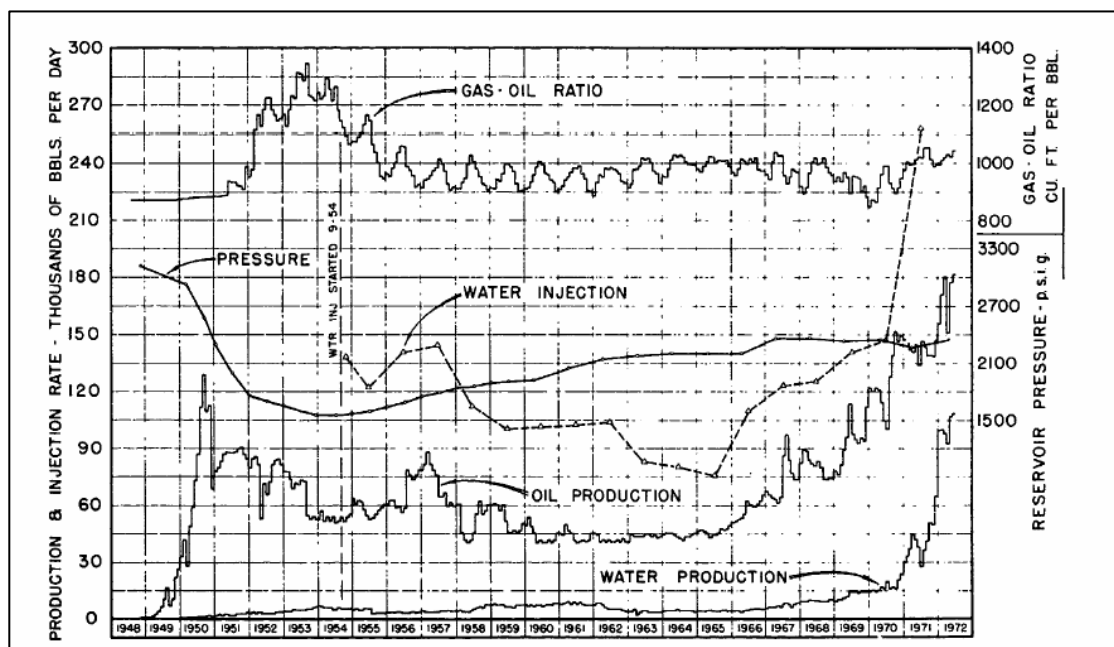
Figure 6: Kelly Snyder Field Reservoir Pressure 1948-1972[5]

9

SACROC Simulation KS080807

In 1948, the initial reservoir pressure was 3,122 psig at 4,300 ft TVDSS. During the first 5 years of operation, less than 5 percent of the oil had been produced but a 50-percent reduction in average reservoir pressure (to 1,560 psia) had occurred and GOR increased. A full-scale pressure maintenance by water injection program began in 1954, which consisted of injecting water at rates of 130,000 to 140,000 BPD in the injections wells and controlling production under unitized operations. Following the water flood, reservoir pressure was successfully restored with 80 percent of the reservoir volume above bubble-point pressure (1850 psig). Before injection, only one percent of the reservoir volume was above bubble-point pressure. Figure 7 depicts the general bottom hole pressure (BHP) conditions in April 1954 (just before water injection) compared to BHP conditions in April 1970[4]. Figure 8 depicts the reservoir pressure in 1992 compared to bubble point pressure and MMP.
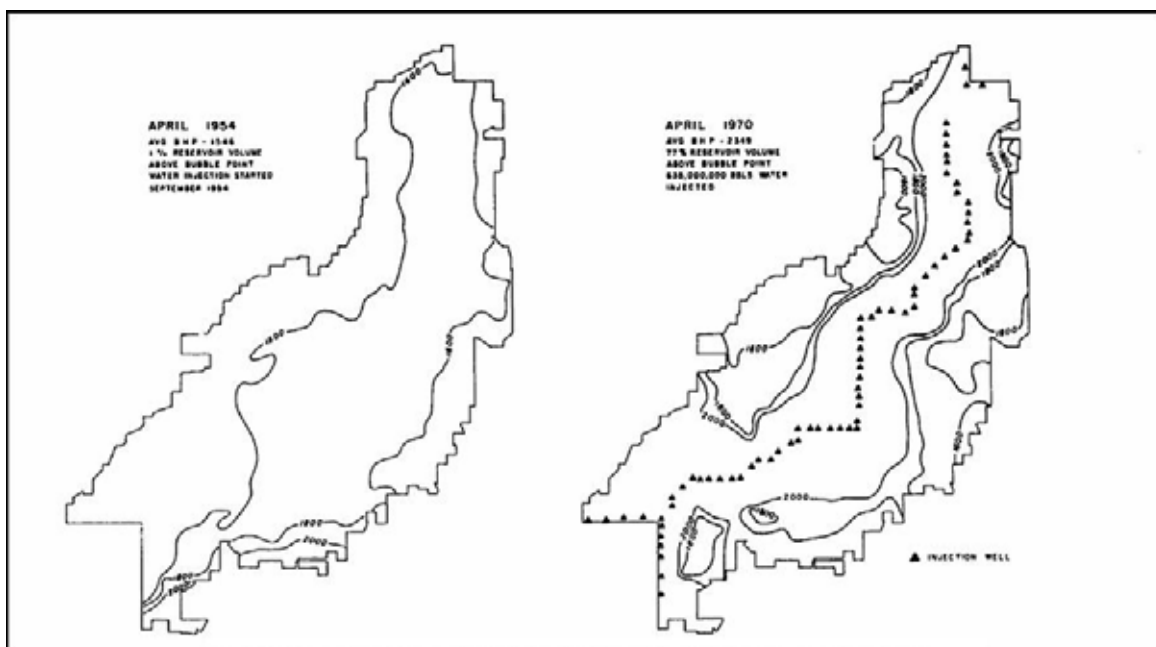
Figure 7: Bottom-Hole Pressure Maps, SACROC Unit Area, Kelly-Snyder Field[5]

Study area
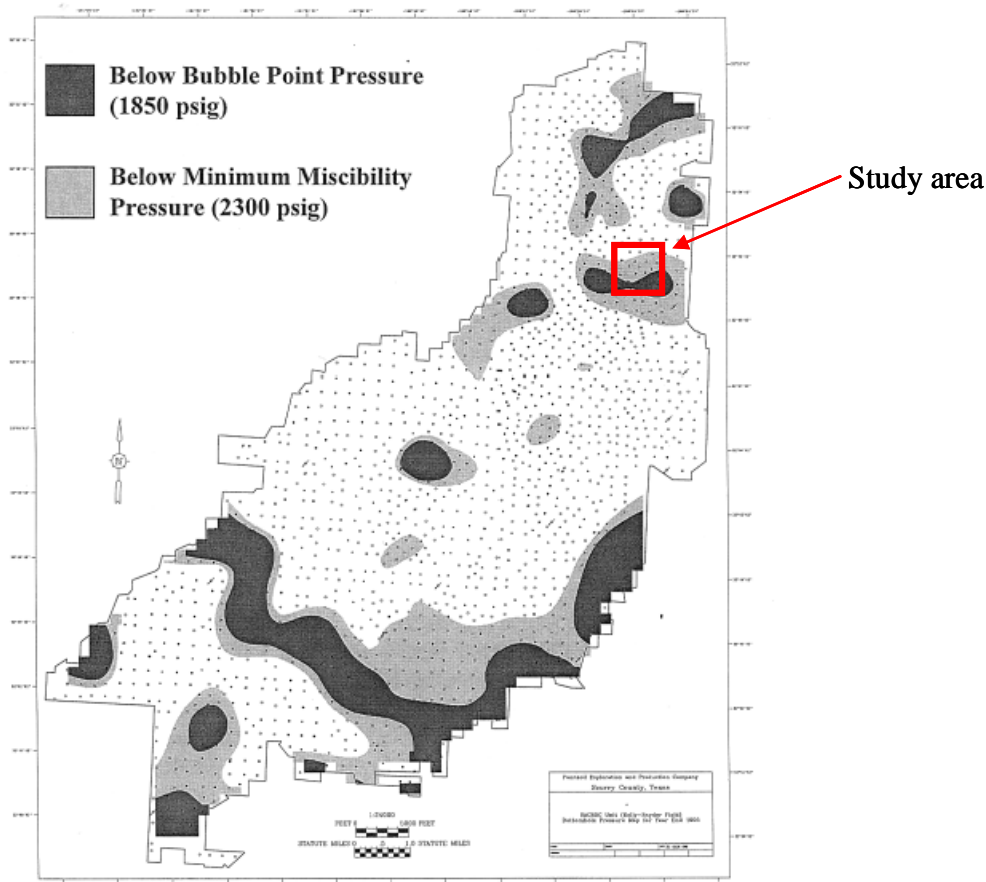
Figure 8: SACROC Unit, 1992 Pressure Contour Map[7]

As seen, reservoir pressure has continued to decrease since 1954 even though Water-Alternating-Gas (WAG) injection[7] has been applied. Since many areas of the field were at a pressure below the MMP and production operations there had mostly ceased by the 1990's, aggressive CO_2 injection and pressure control efforts have been needed to maintain reservoir productivity.

4.2   Reservoir Description: Petrophysical Data

Reservoir parameters are conceived as a random variables varying continuously in space. The basic geostatistical tool used to quantify the spatial variability of a reservoir parameter is the experimental semivariogram[8] (or variogram). The experimental variogram is used for identifying

SACROC Simulation KS080807

the underlying spatial pattern and trends, and reveals the randomness and the structured aspects of the spatial dispersion.

For the SACROC study, actual and pseudo values of core porosity and permeability were used to calculate corresponding experimental and 3D variograms. Using variogram model and the Sequential Gaussian Simulation algorithm[8] of the Stanford Geostatistical Earth Modeling Software[8] (SGEMS), twenty (20) realizations were generated describing possible distributions of porosity. Four typical output images of the porosity distribution[3] obtained from the Gaussian Simulation method are shown in Figure 9. This was followed by the generation of an average characterization from the 20 previous ones. The same method was applied to characterize permeability and the characterization image[3] is presented in Figure 12. The frequency distributions of porosity and permeability simulated values used in the model of the Canyon Reef reservoir[3] are presented in Figure 11 and Figure 13 respectively. The mean porosity value of the characterization is 8.5 %, and the mean permeability is 2.74 mD.
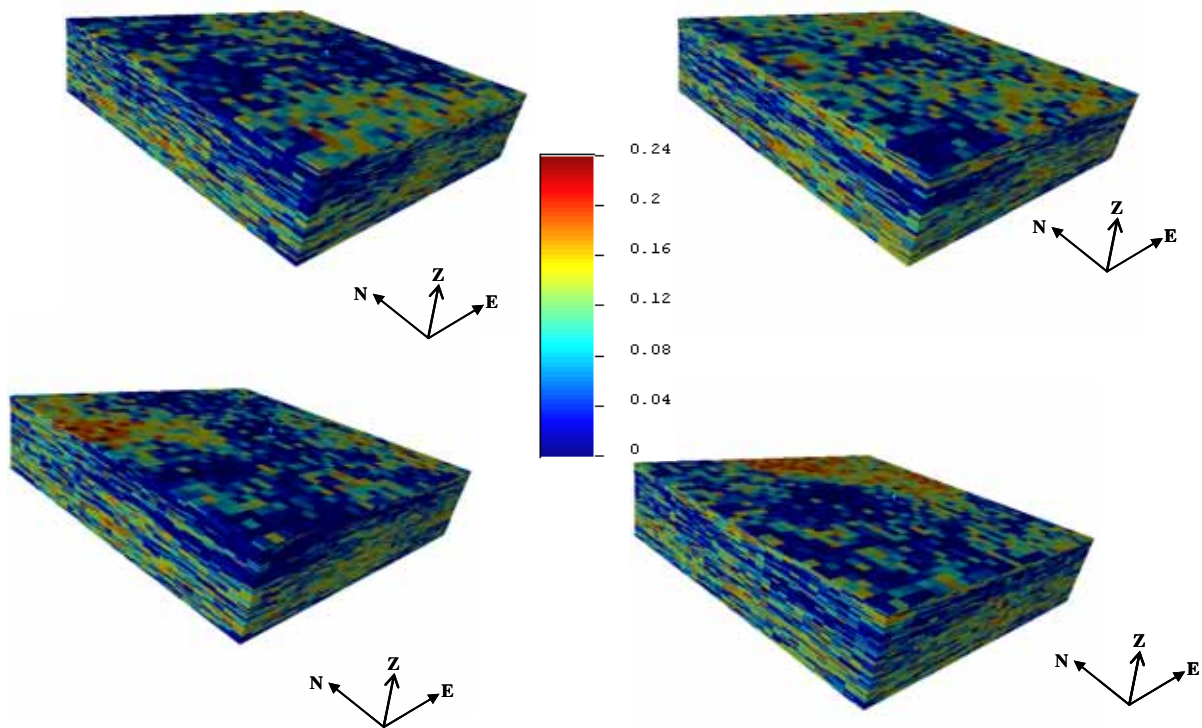
Figure 9: Four Different Geostatistical Realizations of Porosity[3]
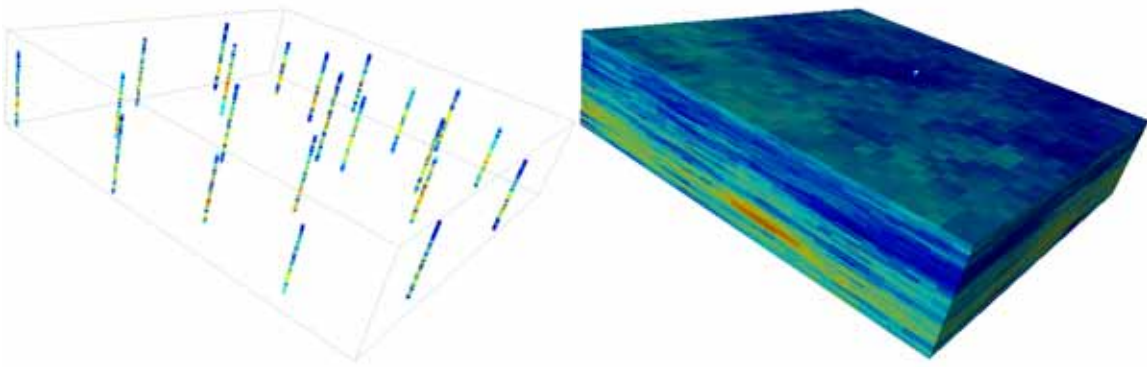
Figure 10: Geostatistical Characterization of Porosity[3] used in the Reservoir Simulation
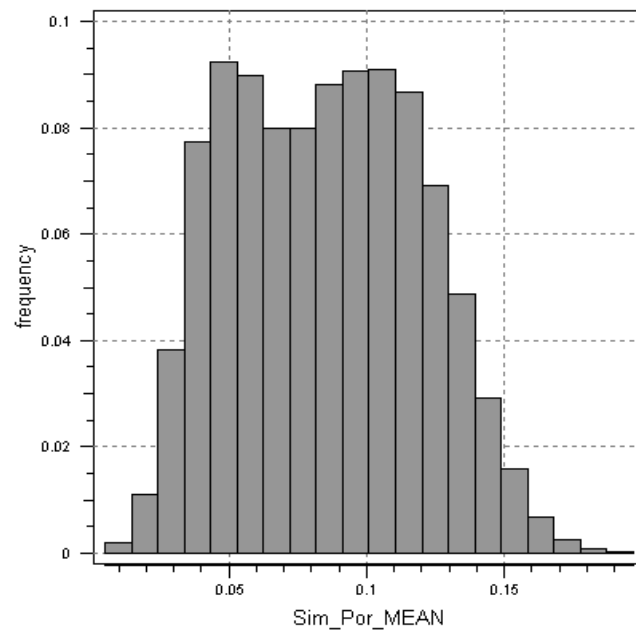
Figure 11: Histogram of Porosity Characterization Values[3] used in the Reservoir Simulation
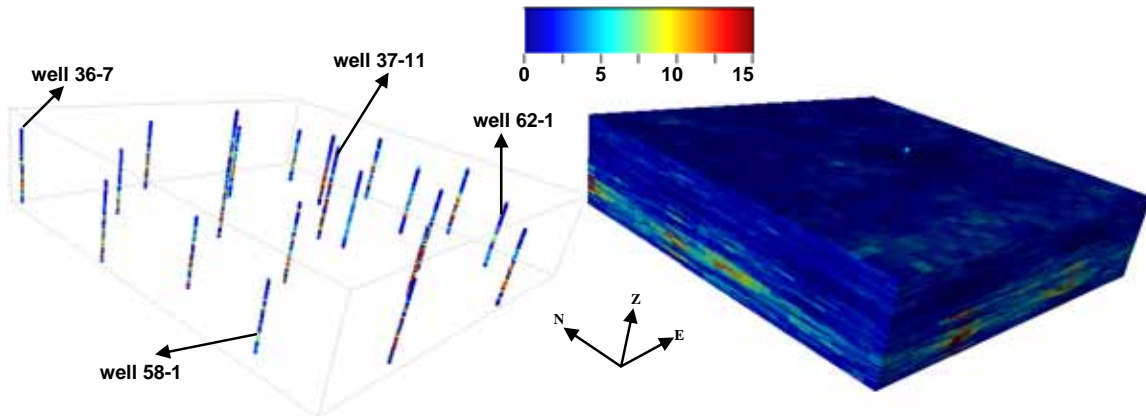
Figure 12: Geostatistical Characterization of Permeability[3] used in the Reservoir Simulation
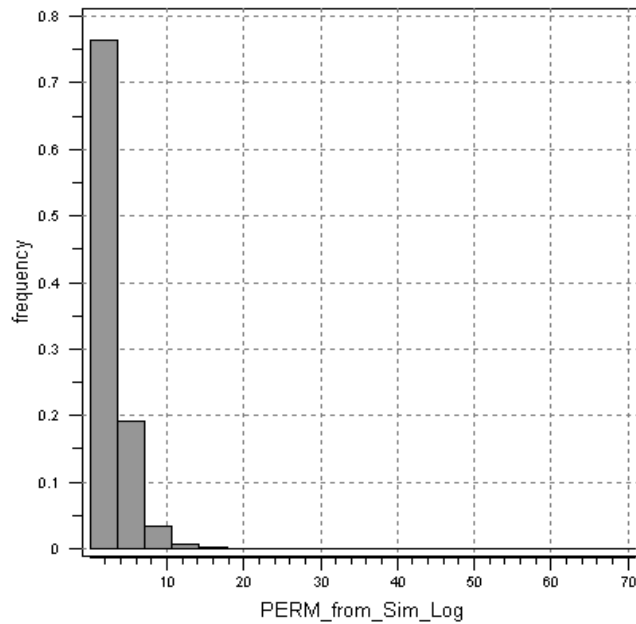
Figure 13: Histogram of the Permeability Characterization Values[3] used in the Reservoir Simulation

Vertical permeability values were available from whole core measurements[2]. However, because of the difference of sizes and resolution existing between core samples and reservoir grid-block, no vertical permeability model was built. Vertical permeability was optimized as a percentage of horizontal permeability during the history matching. For more details on the reservoir characterization, topical reports [2,3] summarize the methodology and results.

14

4.3   Reservoir Description: Fluid Data

Few fluid data were available at the time this study started. The PVT data used in this study came from the published literature[9,10,11,12] and commonly used PVT correlations. The available data and their sources are summarized in Table 1, 2 and 3.

Table 1: Available Formation Properties

Parameter	Units	Value	Source
Initial Pressure	psia	3137	SPE 4083[4], 5536[5], 1259-G[9], 829G[10], 17321[12]
Temperature	F	132	SPE 4083[4], 5536[5], 1259-G[9], 829G[10], 17321[12]

Table 2: Available Fluid Properties

Parameter	Units	Value	Source
Oil Gravity (STC)	API	41	SPE 17321[12]
Bubble Point Pressure	psi	1850	SPE 4083[4], 5536[5], 1259-G[9], 829G[10], 17321[12]
Water Viscosity	cp	0.51	SPE 4083[4], 5536[5], 1259-G[9], 829G[10], 17321[12]

Table 3: Available PVT Data

Pressure	Rs	Bo	Oil Viscosity
(psia)	(cuft/bbl)	(RB/STB)	(cp)
1850	1000	1.55	0.35
3137		1.523	

Note: Data from Table 3 come from literature[4, 5, 11, 12]

Oil-Brine Relative Permeability measurements were available from $KMCO_2$ and include four samples for wells # 32-3 and # 34-6. Those data are presented in Figures 14 and 15.

The different water permeability curves for well 32-3 (Figure 14) were very consistent in terms of shape and end-point. Oil relative permeability curves were somewhat more heterogeneous. Therefore, Corey functions were used: water and oil relative permeability end points (irreducible water saturation, residual oil saturation, etc) were optimized during the history matching process.
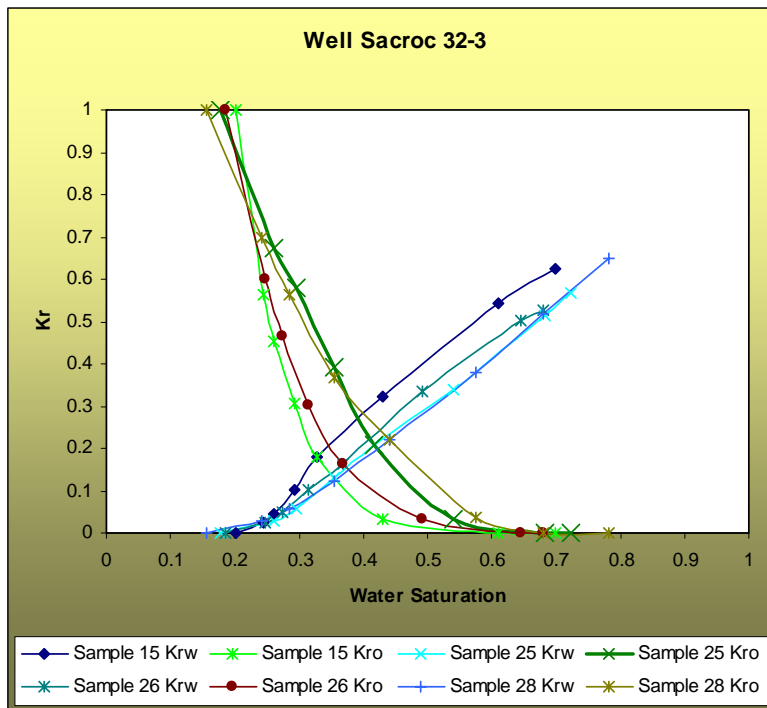
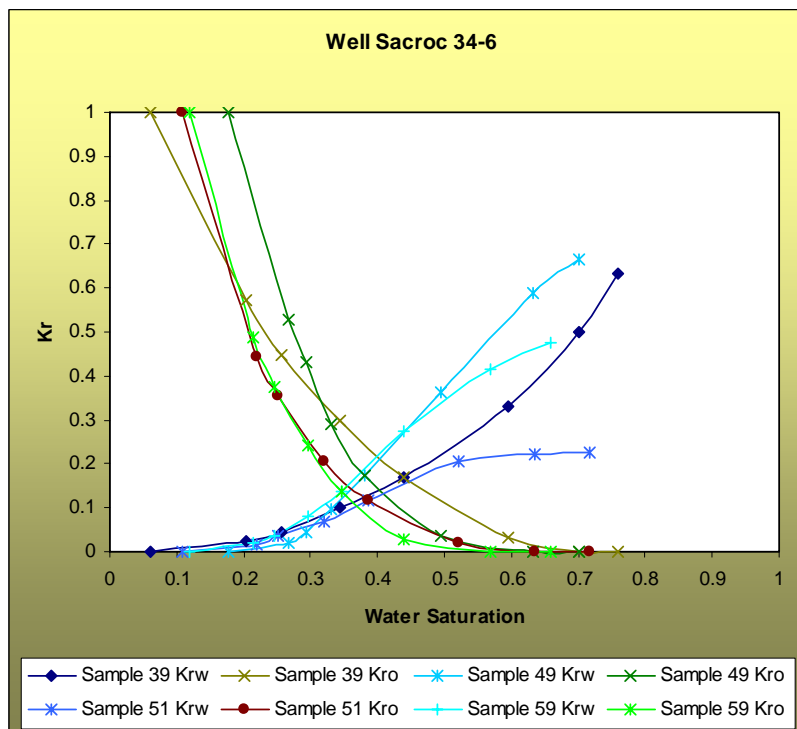**Figure 14: Oil-Water Relative Permeability Curves, Well 32-3**

Figure 15: Oil-Water Relative Permeability Curves, Well 34-6

Advanced Resources
International, Inc.

SACROC Simulation KS080807

The water permeability curves for well 34-6 (Figure 15) have a very different shape and end-points. Oil relative permeability curves were also somewhat homogeneous. This emphasized the need to optimize the end points during the optimization process.

No gas-water relative permeability curves were available for the study. Hence, gas and liquid relative permeability endpoints and exponent were optimized during the history matching process. Seven (7) measurements of centrifugal capillary pressure curves coming from well 65-4 were provided by $KMCO_2$, and are presented in Figure 16. Centrifugal capillary pressure curves are known to accurately define irreducible water saturation. From theses samples, irreducible water saturation varied from 0.22 to 0.38.
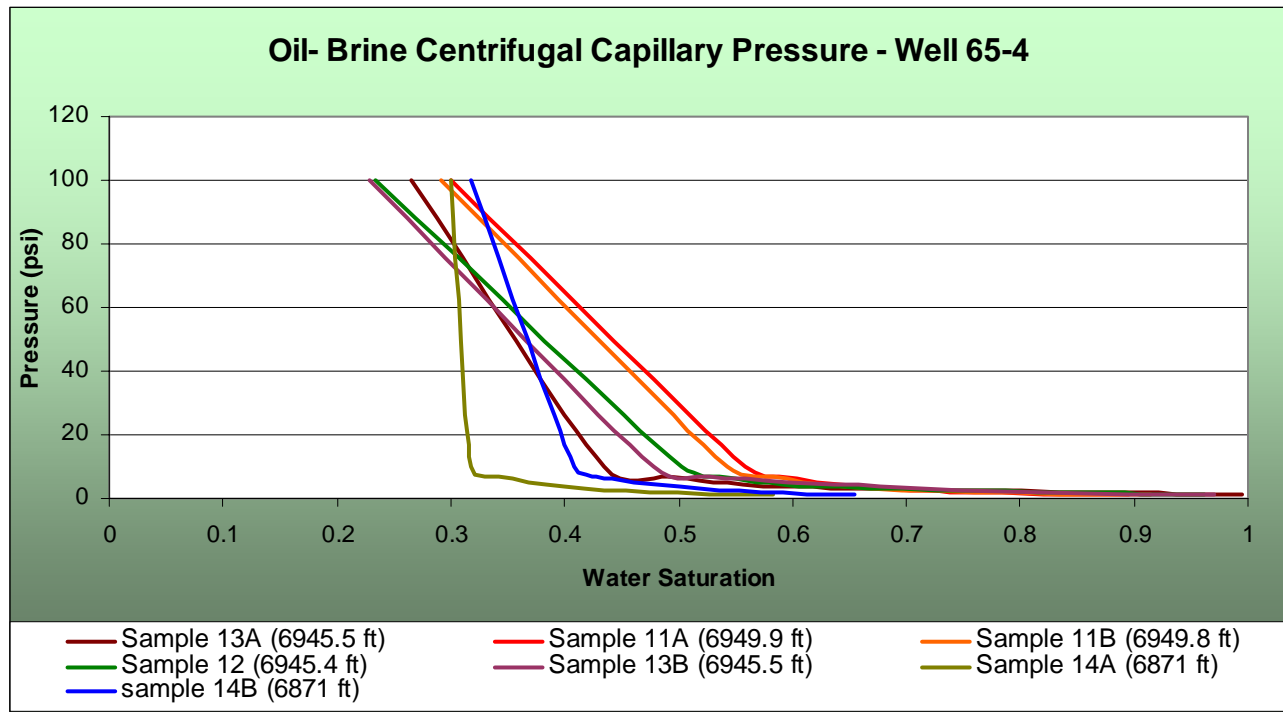
Figure 16: Available Capillary Pressure Curves

No gas-oil capillary pressure curve was available from the operator or in the published literature. Since CO_2 displacement can not be modeled accurately by using a black oil model, it was decided to ignore the gas-liquid capillary effect.

An initial water-oil contact was present in SACROC field Canyon Reef reservoir at a depth of 4,500 ft subsea. This information can be found in the literature[4,5,9,10,12] and is very coherent from one paper to another.

4.4   Production Data

Production data were provided by $KMCO_2$ for the 19 producers in the study area:
- Quarterly Gas Production Rate
- Quarterly Water Production Rate
- Quarterly Oil Production Rate

Injection data were provided by $KMCO_2$ for the 3 producers converted to WAG injectors:
- Quarterly Water Injection Rate
- Quarterly Gas Injection Rate

Figure 17 presents producing and injecting wells within the study area.
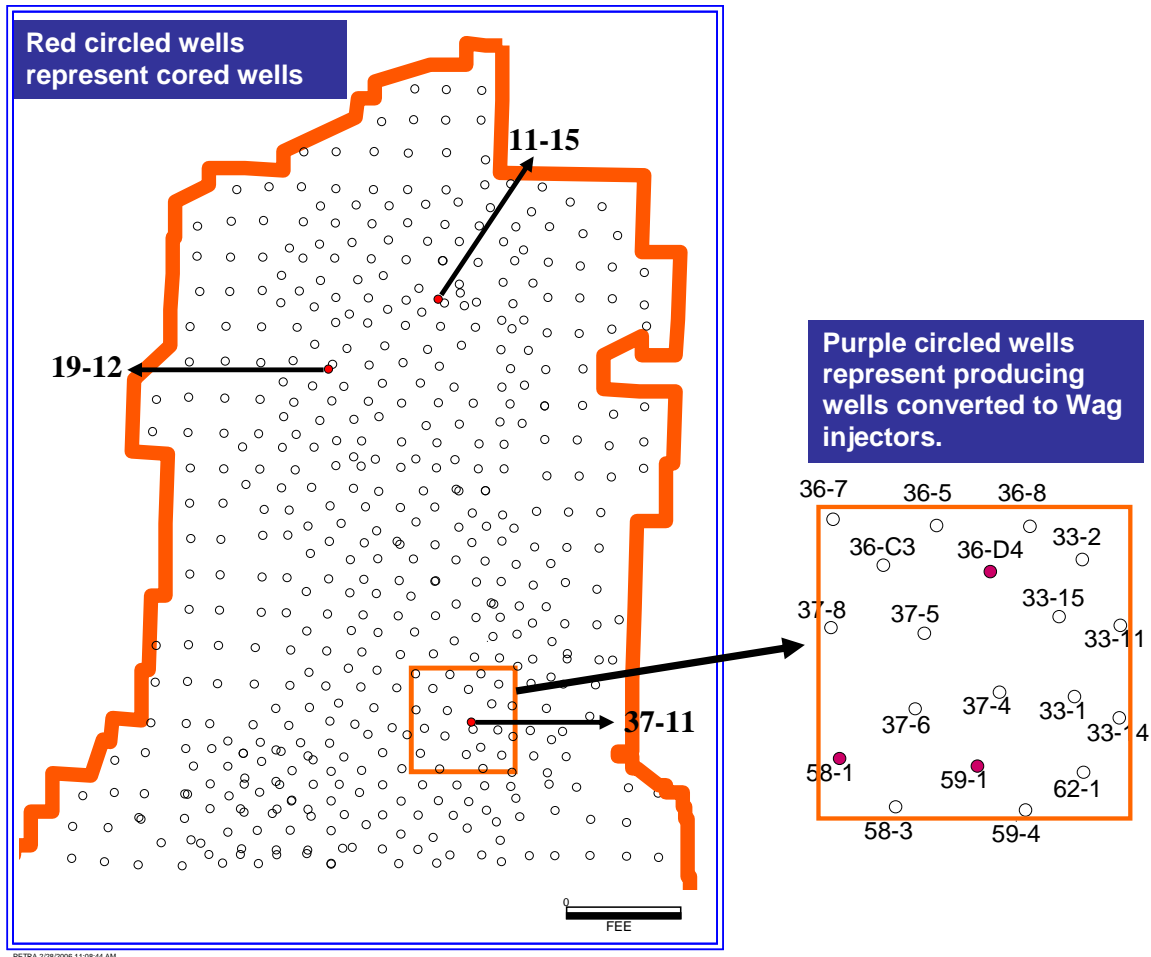
Figure 17: Producing and Injecting Wells Included in the Study Area[2, 3]

The total production and injection rates of the study area are presented Figure 18 and 19.
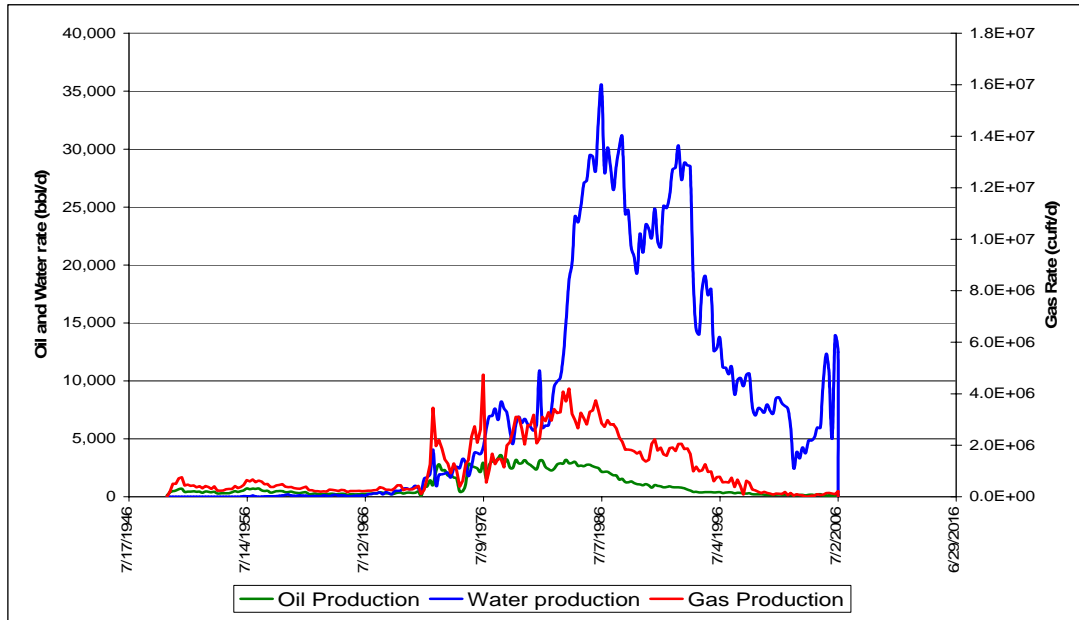
Figure 18: Production Rates for the Modeled Study Area

Production started in August 1949 inside the study area and is still active today.
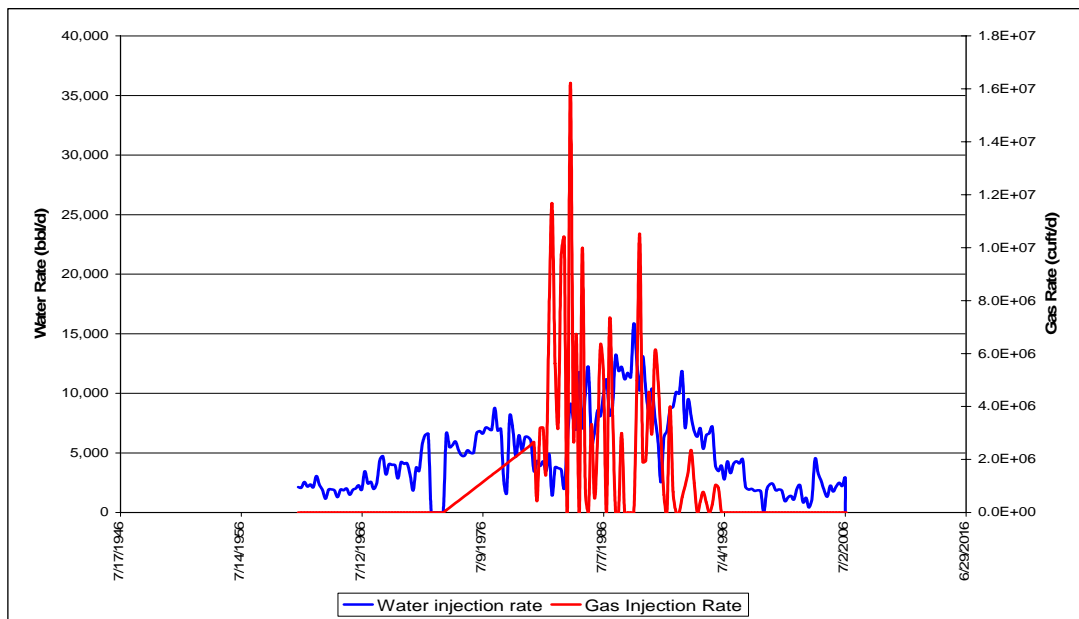
Figure 19: Injection Rates for the Modeled Study Area

19

Water injection started in April 1961 and was then converted to WAG[13] in July 1973 inside the study area. WAG injection is still active today on the Northern Platform. Gas injection stopped in August 1996 inside the study area.

5.0   Reservoir Simulation

5.1   Reservoir Model Construction

The modeled sector represents the area covered by the geostatistical realizations for porosity and permeability presented in topical reports[2,3]. The study area was selected jointly with $KMCO_2$ based on the existence of a completely cored well in this area (well 37-11), a planned crosswell seismic survey inside the area, and a future CO_2 injection procedure to be implemented to improve the production levels.

The reservoir simulator used in this study was IMEX[14] from Computer Modeling Group. The model consists of 65,340 grid-blocks (33 x 33 x 60), each grid block being 112 ft by 112 ft in the horizontal direction and 60 layers 15 ft thick each. All 19 producers and 3 WAG injectors are included in the model. The 3 injectors were originally producers, converted to water injectors and finally converted to WAG, as indicated by actual production history. The completion history for each individual well was respected since this information had been provided by $KMCO_2$. The total area covered by the model is hence 13,660,416 ft^2 or 313.6 acres. The Original Oil In Place (OOIP) for this model was 89.4 MMSTB which only represents a small percentage of the 49,900 acres SACROC region, with OOIP estimated at 2,113 MMSTB[13].

Based on existing information presented in the previous section, the reservoir properties used in the model were as follow:

Porosity: average porosity of this heterogeneous model[3] was 8.5%.

Figure 20 presents the porosity characterization[3] implemented inside the reservoir model.

21
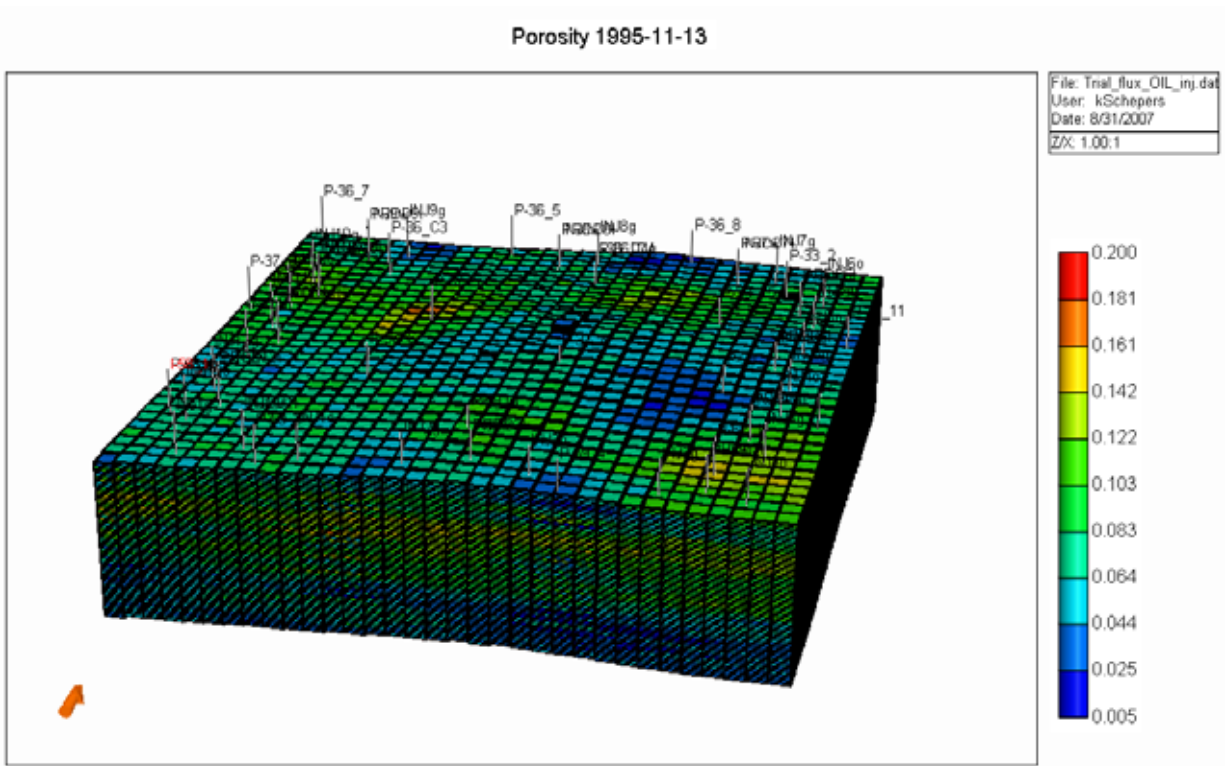
Figure 20: Porosity Model of the Study Area

Horizontal Permeability: average permeability of this characterization[3] was 2.74 mD.

Figure 21 presents the horizontal permeability incorporated into the reservoir model. No permeability anisotropy was introduced (between Kx and Ky) because results derived from the integrated clustering/geostatistical approach for the characterization accounted for it[2,3].

22

Figure 21: Horizontal Permeability Model of the Study Area

The formation, fluid and well properties included in the model are presented in Table 4. They are all based on actual data when available, or on correlation and literature when unavailable.

SACROC Simulation KS080807

Table 4: Formation, Fluid and Well Properties of the Reservoir Model

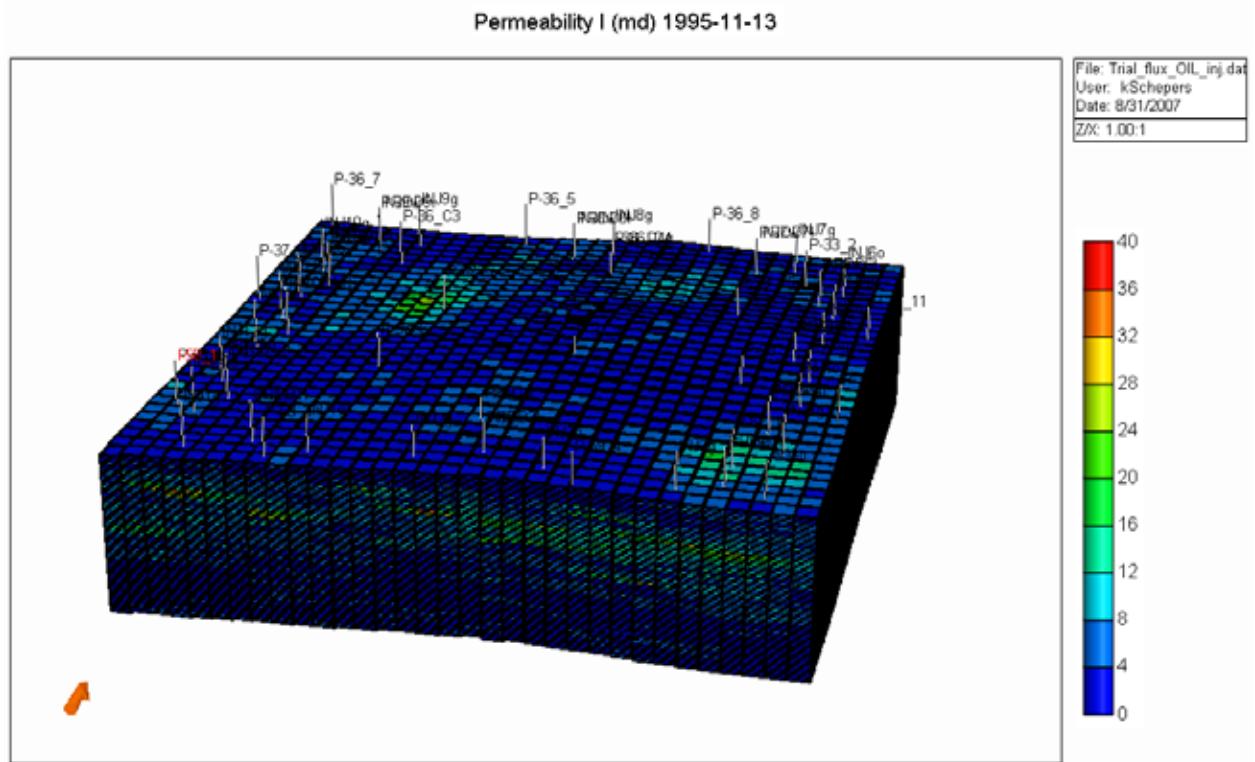| Parameter	Units	Value	Reference Depth/Pressure
Formation Properties			
Initial Pressure	psia	3137	at 4300ft TVDSS (actual data)
Initial Temperature	F	132	at 4300ft TVDSS (actual data)
Initial Water Oil Contact	FT	4500	TVDSS (actual data)
Rock Compressibility	1/psi	5.60E-06	at 3137 psia (actual data)
Fluid Properties			
Bubble Point Pressure	psi	1850	at 4300ft TVDSS (actual data)
Oil Compressibility	1/psi	7.00E-05	at 1850 psia (Ramey's correlation[15])
Oil Density	API	37.2	at STC (actual data and Mc Cain's correlation[16])
Gas Gravity	-	0.67	at STC (Standing and Katz's correlation[17])
Water Compressibility	1/psi	2.90E-06	at 1850 psia (Dodson and Standing's correlation[18])
Water Density	-	62.3	(Earlougher, R.C.[19])
Water FVF	RB/STB	1.013	(Rowe and Chou's correlation[20])
Water Viscosity	cp	0.51	(actual data and Matthews and Russell's correlation[21])
Relative Permeability Relationships			
Krliq	-	1	assumed
Well Parameters			
Skin Producers	-	-1	assumed
Skin injectors	-	-1	assumed

PVT of oil and gas changes versus pressure are presented in Figure 22 to Figure 26.
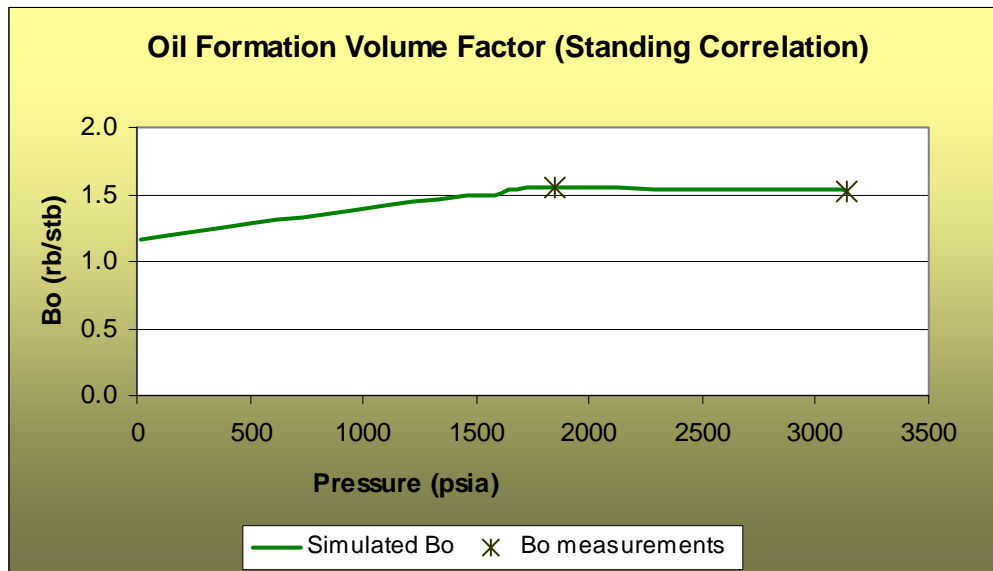
Figure 22: Oil Formation Volume Factor vs. Pressure

24

SACROC Simulation KS080807

The oil formation volume factor was calculated using two data points present in the literature and Standing's correlation[22].
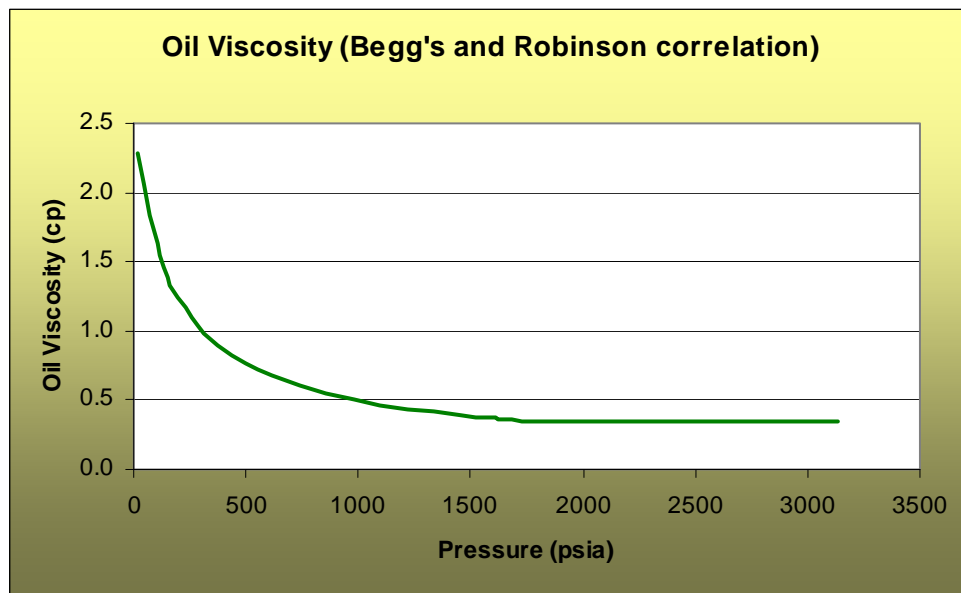
Figure 23: Oil Viscosity vs. Pressure

The oil viscosity was calculated using Beggs and Robinson's correlation[23], based on gravity, temperature and bubble point pressure. No real data was available.

Figure 24: Gas Oil Ratio vs. Pressure

25

The gas-oil ratio was calculated using one data point present in literature and the same trend as the gas-oil ratio of Claytonville field[24].

Figure 25: Inverted Gas Formation Volume Factor vs. Pressure

The gas expansion factor was calculated using Standing and Katz's correlation[17]. No real data was available.

Figure 26: Gas Viscosity vs. Pressure

26

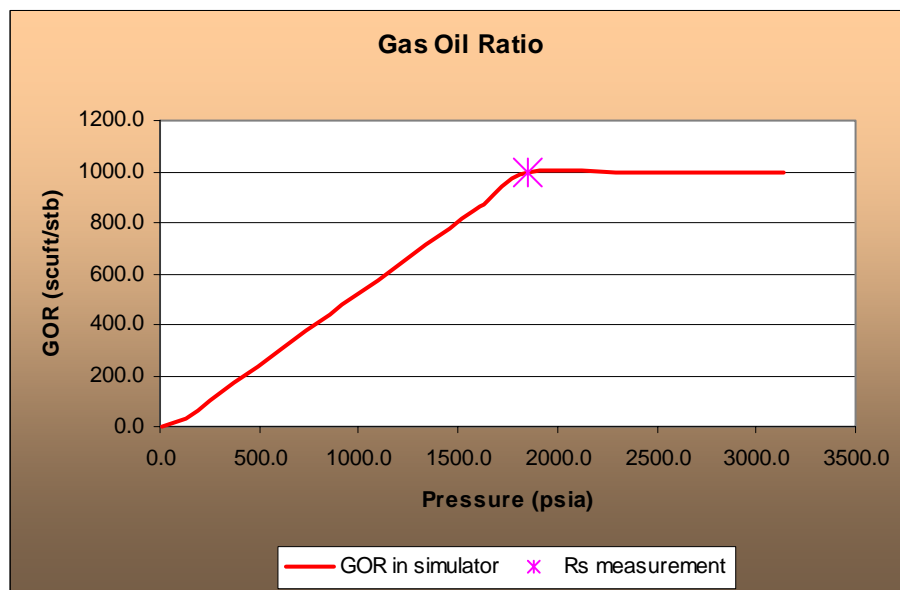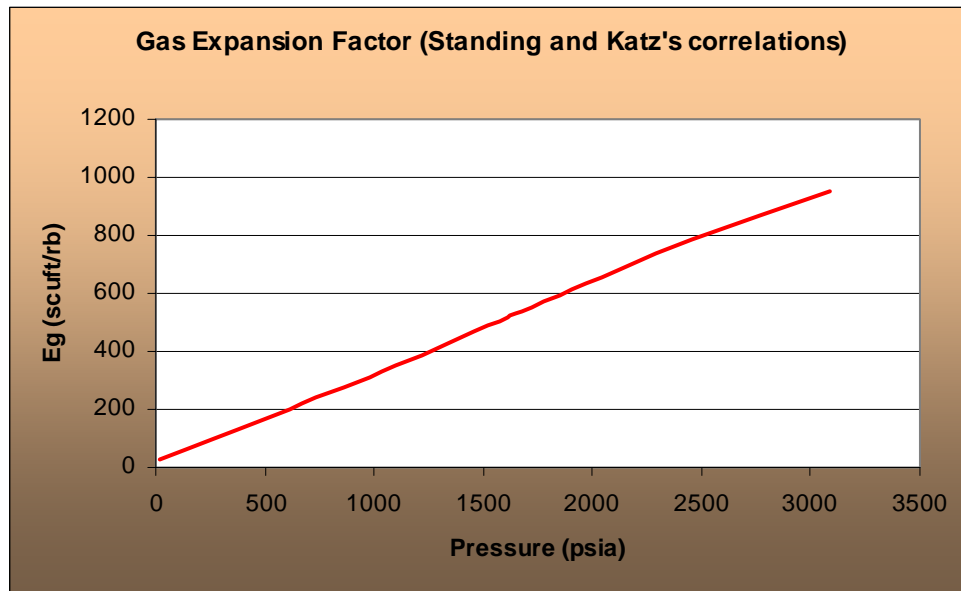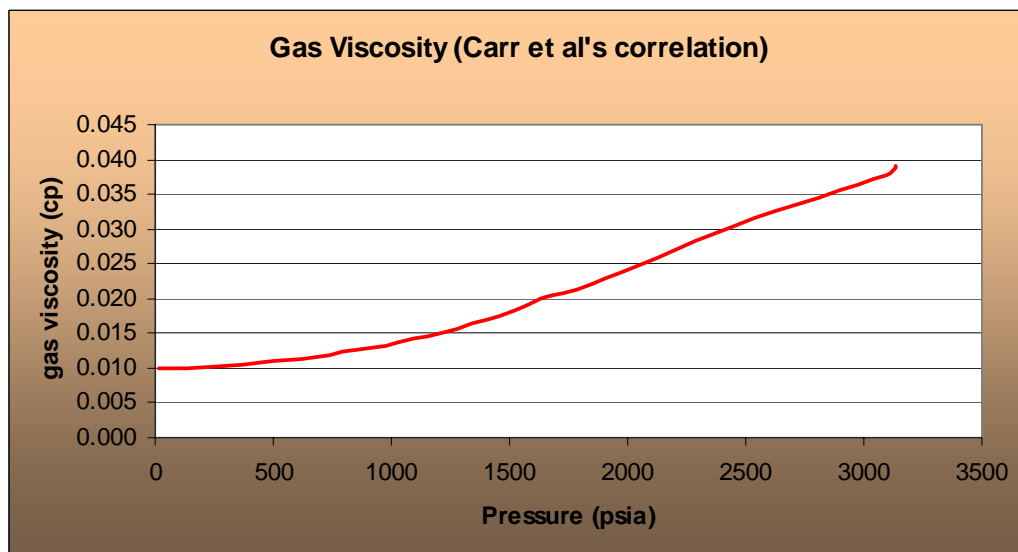No gas viscosity data was available; therefore, it was calculated using Carr et al's correlation[25]. Only one rock type was defined in this model. From the relative permeability samples of wells 32-3 and 34-3, relative permeability (Kr) curves endpoints vary significantly, so it was decided to vary oil-water and gas-liquid relative permeability endpoints and shape using Corey's functions during the optimization process.

Only one oil-water capillary pressure curve has been used, since a gas-liquid was unavailable. Since the shape of the capillary pressure curve is dictated by permeability, the average permeability of the reservoir characterization and the permeability measured on the core samples of the capillary pressure (Pc) measurements were compared: samples 11B and 13B had the closest permeability value. Due to the coherence between those two samples, it was decided to keep a constant capillary curve inside the reservoir model; and an average curve of the two samples was used. This is presented in Figure 27.
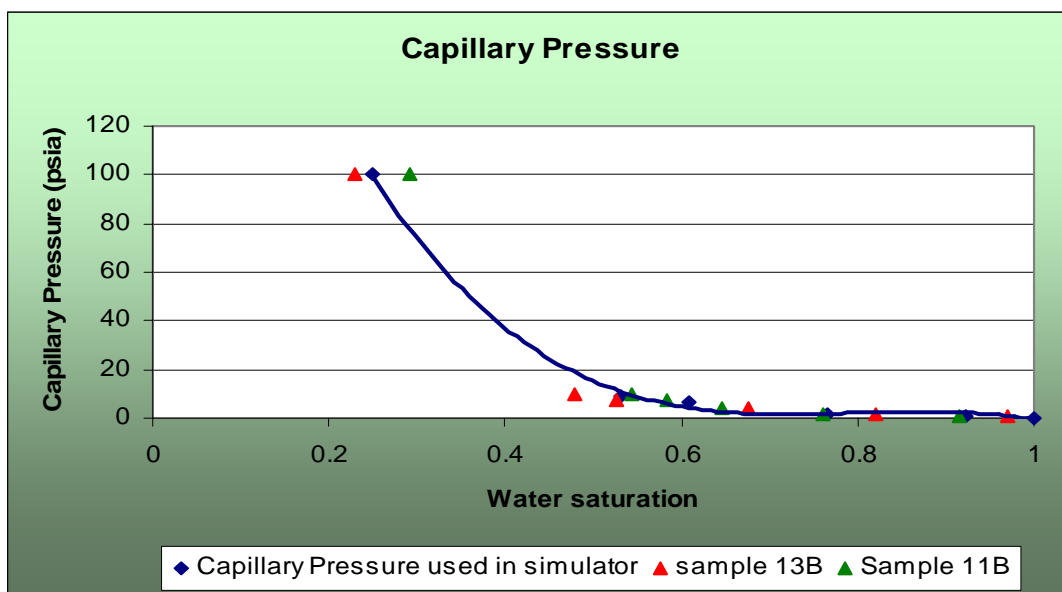
Figure 27: Oil-Water Capillary Pressure Curve vs. Real Data

The reservoir model comprised 19 producers, but 3 were converted to water then to WAG injectors. Twelve (12) pseudo-injection wells were also implemented to reproduce proper boundary conditions. This is explained further in the next section. The model was run on Liquid Production Rate, with a minimum bottom-hole pressure of 28 psia. Injecting wells were controlled by gas and water injection rate. WAG injection consisted of water alternating with CO_2 injection. From the literature[7], miscibility was not achieved in this area of the reservoir due to a reservoir pressure below minimum miscible pressure (MMP). Furthermore, by the time the model was built, no compositional data were available, thus another reason to build a black-oil model.

Because a black-oil model was used, proper CO_2 behavior could not be accurately reproduced. To address this issue:
- Injected gas composition was specified as CO_2: this allowed modeling accurate CO_2 flows inside the wellbore.
- Inside the reservoir, properties of a lean miscible gas were used for injected gas phase (only option available in black oil model).

This definitely had an impact on the recovery factor, but it ended up not being as critical as it will be presented in the Section 6.3 (Results) of this report. Figure 28 and Figure 29 present respectively a planar section (layer 17) and a 3D view of the current reservoir porosity model.
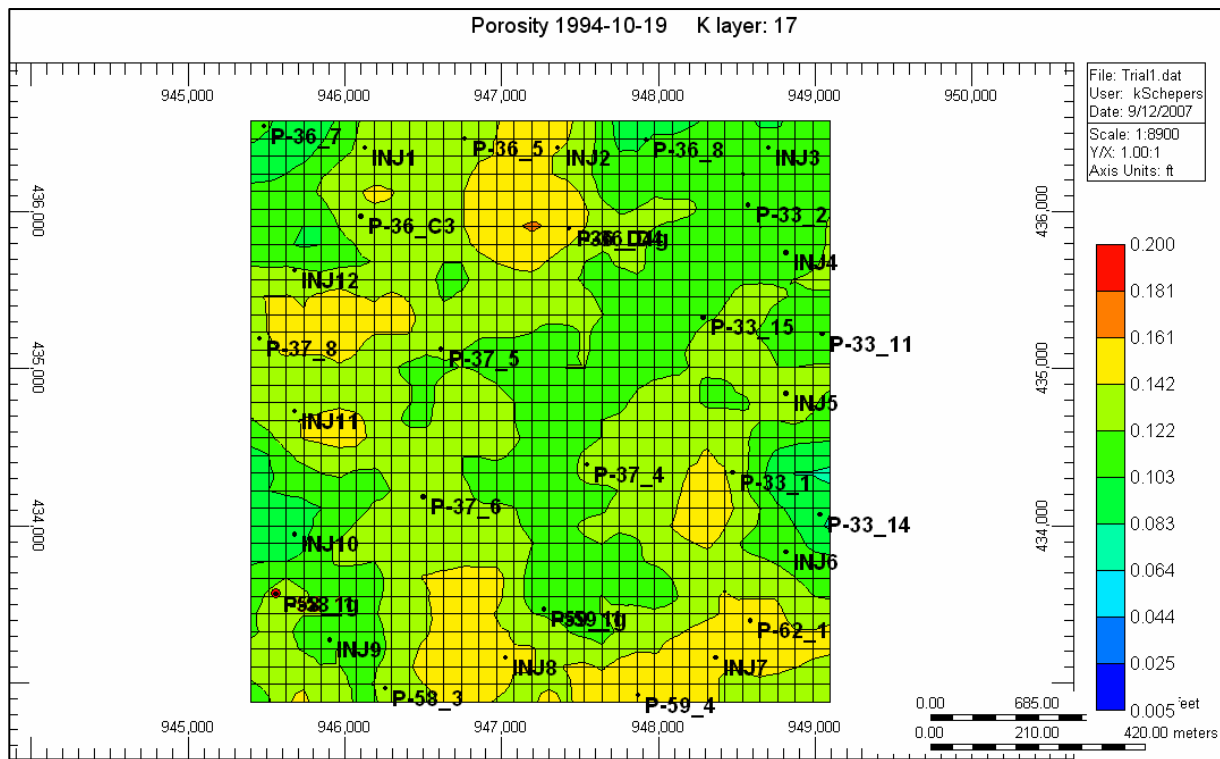

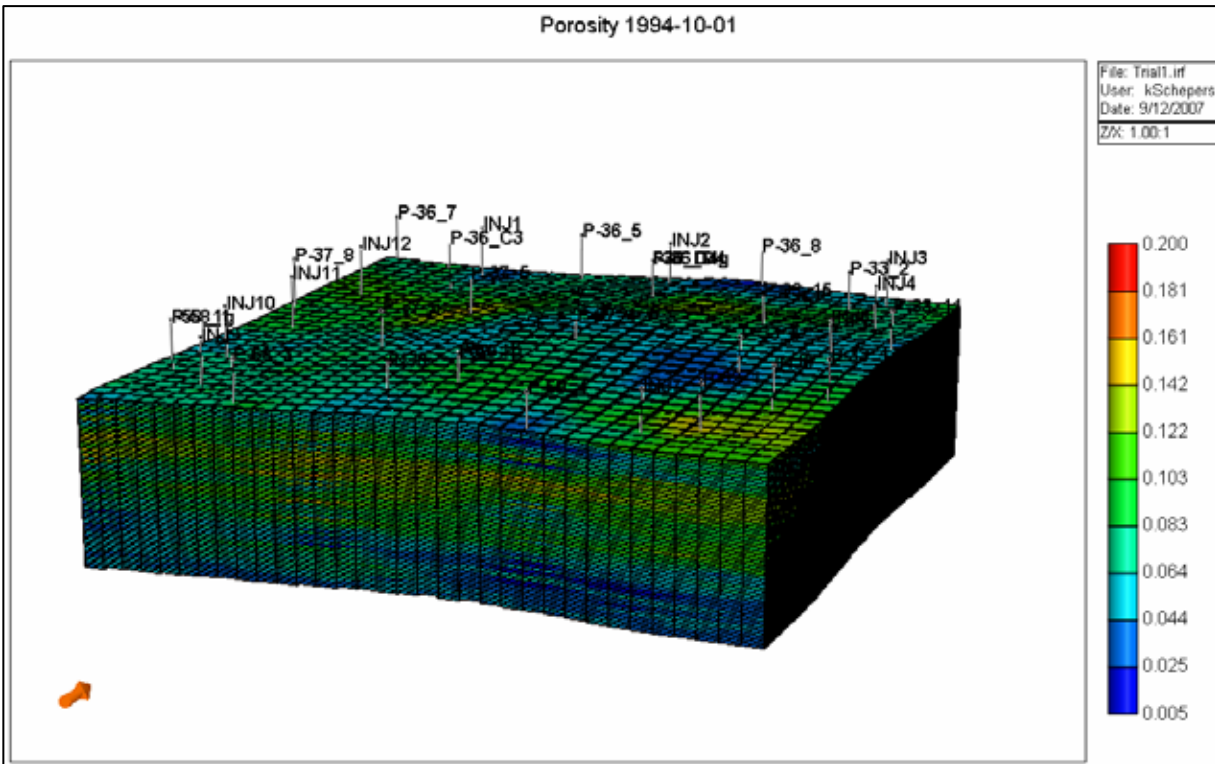**Figure 28: Study Area Reservoir Model - Top View**

SACROC Simulation KS080807

Figure 29: Study Area Reservoir Model - 3D View

5.2   Model Boundary Conditions

The first model built for the study area assumed no-flow boundary conditions, which was obviously not rigorous since the modeled study area is surrounded by producing and injecting wells. Hence, several methods were used to evaluate fluxes entering (influx) and exiting (efflux) the study area.

Method 1

The first method that was used to estimate fluxes was a large-scale model that included the original study area. This model included more than 700 producing and injecting wells within a large part of the SACROC Platform area. Local Grid refinements were used to precisely reproduce the production/injection behaviors inside the study area (Original 7 x 9 x 1 locally refined in 3 x 3 x 5 and/or 11 x 11 x 12). A total of 66,880 grid-blocks composed this model. Planar and 3D views are presented in Figure 30 to Figure 32.

SACROC Simulation KS080807

Large-scale grid defined on the SACROC platform (7 x 9 x 1)

3*3*5 refinement

11*11*12 refinement

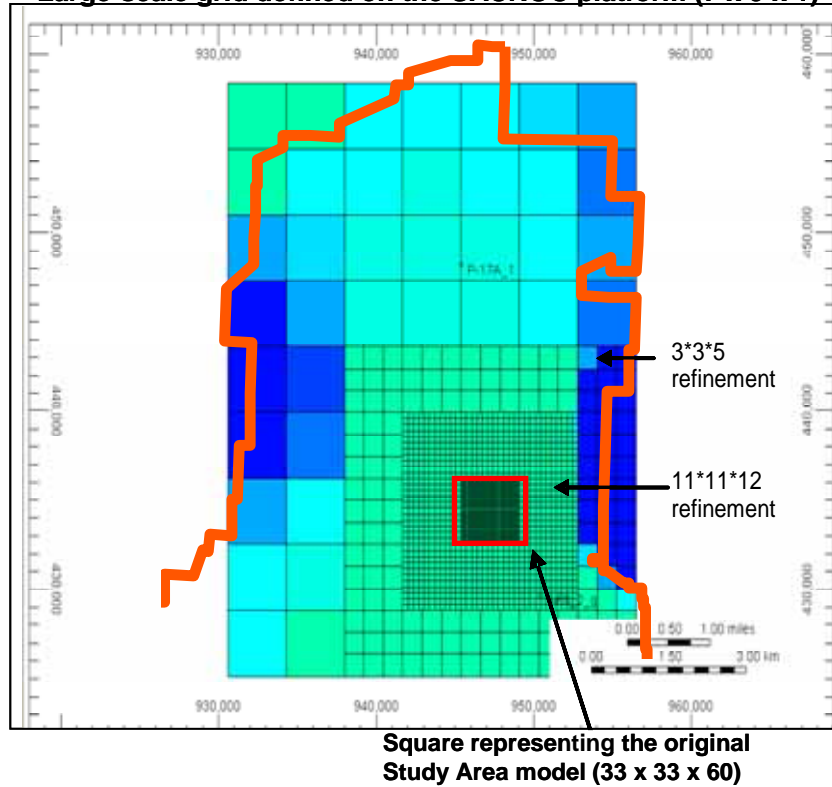Square representing the original Study Area model (33 x 33 x 60)

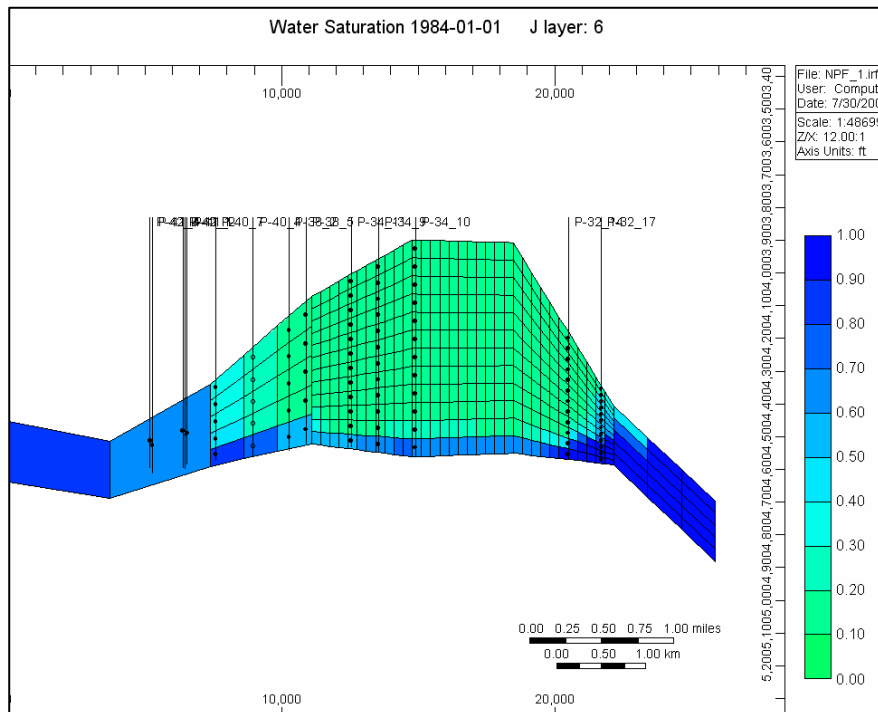**Figure 30: Top View of the SACROC Platform Model**

Figure 31: 2D View of the SACROC Platform Model (IK Plan)
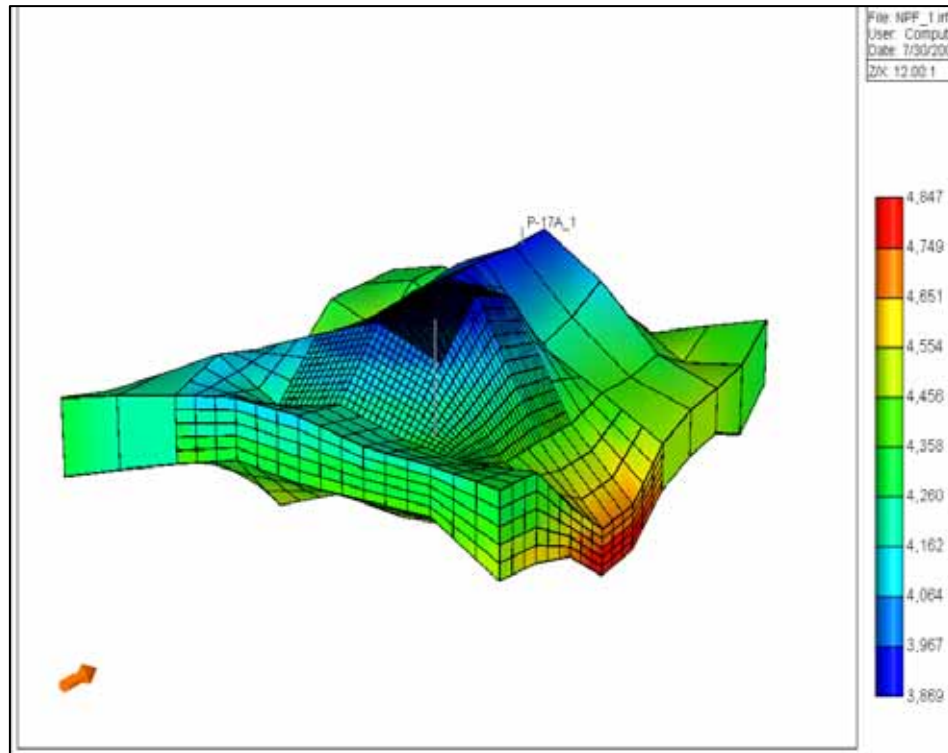
Figure 32: 3D View of the SACROC Platform Model

      The formation and fluid data used in the large-scale model were very similar to the data of the study area model, with the exception that a constant permeability and constant porosity were used for the large scale model. No geological model of porosity and permeability realization were available at the time of this study. No capillary pressure curves were implemented and all wells were completed in all layers. Production and injection history were provided by $KMCO_2$. The model was run on liquid production rate and fluxes were calculated in IMEX[14]. The results of the fluxes are presented in Figure 33 to Figure 37.
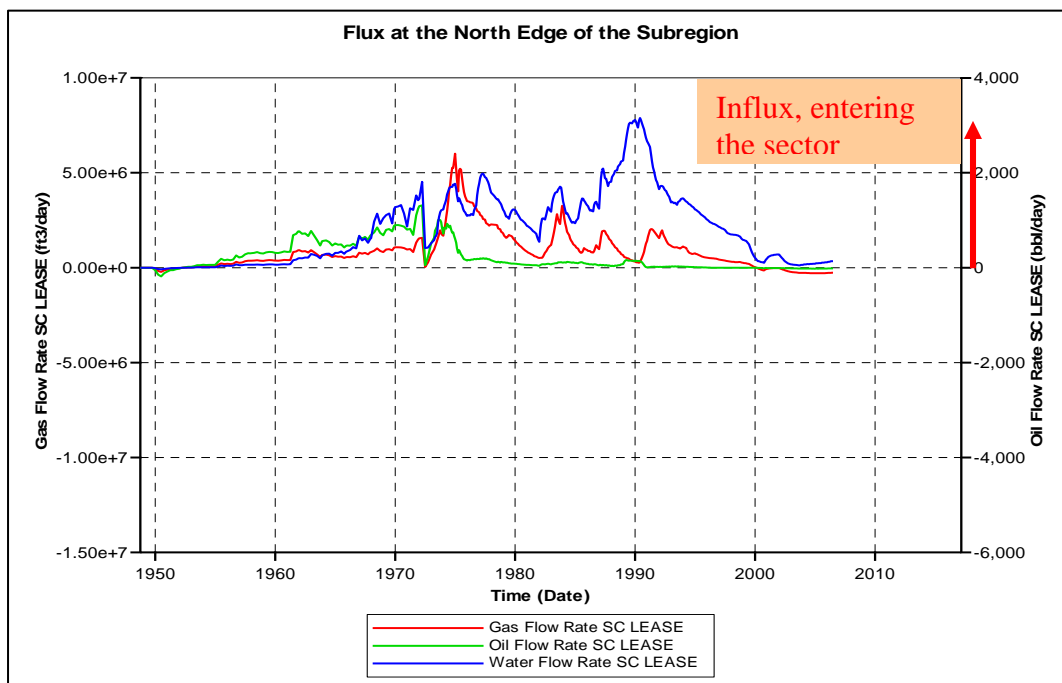
Figure 33: Flux at the North Edge of the Study Area

From this method, influxes were dominant at the north edge of the study area.
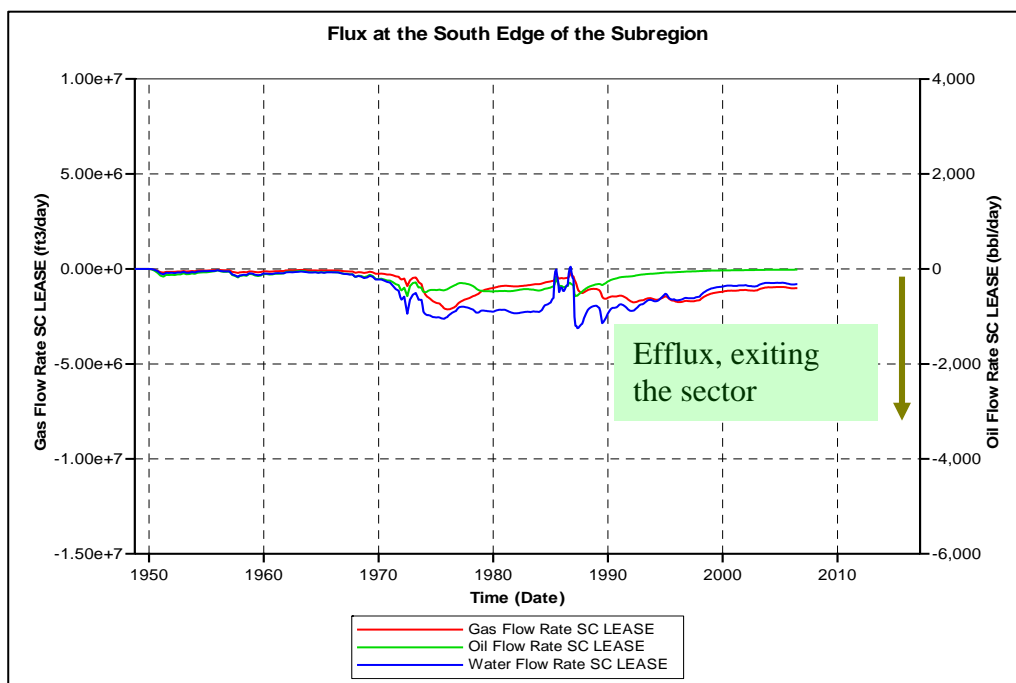
Figure 34: Flux at the South Edge of the Study Area

At the south edge of the study area, effluxes were dominant but not as large as at the north edge.
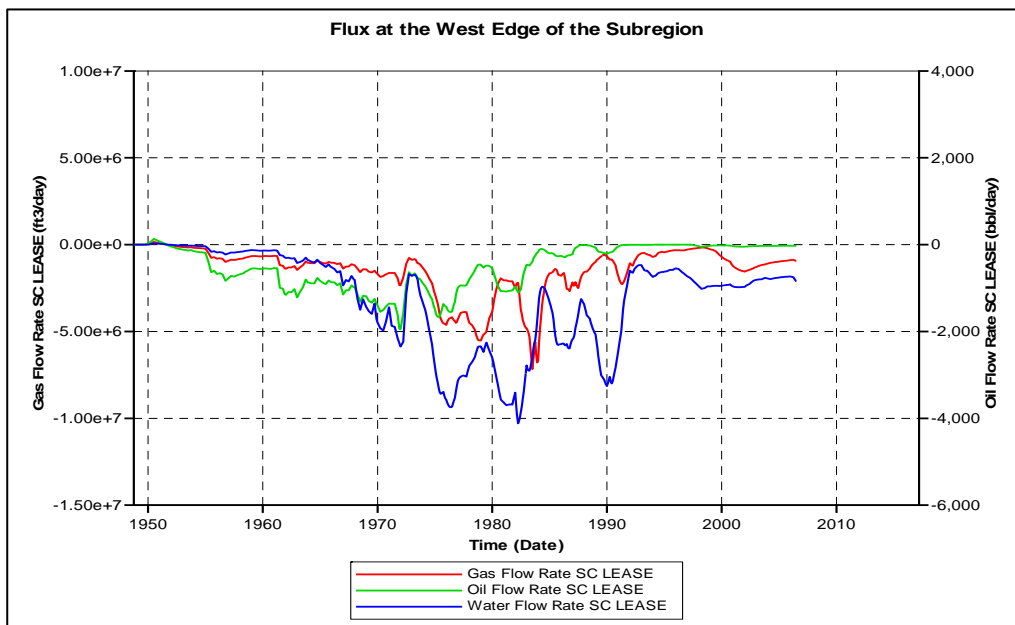
Figure 35: Flux at the West Edge of the Study Area

At the west edge of the area, effluxes were dominant and important in magnitude.
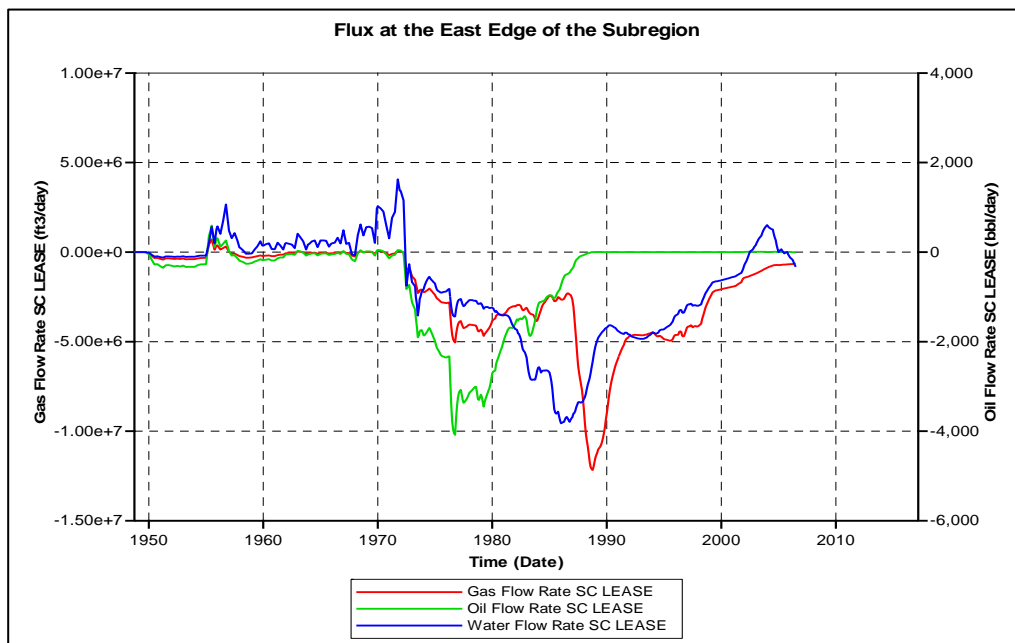
Figure 36: Flux at the East Edge of the Study Area

33

Advanced Resources
International, Inc.

SACROC Simulation KS080807

At the east edge of the study area, effluxes were dominant and represented very significant volumes, especially for gas and oil. From the flux calculated using the large-scale model, effluxes were dominant in the study area as shown in Figure 37. However, constant porosity and permeability assumptions likely had a strong impact on those results. Hence, a volumetric approach was used to cross check this conclusion (Method 2).

Figure 37: Total Fluxes at Edges of the Study Area

Method 2

This method was purely volumetric and used actual production and injection data from the wells within the study area. The difference between total water production and water injection rates was calculated, and the results are presented in Figure 38.
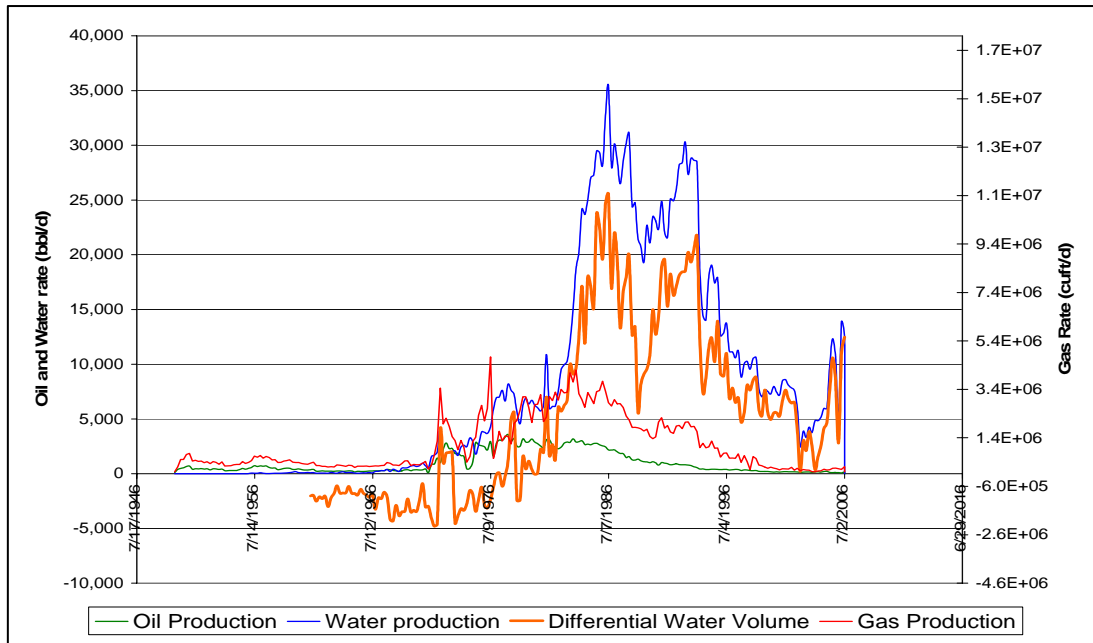
Figure 38: Differential Water Volume for the Model (Water Production - Water Injection)
Note: Differential Water Volume = Total Water Production Rate – Total Water Injection Rate

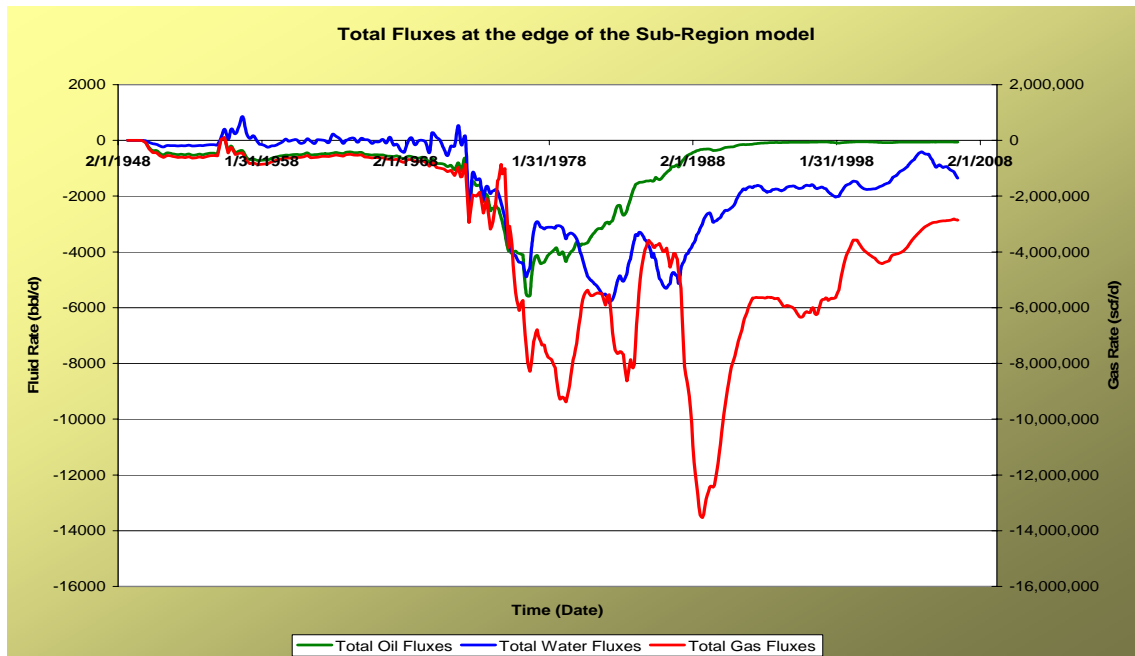The orange curve represents the difference between water production and injection versus time. From this plot, it was apparent that the volume of produced water by far exceeded the quantity of water that had been injected inside the sector. This suggested strong water influxes. The cumulative water influx calculated from this method was **89 MMSTB**.

This approach indicated strong influxes entering the study area, and also provided a good picture of the fluxes versus time. However, it did not define precisely the time of water breakthrough. Indeed, there is always a delay between the time the water is injected and the time it is recycled or reproduced. Therefore, some uncertainties were inherent to this method. Finally, results obtained from Method 1 differed completely from those computed using Method 2, as Figure 39 illustrates. For these reasons, a third method to estimate volumetric water influxes was attempted.

35

SACROC Simulation KS080807
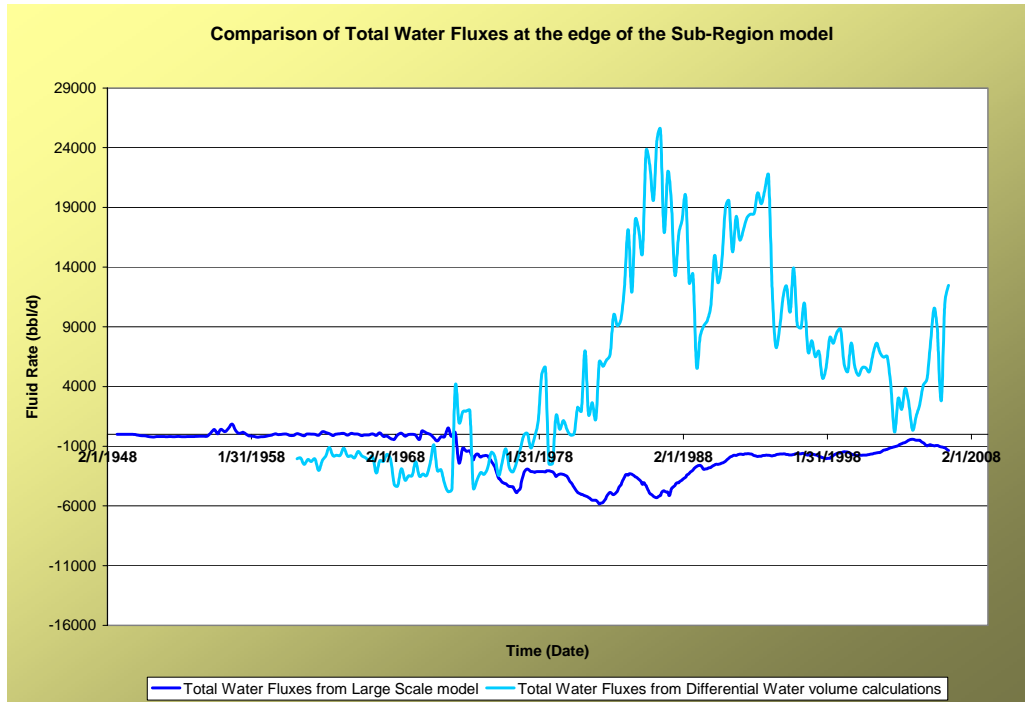
Figure 39: Comparison of Total Water Fluxes Computed from Method 1 and Method 2

Method 3

The third method was a simple material balance calculation performed over the entire period of production in order to estimate cumulative water influx. First, cumulative water influx was calculated using the equation from Van Everdingen *et al*[26]: The symbols for this equation are presented in Table 5.

$$N(Bo\text{-}Boi) + N(Rsi\text{-}Rs)Bg = NpBo + (Gps\text{-}NpRs)Bg - GiBg + WpBw - WiBw - WeBw$$

Note 1: since pressure dropped below bubble point (1850 psia), water and rock expansions were neglected.

Note 2: No original gas cap was present.

Table 5: Material Balance Symbols[25]

Symbol	Name	Units
N	Original Oil In Place	STB
Bo	Oil Formation Volume factor	RB/STB
Boi	Initial Oil Formation Volume factor	RB/STB
Rsi	Initial Solution Gas Oil Ratio	scf/STB
Rs	Solution Gas Oil Ratio	scf/STB
Bg	Gas Formation Volume Factor	RB/scf
Np	Cumulative Oil Produced	STB
Gps	Gas produced initially in solution	scf
Gi	Cumulative Gas Injected	scf
Wp	Cumulative Water Produced	STB
Bw	Water Formation Volume Factor	RB/STB
Wi	Cumulative Water Injected	STB
We	Cumulative Water Influx	STB

The cumulative water influx calculated from material balance was **35 MMSTB**. This confirmed that influxes were dominant inside the study area. Cumulative water influx from Method 2 was compared to the material balance results. The cumulative water influx calculated with material balance represented 40% of the cumulative water influx calculated using differential water volume method.

Considering the difference between material balance and differential volumes calculations, some uncertainties existed around the fluxes calculation. To account for those uncertainties, water influxes were implemented but varied at the edge of the model.

Calculation of Water Influxes

Water injection rate at the edges of the study area were implemented using Methods 2 and 3 (orange curve from Figure 38). Twelve (12) pseudo-injectors were implemented at the boundaries of the study area (3 injecting wells on each side). Water injection rate for each well was then calculated as follow:

The model was subdivided in four areas, represented in Figure 40. For each quadrant, total water injection was subtracted from total water production. This defined a total water influx rate per quadrant, as presented in Figure 41.

Since three injecting wells were present inside each quadrant, total water injection rate per quadrant was divided by three to get an injection rate for each injection well along the entire period of production.

Variation of the Water Influxes

To vary water influxes at the edge of the model, the water injection rate of each pseudo-injector was multiplied by a factor varying between 0.2 and 1. This factor was optimized during the history matching process.
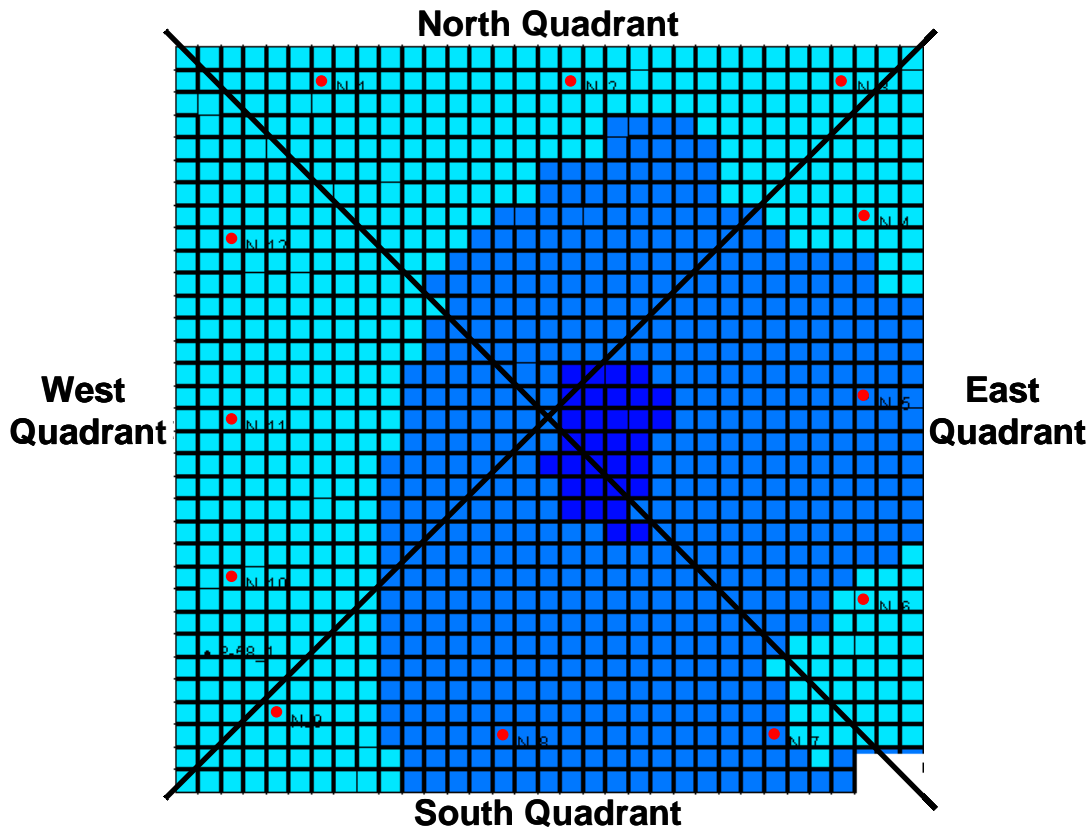

Figure 40: Location of the 12 Pseudo-Injectors (in Red) Inside the Four Quadrants of the Study Area
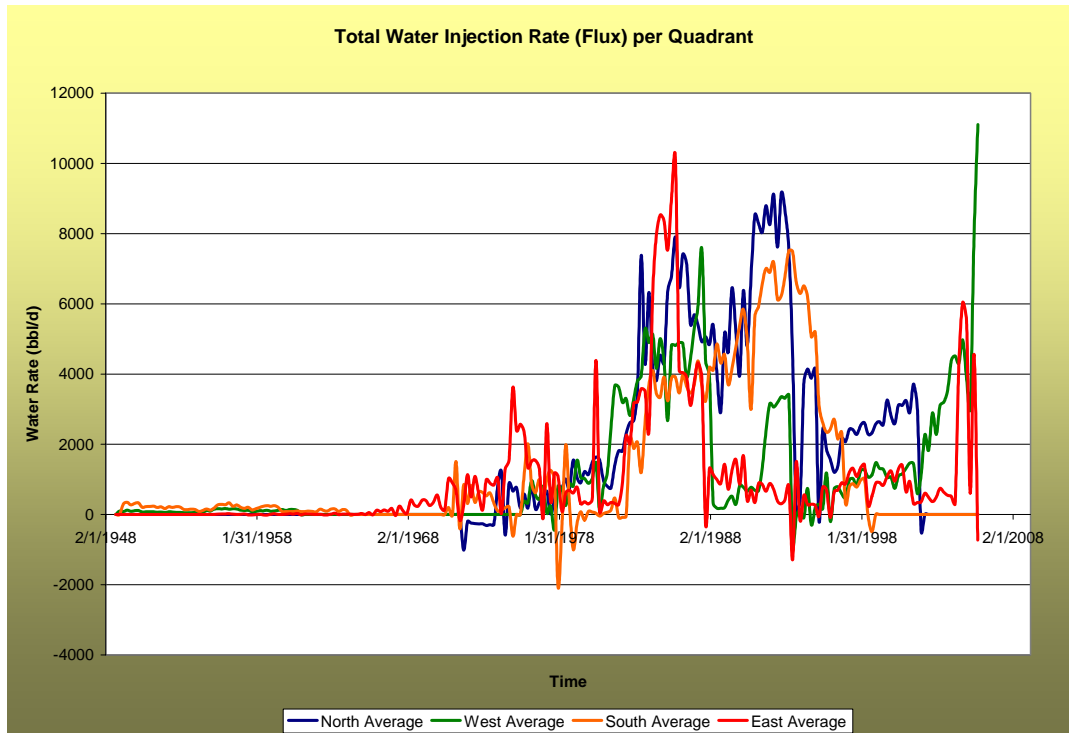
Figure 41: Water Flux per Quadrant (from Method 2)

6.0 History Matching

6.1 Procedure

The automated history matching is an iterative technique utilizing two software programs, the global optimizer[27] (*ClearVu*) and a black-oil reservoir simulator (*IMEX - CMG).* The first step begins with a spreadsheet version of an IMEX[14] input file that is built in order to facilitate the variation of input parameters through the addition of formulas (Corey correlations for relative permeability curves, for example). Before the optimization process is started, the case is defined by generating possible ranges for uncertain input parameters (minima and maxima) as well as the total number of simulations to be run and the number of simulations per batch (also referred to as an iteration).

The current set of input parameter values is generated by the optimizer based on the probability distributions previously defined by the user. These parameter values are then inserted into the simulator input file in their appropriate locations and the spreadsheet is converted to a standard ASCII input file.

Simulations are executed one after the other and at the end of each iteration, the output data from each simulation is saved and compared to historical data. At this point, the corresponding error value is computed using Equations 1, 2, and 3 shown below. Equation 1, weighted sum of squares of the difference between actual data and simulation data, is used most frequently and recognizes the goodness-of-fit measure for optimization purposes.

$$ErrorValue = \frac{\sum \left(\dfrac{(SimData - ActualData)^2}{2*Variance} \right)}{NumberofData} \qquad (1)$$

with

$$Variance = \frac{\sum (ActualData - Mean)^2}{NumberofData} \qquad (2)$$

and

$$Mean = \frac{\sum ActualData}{NumberofData} \qquad (3)$$

These computed error values serve as objective (goodness-of-fit) function values and are evaluated by the optimizer, which produces a new set of input parameters. The next iteration can then be initialized. When several output parameters are to be matched, the objective function is computed separately for each parameter with the final error value being the sum (or some other combination) of the independent error values[27]. The workflow of the process is outlined in Figure 42. The algorithm used by the optimizer is described in more detail in the next section.
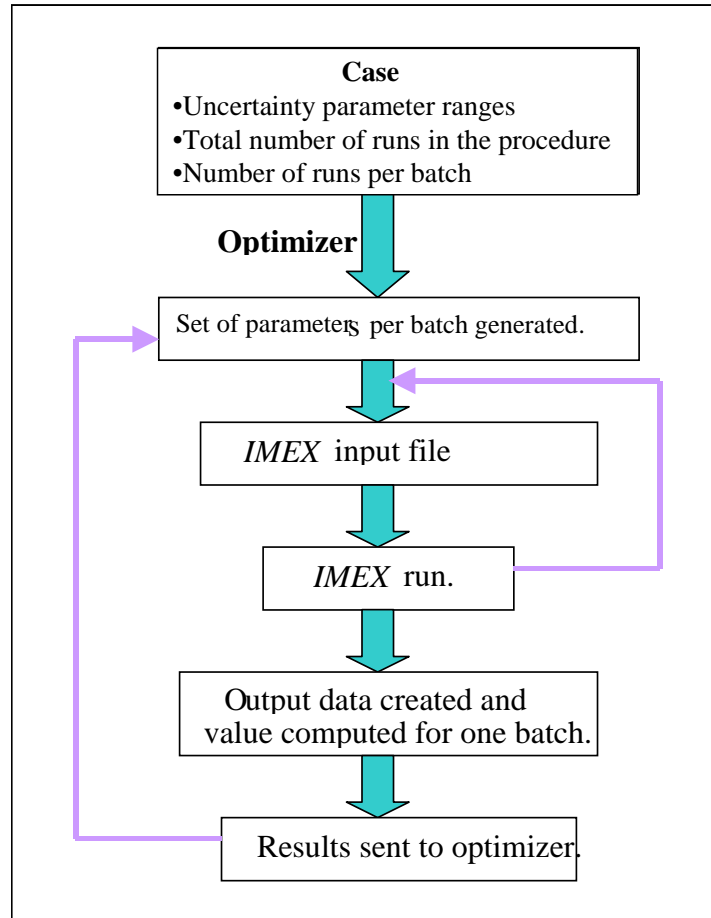

Figure 42: Optimization Process Workflow

The optimizer consists of an "evolution strategy"[27,28], more exactly a (μ,λ)-evolutionary strategy. Evolutionary strategies were invented by H.P. Schwefel and I. Rechenberg in the late 1960s in Germany. The basic idea of such a strategy is to mimic biological evolution, also known as mutation-selection-mechanism (Darwinian Theory). Numerically, the great advantage of employing evolutionary strategy is that it is not necessary to calculate derivatives. Consequently, it is possible to deal with non-linear functions more easily than with any other optimization techniques.

41

The algorithm is initialized with a set of λ individuals, where an individual represents a solution in the given search space. The optimizer can support the distribution of λ individuals in the search space completely arbitrarily or via initialization with a given start point. The latter can be used if an optimization will be based on a known good solution.

The λ individuals are then evaluated -- meaning in this particular case, that for each set of individuals a complete set of simulation iterations are executed. Once completed, the objective value can be calculated as previously described. The next step in the optimization loop is the "selection" mechanism where the individuals are sorted according to their objective values. The population for the next generation is then created by taking the best μ individuals from the λ individuals (also called "comma-selection").

In order to exchange information about the topology between the individuals, the next applied operator is the recombination operator. Usually two individuals from these μ are taken randomly to create a new individual. Here an "intermediate recombination" is used, i.e. for each dimension the average of the values of the two participating parent individuals is calculated. This is done until λ offspring are generated.

Since the recombination is responsible for large moves in the search space, the subsequent "mutation" is applied to make smaller moves and hence to search more locally. The value of each individual's dimension is mutated by adding a normal distributed term which is calculated based on the parameters of global sigma (σ) and local sigma (σ_i). These additional variables are called "step sizes" or "strategic variables" and belong to the individual's gene type as the objective variables (input variables) do. Due to the normal distribution, smaller changes are more likely than greater changes. The σ, σ_i itself are also underlying a normal distributed variation. This means the step sizes change and should always be adapted to the current fitness landscape. This mechanism is called "self-adaptation"[27,28]

Although an evolutionary algorithm is a very general and robust optimization technique, it is possible in each specific case to make the optimization more efficient and converge faster by applying known domain knowledge and good parameter settings.

6.2   Optimized Parameters

Some input parameters were unavailable for the study. Those parameters were varied during the history matching as were uncertain parameters. The porosity and permeability characterizations were developed in a grid that could work directly in the flow simulator[3]. Both the geostatistical characterizations and the reservoir flow simulations were conducted on the same Cartesian grid. Confidence in the porosity model developed with this grid definition was high, but it was suspected that the values of permeability populating the model grid-blocks could have been underestimated.

Therefore, the permeability characterization was varied quantitatively. This geostatistical characterization was kept the same in order to preserve geological trends and heterogeneities that were identified during the geostatistical process. But the entire characterization was multiplied by a factor varying between 1 and 5 that needed to be optimized during the history matching process. Hence, each value of permeability of the geostatistical model was multiplied by the same factor.

Additionally, as mentioned in previous sections, the factor multiplying water influxes at the edge of the model was also optimized. Table 6 presents the known or fixed parameters (and their corresponding values) inside the reservoir model. Likewise, Table 7 presents the 13 unknown or varying parameters that had to be optimized during the history matching.

The tactics used to achieve this history match were:
- Vary horizontal permeability
- Evaluate effects of vertical permeability variability
- Evaluate effects of changes in relative permeability
- Evaluate the effects of injection rate variability of the pseudo-wells at the edge of the model

Table 6: Fixed Parameters During History Matching

Parameter	Units	Value	Source
Formation Properties			
Average Thickness	ft	900	Geostatistical Characterization[2,3]
Initial Pressure	psia	3137	SPE 4083[4], 5536[5], 1259-G[9], 829G[10], 17321[12]
Temperature	F	132	SPE 4083[4], 5536[5], 1259-G[9], 829G[10], 17321[12]
Average Porosity	%	8.5	Geostatistical Characterization[2,3]
Rock Compressibility	1/psi	5.60E-06	Correlation
Fluid Properties			
Oil Gravity	API	41	SPE 17321[12]
Bubble Point Pressure	psi	1850	SPE 4083[4], 5536[5], 1259-G[9], 829G[10], 17321[12]
Gas Gravity	-	0.7	Assumed
Water Density	-	62	Assumed
Water Formation Volume Factor	RB/STB	1.013	Assumed
Water Compressibility	1/psi	2.90E-06	Correlation
Water Viscosity	cp	0.51	SPE 4083[4], 5536[5], 1259-G[9], 829G[10], 17321[12]
Relative Permeability Relationships			
Maximum Corey Kr liquid	-	1	assumed
Well Parameters			
Skin Producers	-	-1	assumed
Skin injectors	-	-1	assumed

SACROC Simulation KS080807

Table 7: Varying parameters during History Matching

Parameter	Units	Minimum	Maximum	Source
Formation Properties				
Permeability Multiplier	-	1	5	Geostatistical Characterization[2,3]
Vertical Permeability Ratio	-	0.01	1	
Relative Permeability Endpoints				
Irreducible Water Saturation	-	0.10	0.22	$KMCO_2$
Residual Oil Saturation	-	0.20	0.30	$KMCO_2$
Maximum Kr water (oil-water system)	-	0.40	1.00	$KMCO_2$
Maximum Kr oil (oil-water system)	-	0.40	0.90	$KMCO_2$
Kro Corey's Exponent (oil-water system)	-	1	4	$KMCO_2$
Krw Corey's Exponent (oil-water system)	-	1	4	$KMCO_2$
Residual gas Saturation	-	0.01	0.1	$KMCO_2$
Maximum Krg (gas-liquid system)	-	0.1	0.7	$KMCO_2$
Krg Corey's Exponent (gas-liquid system)	-	1	4	$KMCO_2$
Krliquid Corey's Exponent (gas-liquid system)	-	1	4	$KMCO_2$
Production Data				
Injection Rate Ratio	-	0.2	1	Calculations

6.3   Results

The dependent (history match) parameters were, for each individual producing well, Gas Production rate, Liquid Production Rate, and Water Production Rate. Average Reservoir Pressure was matched as well. One hundred and ninety eight (198) runs were necessary to achieve a good match and convergence of the parameters.

Figure 43 to Figure 57 present the comparison of the actual versus simulated gas, liquid and water production rates for each individual well located in the center of the model. It is believed boundary conditions were properly reproduced for those wells. History matching results of outer wells are presented in Appendix A. Figure 59 presents the actual versus simulated average reservoir pressure.

The modeling efforts resulted in a very good history match for the center wells in the study area. A good match was also obtained for the outer producing wells, and was achieved due to an optimized boundary effect. A good reservoir pressure match was also obtained, even though the implementation of effluxes would have helped to improve the pressure match between 1972 and 1988.
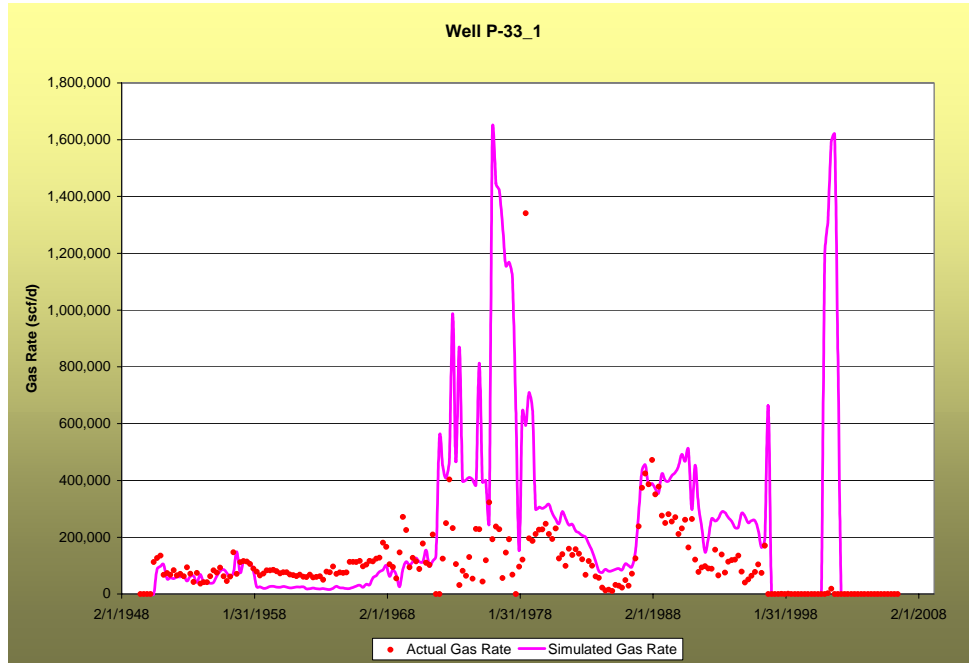
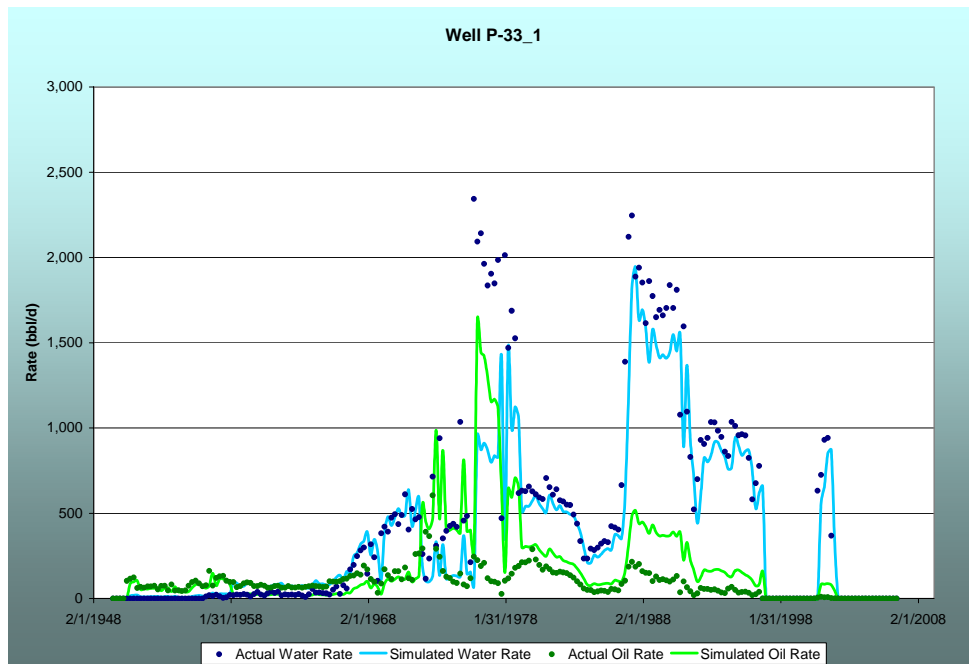**Figure 43: History Match of Gas Rate, Well P-33-1**

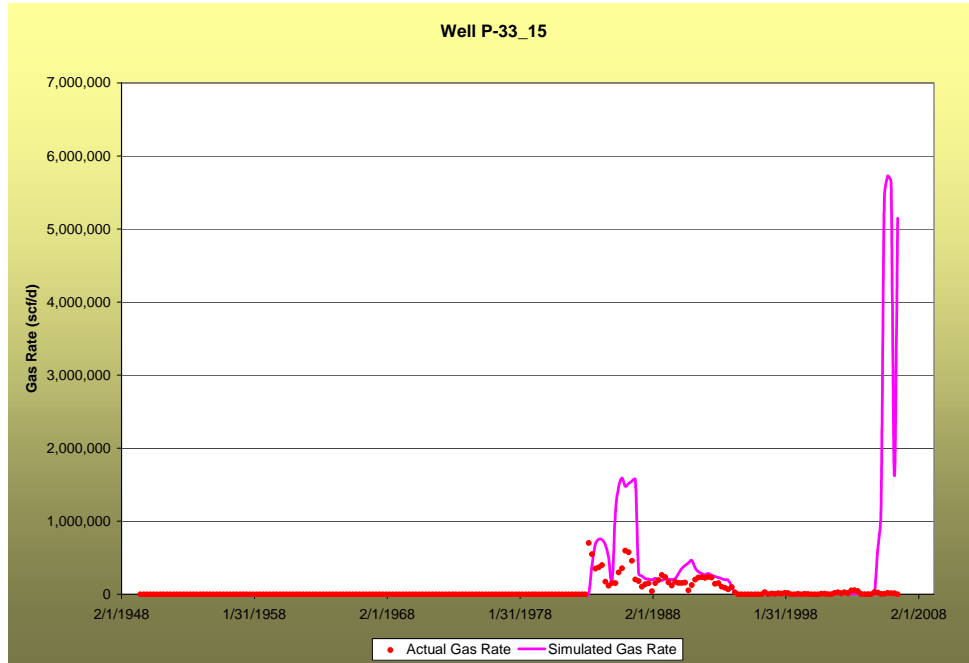**Figure 44: History Match of Oil and Water Rates, Well P-33-1**

45

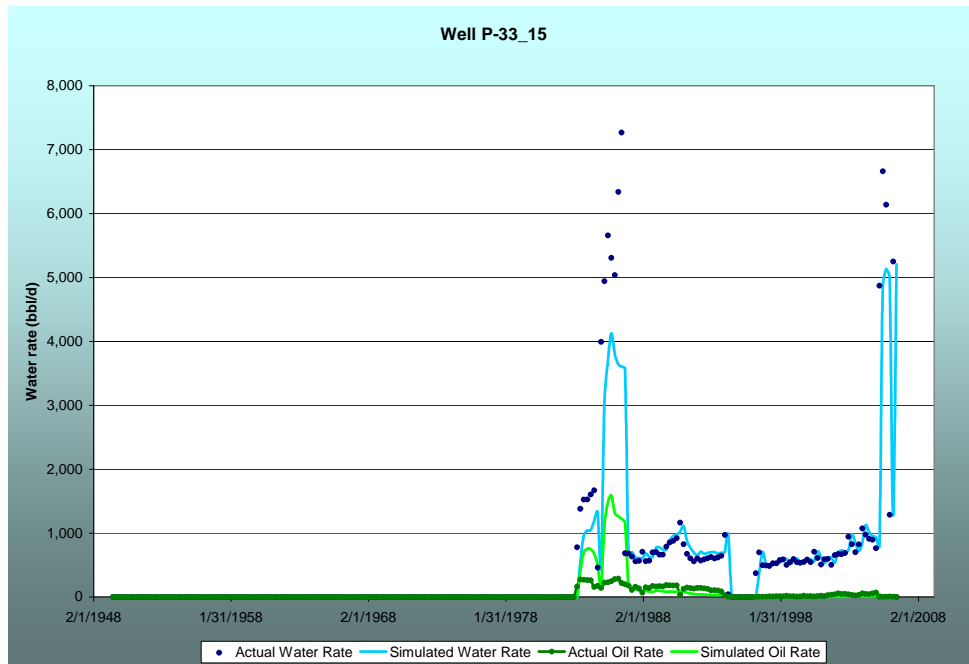**Figure 45: History Match of Gas Rate, Well P-33-15**

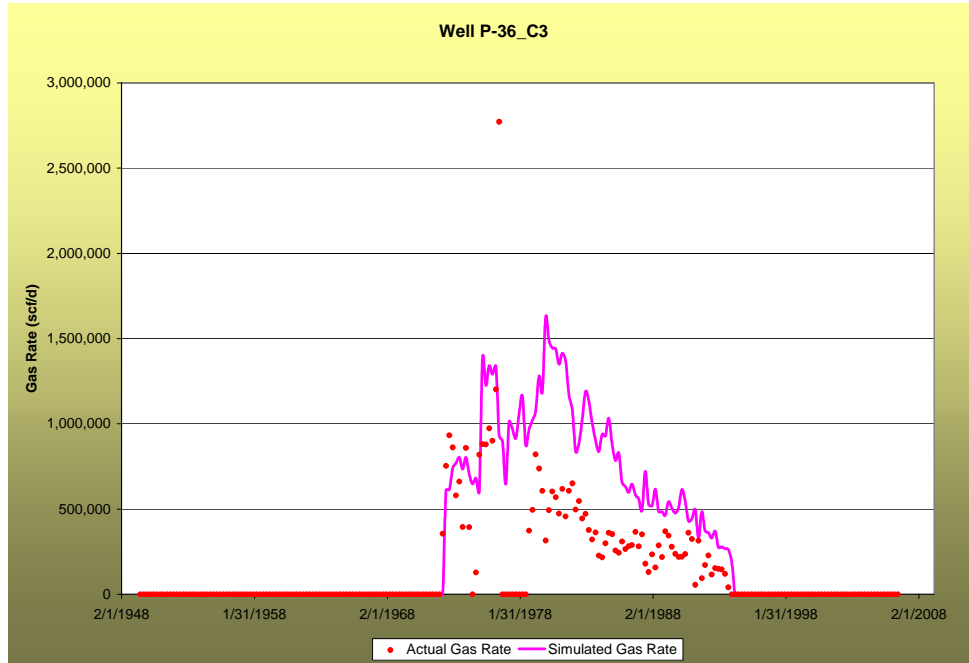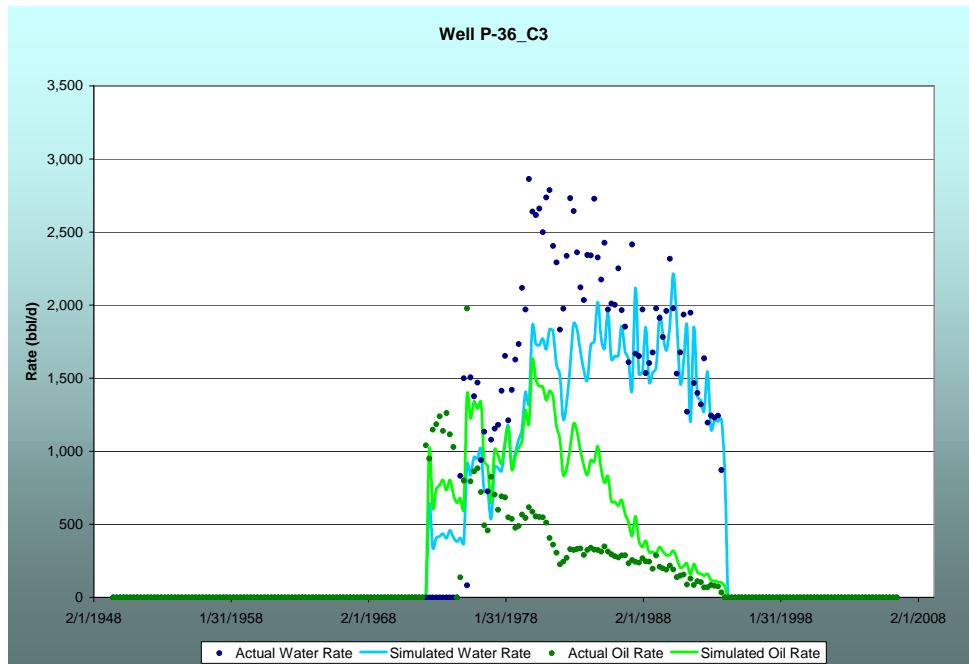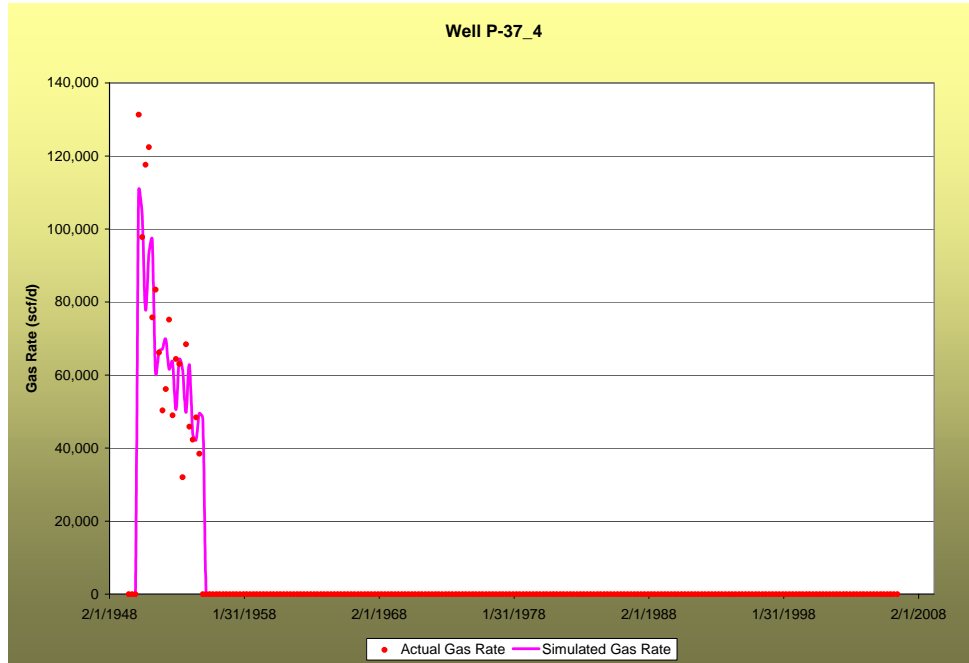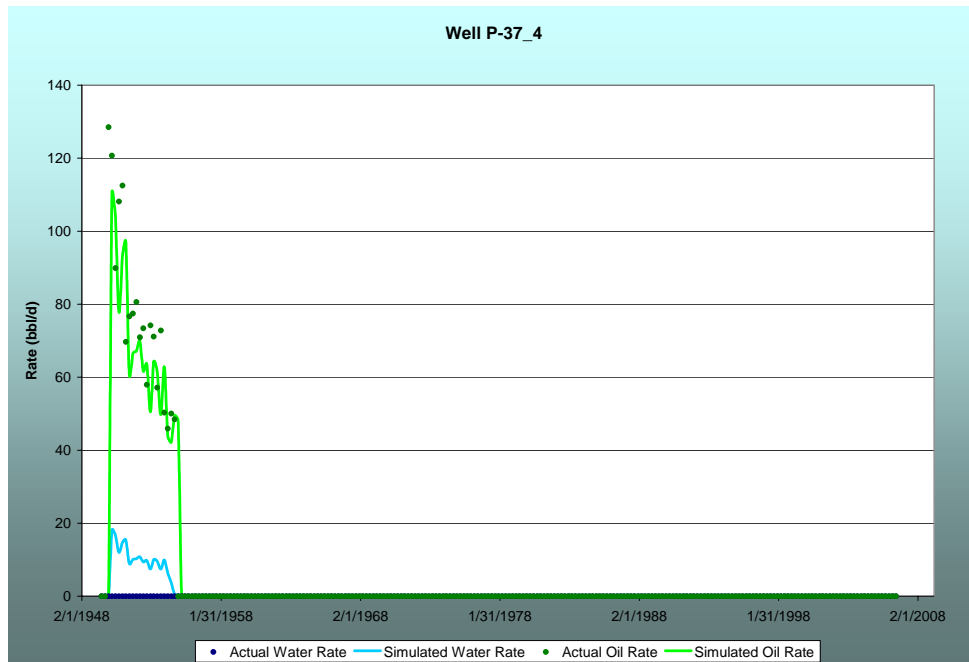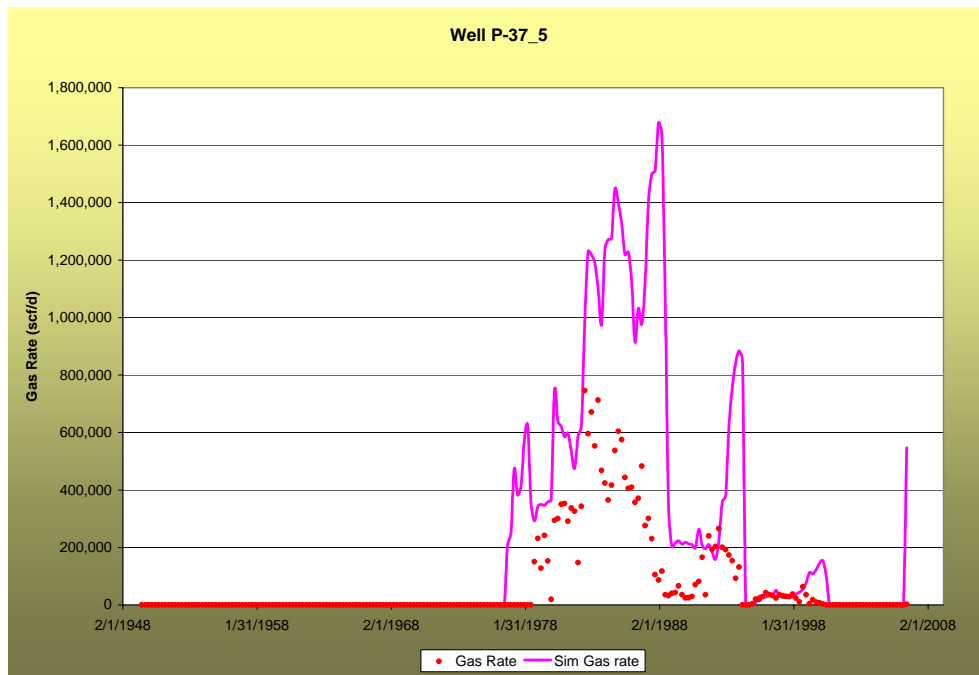**Figure 46: History Match of Oil and Water Rates, Well P-33-15**

46

SACROC Simulation KS080807

Figure 47: History Match of Gas Rate, Well P-36-C3

Figure 48: History Match of Oil and Water Rates, Well P-36-C3

47

Figure 49: History Match of Gas Rate, Well P-37-4

Figure 50: History Match of Oil and Water Rates, Well P-37-4

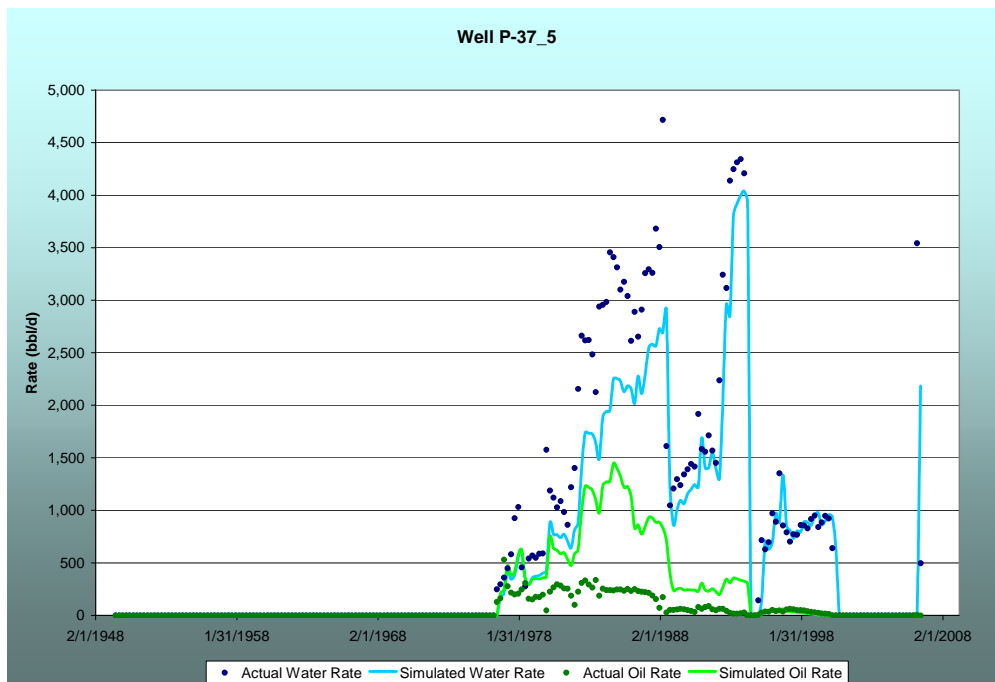48

Figure 51: History Match of Gas Rate, Well P-37-5

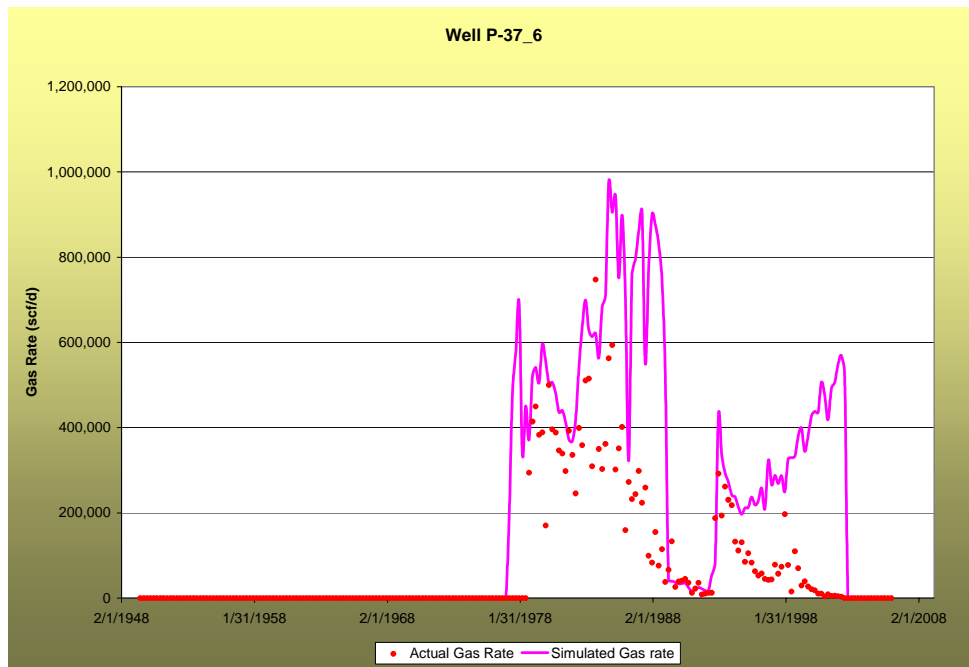**Figure 52: History Match of Oil and Water Rates, Well P-37-5**

49

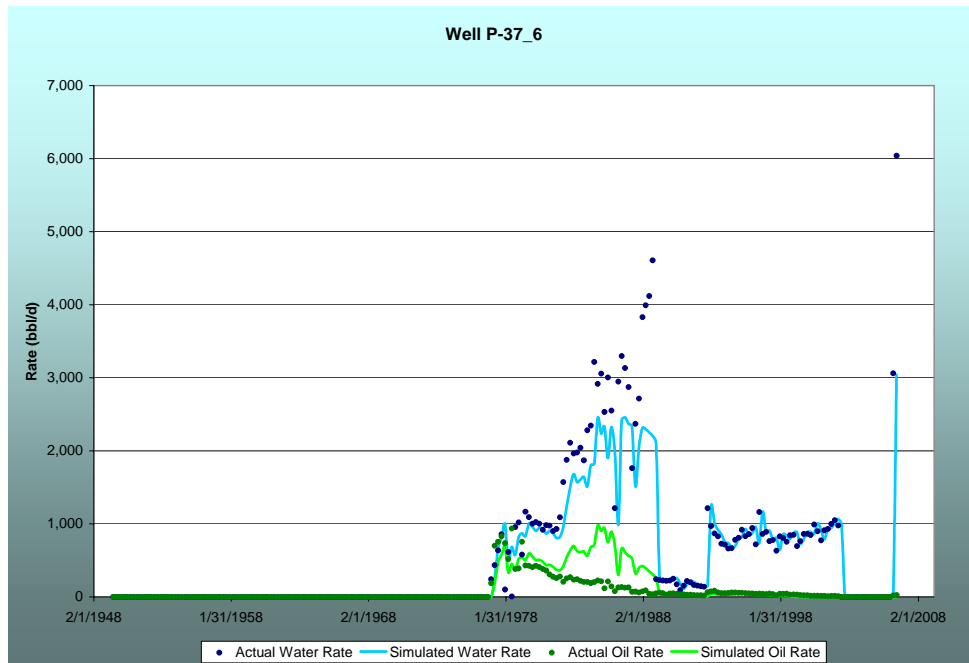**Figure 53: History Match of Gas Rate, Well P-37-6**
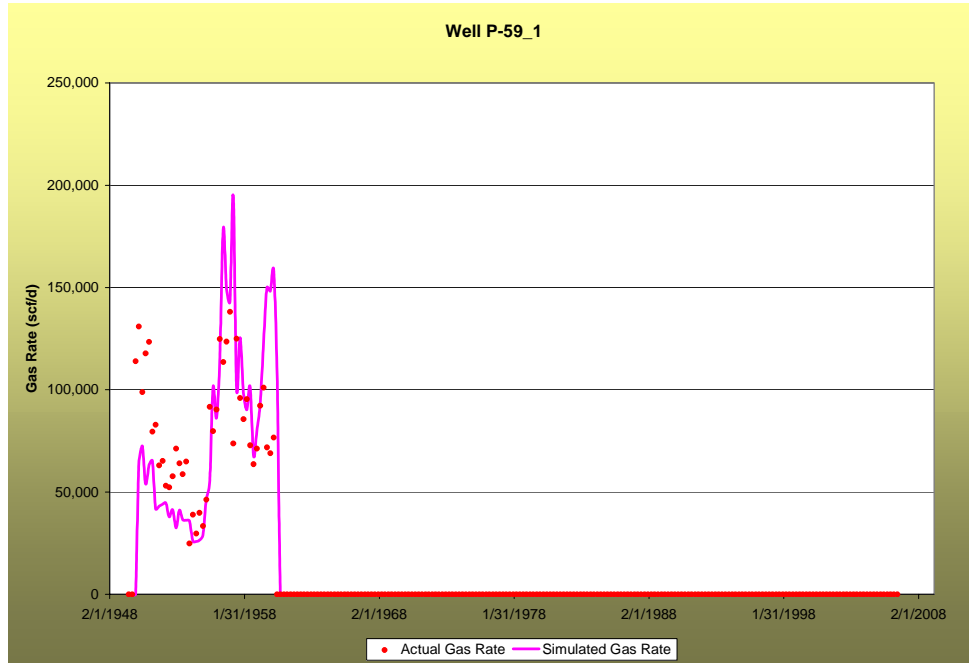

Figure 54: History Match of Oil and Water Rates, Well P-37-6
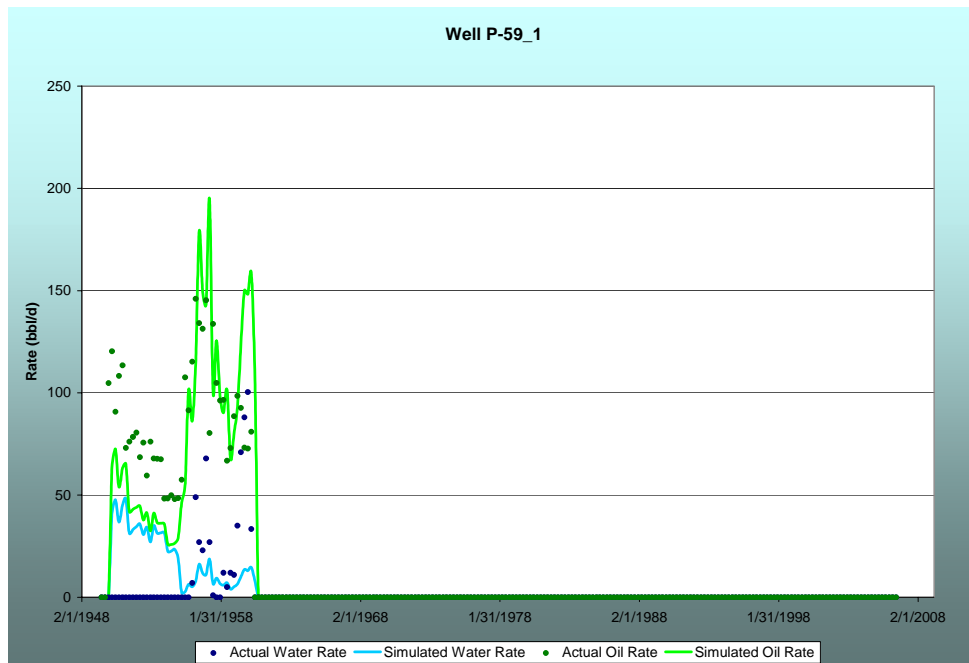
50

Figure 55: History Match of Gas Rate, Well P-59-1

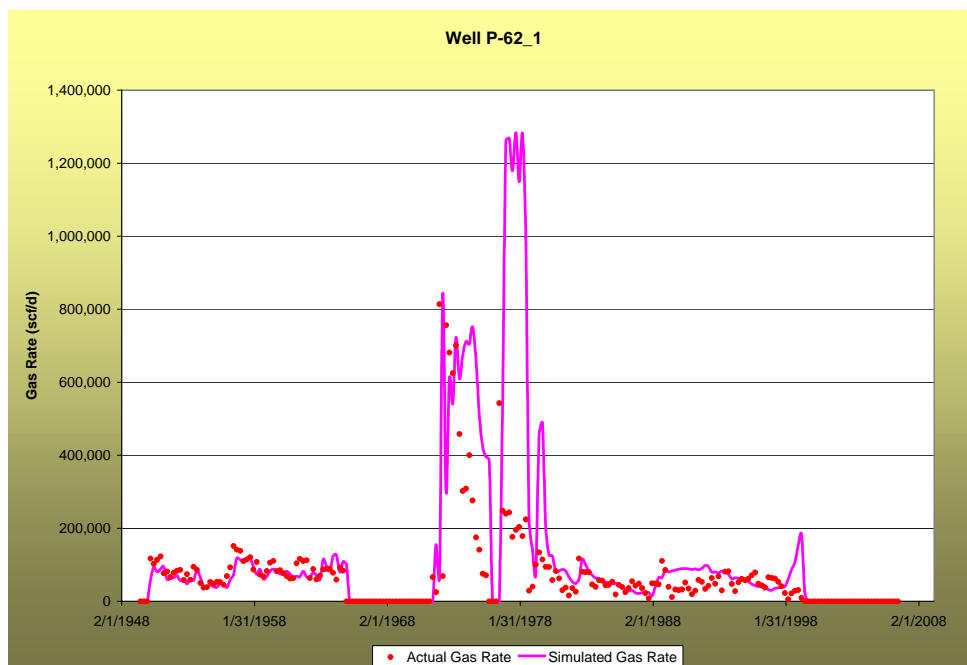**Figure 56: History Match of Oil and Water Rates, Well P-59-1**

51

SACROC Simulation KS080807

Figure 57: History Match of Gas Rate, Well P-62-1
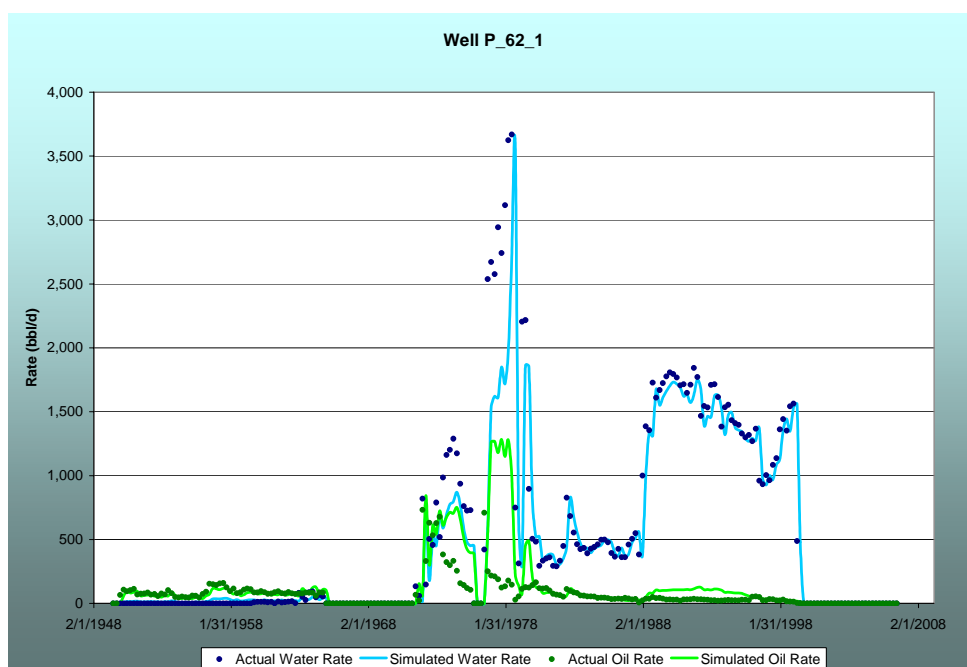
Figure 58: History Match of Oil and Water Rates, Well P-62-1
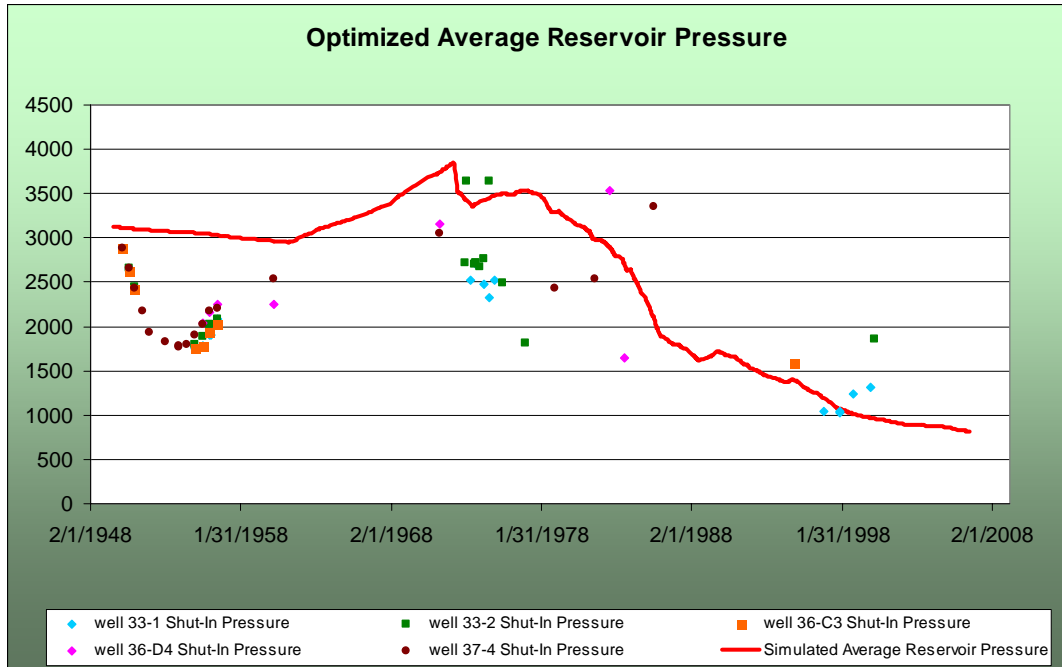
52

SACROC Simulation KS080807

Figure 59: History Match of Average Reservoir Pressure

Note: actual pressure measurements were originally Shut-in pressures. Peaceman's correction was applied to those pressures to be properly compared to Average Reservoir pressure.

Overall, the match of liquid production rate was very well achieved. Matches of oil, gas and water production rates were satisfactory to very good. The average reservoir pressure match is also of good quality although it is slightly high between 1972 and 1988. Oil cut and gas production rate could be improved for wells 36-C3, 37-5, 37-6 and 59-1. Wells 36-C3, 37-5 and 37-6 produced too much oil compared to actual data. Since the reservoir pressure is above the bubble point pressure, too much gas is also produced (GOR=1,000 scf/bbl). Well 59-1 doesn't produce enough oil compared to actual data, hence not enough gas. Wells 36-C3, 37-5 and 37-6 are located in areas where permeability and porosity are particularly heterogeneous from one layer to another. Well 59-1 is located in a high porosity zone.

As explained in Section 5.1, only one rock type (one set of relative permeability curves for oil-water and gas-liquid) was used in this model. The match of production rates for all wells could probably be improved if several rock types were defined inside the model, so that each rock type could be assigned different relative permeability curves.

Additionally, only water influxes have been simulated at the edge of the model. Water efflux and oil/gas fluxes have not been simulated. The match of the average reservoir pressure

SACROC Simulation KS080807

could probably be improved if flux for all phases were implemented, allowing some efflux to occur, hence decreasing the average reservoir pressure.

The history matching process gave the following values for the optimized parameters:

Table 8: Optimized Parameters Obtained for the Match

Parameter	Units	Minimum	Maximum	Optimized	Source
Formation Properties					
Permeability Multiplier	-	0.5	5	3	Geostatistical Characterization[2,3]
Vertical Permeability Ratio	-	0.01	1	0.9	
Relative Permeability Endpoints					
Irreducible Water Saturation	-	0.10	0.22	0.21	$KMCO_2$
Residual Oil Saturation	-	0.20	0.30	0.24	$KMCO_2$
Maximum Kr water (oil-water system)	-	0.40	1.00	0.85	$KMCO_2$
Maximum Kr oil (oil-water system)	-	0.40	0.90	0.86	$KMCO_2$
Kro Corey's Exponent (oil-water system)	-	1	4	3.5	$KMCO_2$
Krw Corey's Exponent (oil-water system)	-	1	4	1.2	$KMCO_2$
Residual gas Saturation	-	0.01	0.1	0.09	$KMCO_2$
Maximum Krg (gas-liquid system)	-	0.1	0.7	0.66	$KMCO_2$
Krg Corey's Exponent (gas-liquid system)	-	1	4	1.7	$KMCO_2$
Krliquid Corey's Exponent (gas-liquid system)	-	1	4	2	$KMCO_2$
Production Data					
Injection Rate Ratio	-	0.2	1	0.8	Calculations

Average porosity from the geostatistical characterization was 8.5%. Values ranging from 7 to 10% were found in the literature. Average permeability defined by history matching is 2.74 mD multiplied by a factor of 3, so 8.22 mD. Values of average permeability found in the literature are around 15 mD. The injection ratio defining water influxes converged at 0.8. This is not far from the predicted injection rate. Simulated oil and water relative permeability curves are compared to actual data provided by $KMCO_2$ in Figure 60. As seen, the simulated curves perfectly match the real data. Figure 61 presents the simulated relative permeability curves derived from the optimization process for gas and liquid.
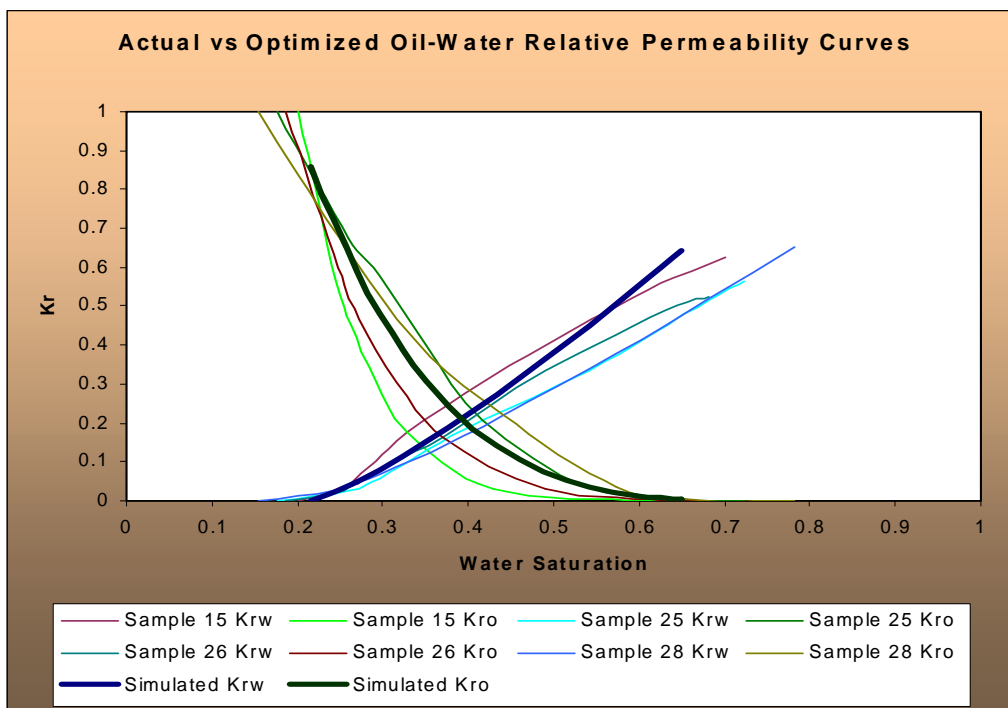
Advanced Resources
International, Inc.

SACROC Simulation KS080807

Figure 60: Optimized Oil-Water Relative Permeability Curves
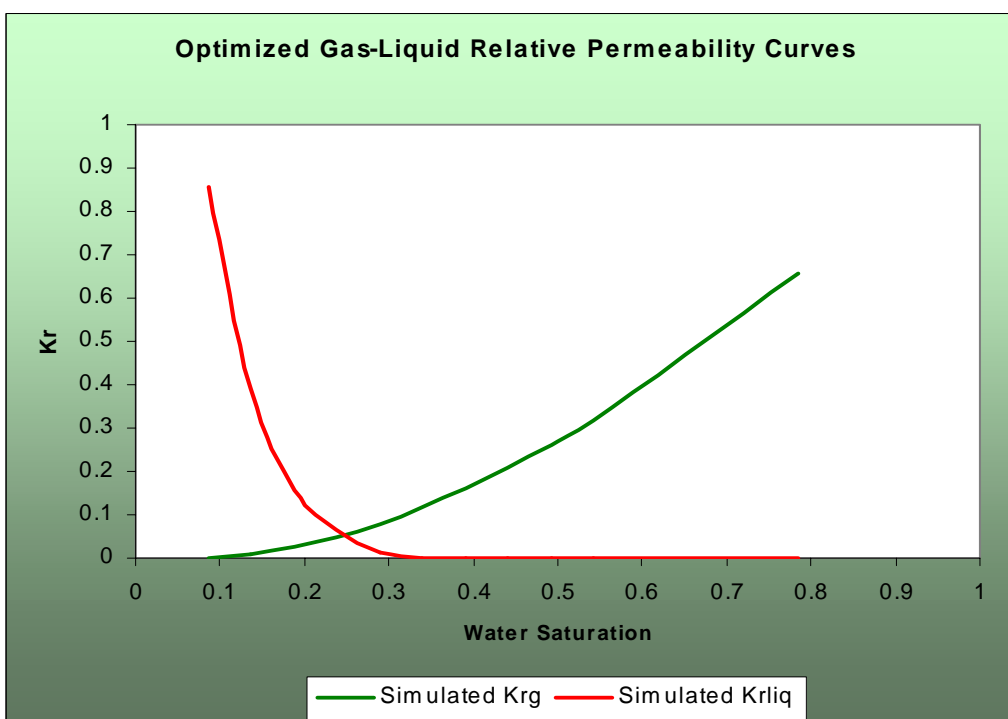

Figure 61: Optimized Gas-Liquid Relative Permeability Curves

An illustration of how the Total Error Function decreases as a function of the number of runs is presented in Figure 62. Once proper boundary conditions were determined for the model, 198 runs were necessary to achieve good history matching. Two examples of converging parameters are presented in Figure 63 and Figure 64.
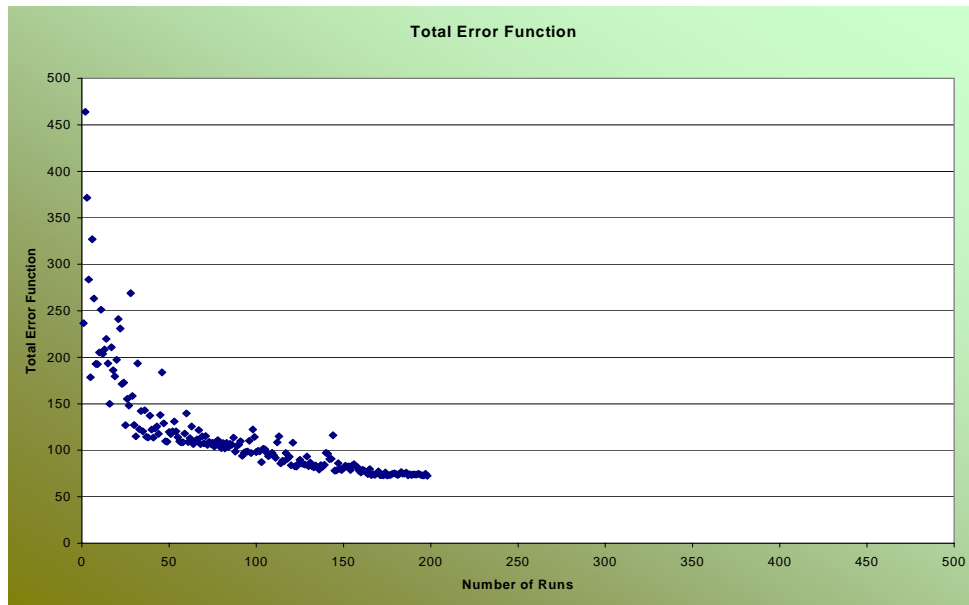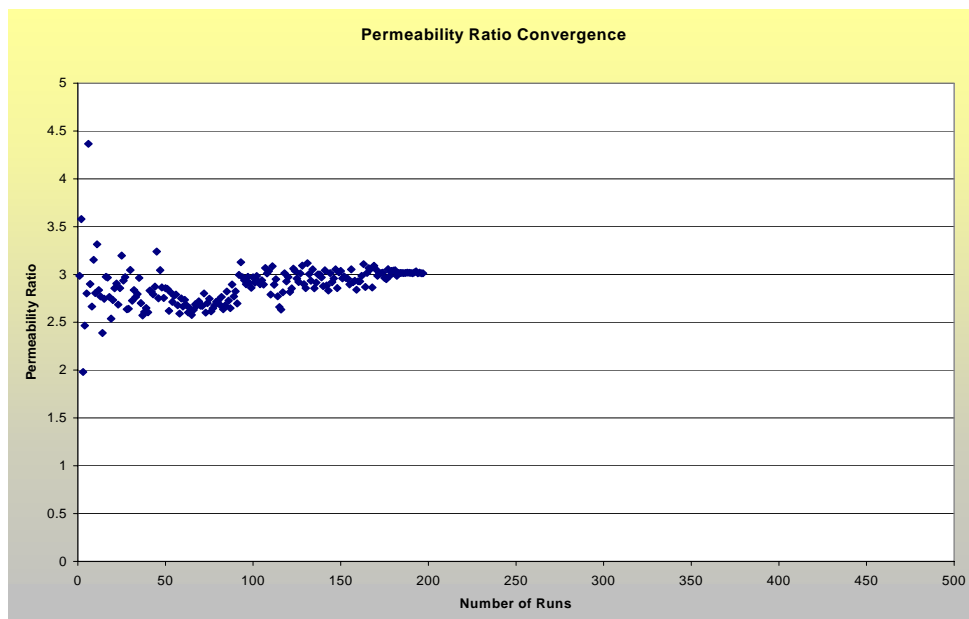

Figure 62: Total Error Function vs. Number of Runs

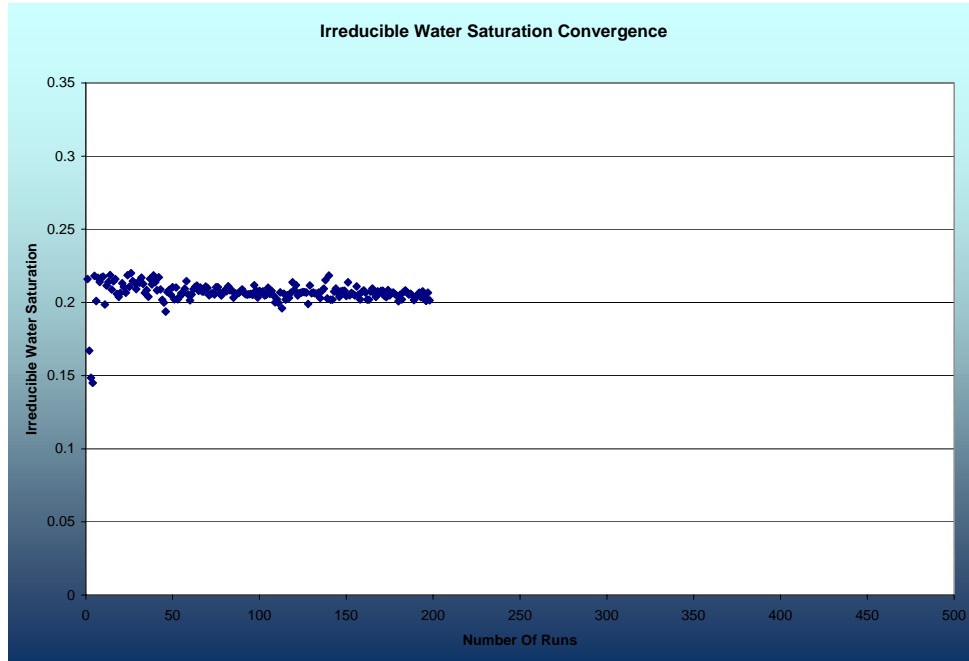**Figure 63: Convergence of the Permeability Multiplier**

56

Figure 64: Irreducible Water Saturation Convergence

A 3D view of the residual oil saturation at the end of the producing period is presented in Figure 65. Based on those irreducible water and residual oil saturations, the recovery factor from the reservoir model is equal to 46%. In published literature[12] a maximum of 39% was reported for the entire SACROC unit. The recovery factor is likely overestimated in our model due to the injection of miscible gas in the black-oil model, when immiscibility injection should occur. However, this simple black oil model was accurate enough to understand the reservoir behavior of SACROC Unit, Canyon Reef Formation. Better understanding of water and gas breakthrough could be more accurately modeled using a compositional model, based on the knowledge acquired in this study. A compositional model could probably give more accurate answers regarding the CO_2 injection dynamic.
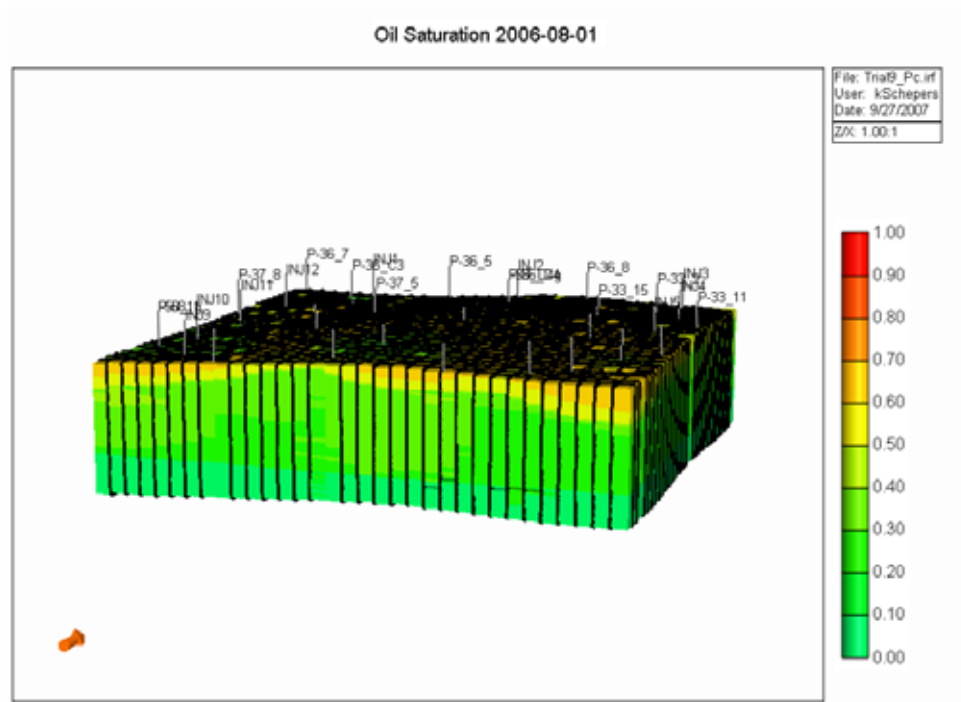
Figure 65: 3D View of Residual Oil Saturation at the End of the Simulation

7.0   Conclusions

1. An assisted history match was achieved using a global optimization method (evolutionary algorithms). This history match, in which several results were produced, was based on the matching of oil, gas and water production rates, and the average reservoir pressure. The match was accomplished by manipulating 13 uncertain design parameters which included two formation properties, other ten variables related with the corresponding relative permeability curves, and one variable linked to the reservoir production.

2. Evolutionary algorithms are widely accepted as robust optimization methodologies that can handle a large amount of input design parameters. And, in this work, they were successfully applied for history matching complex reservoir performance drivers thanks to their capabilities to explore an enormous range of parameter combinations and produce lots of results related to the reservoir performance.

3. History match results confirmed that the 3D reservoir models of porosity and permeability constructed applying the combined reservoir characterization approach (advanced pattern recognition techniques and geostatistical algorithms) were legitimate representations of the spatial distribution of these parameters in the reservoir.

4. The assisted history match procedure confirmed initial assumptions that the developed porosity model was highly trustworthy, whereas the permeability model, despite of capturing correctly geological trends and heterogeneities of Canyon Reef reservoir (SACROC field) presented slightly underestimated values.

5. The modeling efforts resulted in a very good history match for the center wells in the study area. A good match was also achieved for the outer producing wells and the average reservoir pressure. These achievements were thanks to the setting up of proper boundary conditions that described the flow behavior at the boundary of the analyzed region.

6. Overall, the match of liquid production rate was very well achieved. Matches of oil, gas and water production rates were from satisfactory to very good. The average reservoir pressure match was also of good quality although slightly high between years 1972 and 1988.

7. Application of several techniques for estimating water influxes allowed the definition of proper boundary conditions for the simulation model. The adopted influxes techniques were very important to achieve very good history match results.

8. The implementation of twelve pseudo-injectors at the boundaries of the study area reproduced accurately water influxes at the edge of the model. The use of a multiplicative factor for water influxes at the edge of the model was determinant in this process. This factor, varied between 0.2 and 1, converged at 0.8 which was close to calculated injection rates using differential water volume technique (Method 2).

9. The simple black oil model developed here was sufficient to capture the reservoir behavior of SACROC Unit, Canyon Reef Formation:

   - Simulated oil-water relative permeability curves match perfectly actual core measurements
   - The recovery factor from the simulated reservoir model is equal to 46%; a maximum of 39% was mentioned in literature.

59

10. The recovery factor was probably overestimated due to the injection of miscible gas in our black-oil model, when immiscibility injection should have occurred. Better understanding of water and gas breakthrough could be more accurately modeled using a compositional model.

11. Based on the knowledge acquired in this study, most of the discrepancies reported here could be alleviated or completely removed with the use of a compositional model, and the extension of the reservoir model to a larger drainage area.

12. The addition of optimization methods (for assisted history matching) to the combined soft-computing/geostatistical approach (utilized for reservoir characterization purposes) constitutes a powerful triad of mathematical techniques ideally suited for addressing reservoir integrated studies, with the capacity of facing these complex tasks more rapidly and efficiently than using traditional methodologies.

8.0 References

1. Reeves, S.R., Mohaghegh, S.D., Fairborn, J.W., and Luca, G.; "Feasibility Assessment of a New Approach for Integrating Multiscale Data for High-Resolution Reservoir Characterization", SPE 77795, presented at the SPE Annual Technical Conference and Exhibition, San Antonio, Texas, September 29 - October 2, 2002.
2. González, R.J., Reeves, S.R., and Eslinger, E.; "Predicting Porosity and Permeability for the Canyon Formation, SACROC Unit (Kelly-Snyder Field), Using the Geologic Analysis via Maximum Likelihood System", Topical Report prepared for U. S. Department of Energy, Contract Number DE-FC26-04NT15514, September, 2007.
3. González, R.J., Reeves, S.R., and Eslinger, E.; "Geostatistical Reservoir Characterization of the Canyon Formation, SACROC Unit, Permain Basin", Topical Report for U. S. Department of Energy, Contract Number DE-FC26-04NT15514, September, 2007.
4. Dicharry, R.M., Perryman, T.L., Ronquille, J.D.; "Evaluation and Design of a CO_2 Miscible Flood Project – SACROC Unit, Kelly-Snyder Field", SPE 4083, prepared for the Journal of Petroleum Technology, pg. 1309 - 1318, November, 1973.
5. Brummett, W.M., Jr., Emanuel, A.S., Ronquille, J.D.; "Reservoir Description by Simulation at SACROC – A Case History", SPE 5536, prepared for the Journal of Petroleum Technology, pg. 1241 – 1255, October, 1976.
6. Reeves, S.R.; "Demonstration of a Novel, Integrated, Multi-Scale Procedure for High-Resolution 3D Reservoir Characterization and Improved CO_2-EOR/Sequestration Management, SACROC Unit", prepared for U. S. Department of Energy, Solicitation Number DE-PS26-04NT15450-2C, February 10, 2004.
7. Hawkins, J.T., Benvegnu, A.J., Wingate, T.P., McKamie, J.D., Pickard, C.D., Altum, J.T.; "SACROC Unit CO_2 Flood: Multidisciplinary Team Improves Reservoir Management and Decreases Operating Costs", SPE 35359, presented at the 1996 SPE/DOE Symposium on Improved Oil Recovery, Tulsa, OK, April 21-24, 1996.
8. Remy, N.: "SGEMS: The Stanford Geostatistical Earth Modeling Software. User's Manual", http://sgems.sourceforge.net/doc/sgems_manual.pdf, May 2004.
9. Allen, H.H., Thomas, J.B.; "Pressure Maintenance in SACROC Unit Operations", SPE 1259-G, presented at the Permian Basin Section Oil Recovery Conference, Midland, TX, May 7-8, 1959.
10. Allen, H.H., LaRue, C.R.; "SACROC Unit Operations", SPE 829-G, presented at Permian Basin Oil Recovery Conference, Midland, TX, April 18-19, 1957.
11. Graue, D. J., Blevins, T.R.; "SACROC Tertiary CO_2 Pilot Project", SPE 7090, presented at the Fifth Symposium on Improved Methods for Oil Recovery of the Society of Petroleum Engineers of AIME, Tulsa, OK, April 16-19, 1978.
12. Langston, M.V., Hoadley, S.F., Young, D.N.; "Definitive CO_2 Flooding Response in the SACROC Unit", SPE 17321, prepared for the SPE/DOE Enhanced Oil Recovery Symposium, Tulsa, OK, April 17-20, 1988.
13. Kane, A.V.; "Performance Review of a Large-Scale CO_2-WAG Enhanced Recovery Project, SACROC Unit, Kelly-Snyder Field", SPE 7091, presented at the SPE/AIME

Fifth Symposium on Improved Methods for Oil Recovery, Tulsa, OK, April 16-19, 1978.

14. "IMEX. Advanced Oil/Gas Reservoir Simulator. 2007 User's Guide", Computer Modelling Group Ltd., 2007.
15. Ramey, H.J. Jr.; "Rapid Methods for Estimating Reservoir Compressibilities," JPT (April 1964) 447; Trans., AIME, 231.
16. McCain, W.D. Jr; "Reservoir-Fluid Property Correlations - State of the Art", SPERE (May 1991) 266.
17. Standing, M.B. and Katz, D.L.; "Density of Natural Gases", Trans. AIME (1942) 146, 140-149.
18. Dodson C.R. and Standing, M.B.; "Pressure, Volume, Temperature and Solubility Relations for Natural Gas-Water Mixtures", Drill. & Prod. Prac. (1944) 173-179.
19. Earlougher, R.C., Jr.; "Advances in Well Test Analysis", SPE Monograph Series, SPE, Richardson, Texas (1977) 5.
20. Rowe, A.M. Jr. and Chou, J.C.S.; "Pressure-Volume-Temperature-Concentration Relation of Aqueous NaCl Solutions," J. Chem. Eng. Data (1970), 15, 61.
21. Matthews, C.S. and Russell, D.G.; "Pressure Buildup and Flow Tests in Wells", Monograph Series, SPE, Dallas (1967) 1, Appendix G.
22. Standing, M.B.; "Volumetric and Phase Behavior of Oil Field Hydrocarbon Systems", SPE, Richardson, TX, 1981.
23. Beggs, H.D. and Robinson J.R.; "Estimating the Viscosity of Crude Oil Systems", J. Pet. Tech. (Sept. 1975) 1140-41.
24. Holtz, M.H., Smith, R.C., McPherson, B. and Han, W.C.; "Subsurface Site Characterization Methodology; Example from Pennsylvanian Carbonate Reef, West Texas", prepared for DOE Southwest Partnership Pilot at SACROC and Claytonville oil field sites, February 16, 2006.
25. Carr, N.L., Kobayashi, R., and Burrows, D.B.; "Viscosity of the Hydrocarbon Gases Under Pressure," Trans., AIME (1954) 201, 264-78.
26. Van Everdingen, A.F., Timmerman, E.H., and McMahon, J.J.; "Application of the Material Balance Equation to a Partial Water-Drive Reservoir", Trans., AIME (1953) 198, 51-60.
27. Oudinot, A., Sultana, A., Gonzalez, R.J., Reeves, S.R., and Wörmann, M.; Development of Optimized History-Matched Models for Coalbed Methane Reservoirs.
28. Baeck, T., Fogel, D.B., Michalewicz, Z.; "Handbook of Evolutionary Computation"; Oxford University Press, New York, Oxford, 1997.
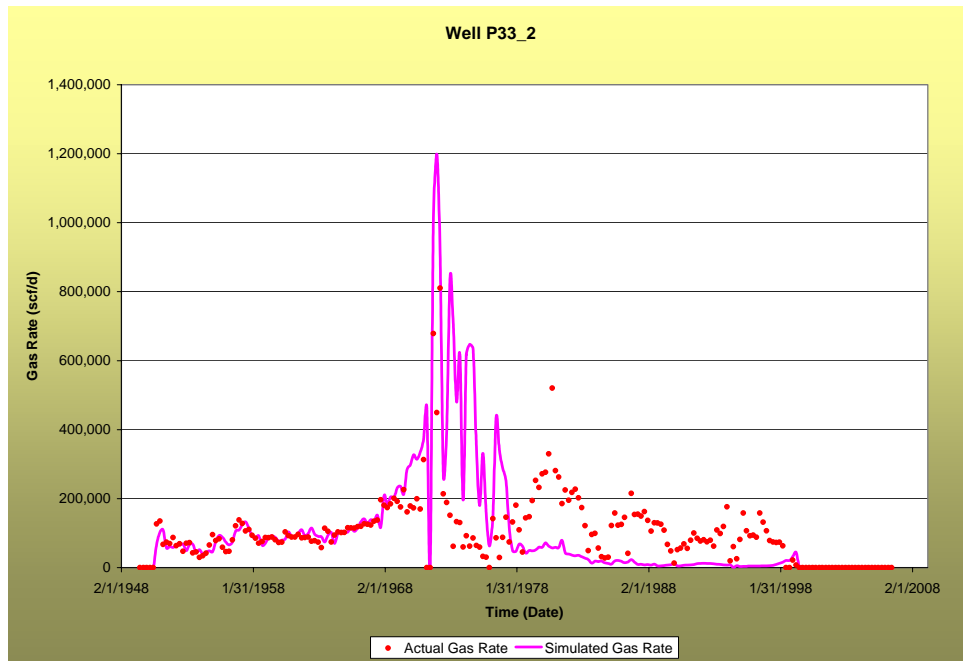
Appendix A: History Matching Results – Outer Wells

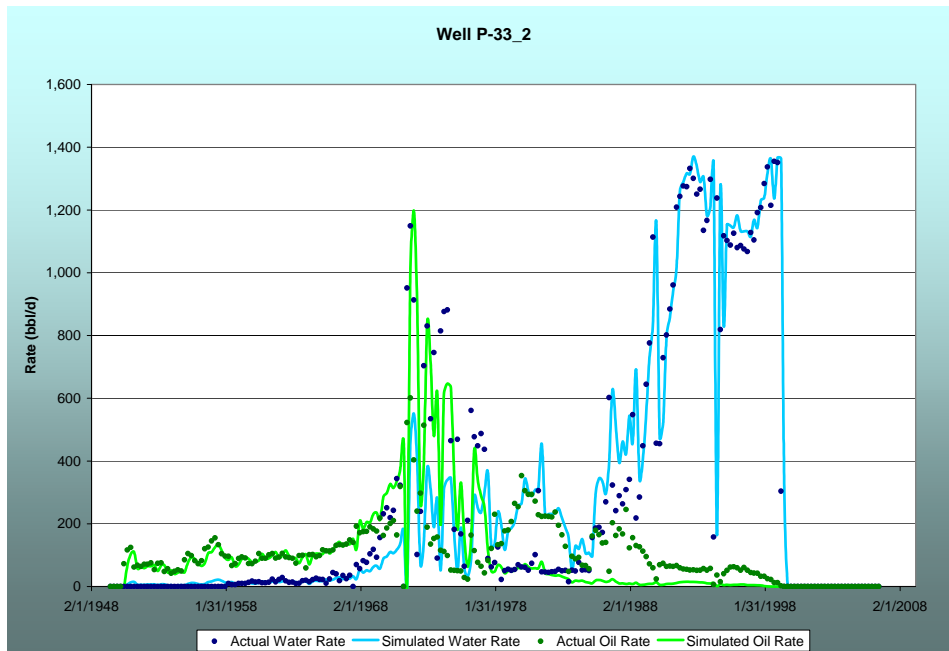**Figure A-1: History Match of Gas Rate, Well P-33-2**

Figure A-2: History Match of Oil and Water Rates, Well P-33-2
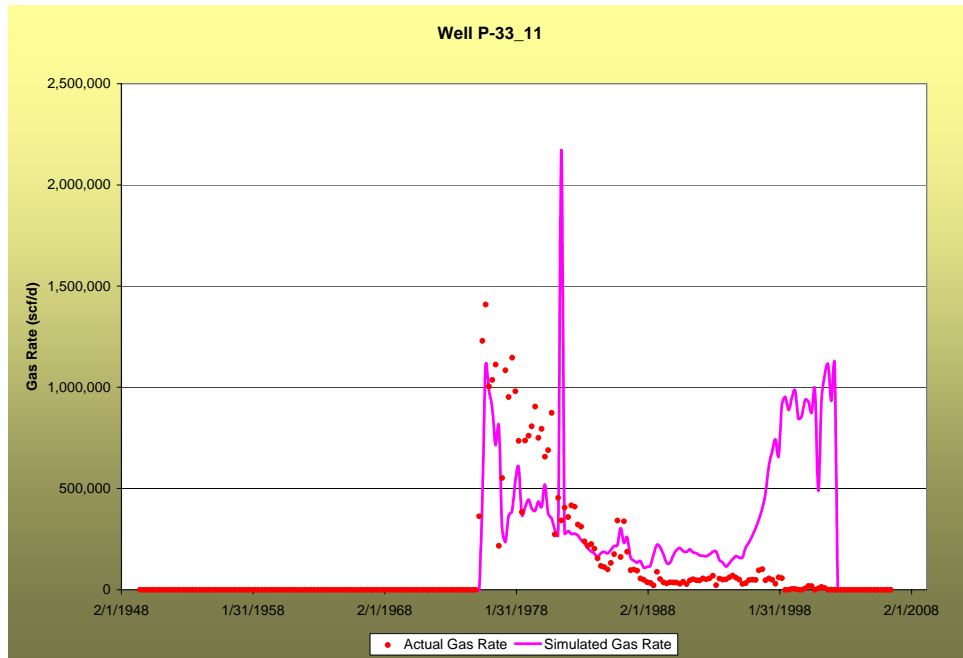
A-1

SACROC Simulation KS080807

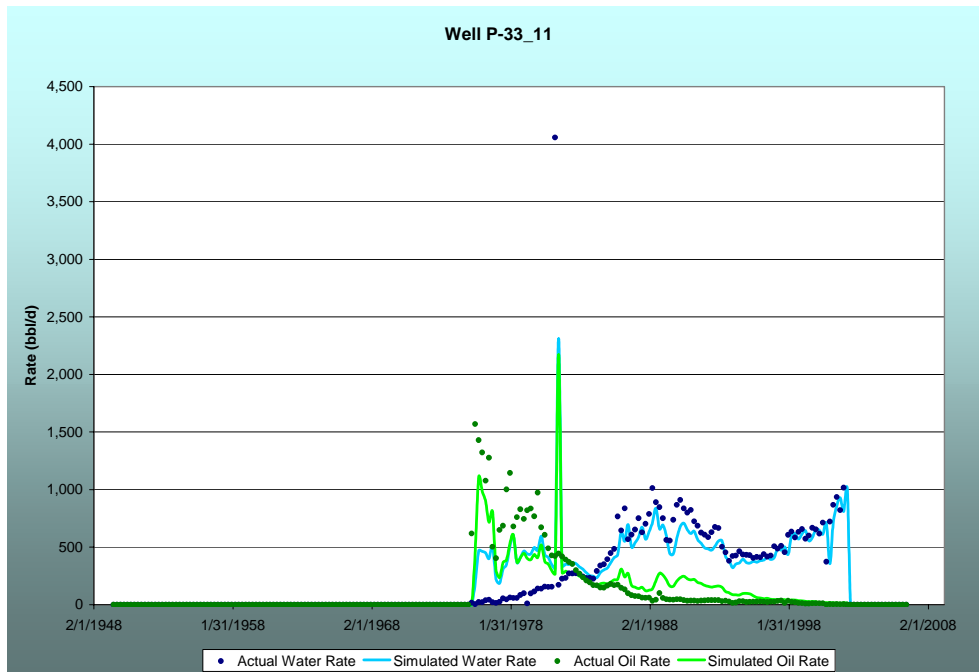**Figure A-3: History Match of Gas Rate, Well P-33-11**

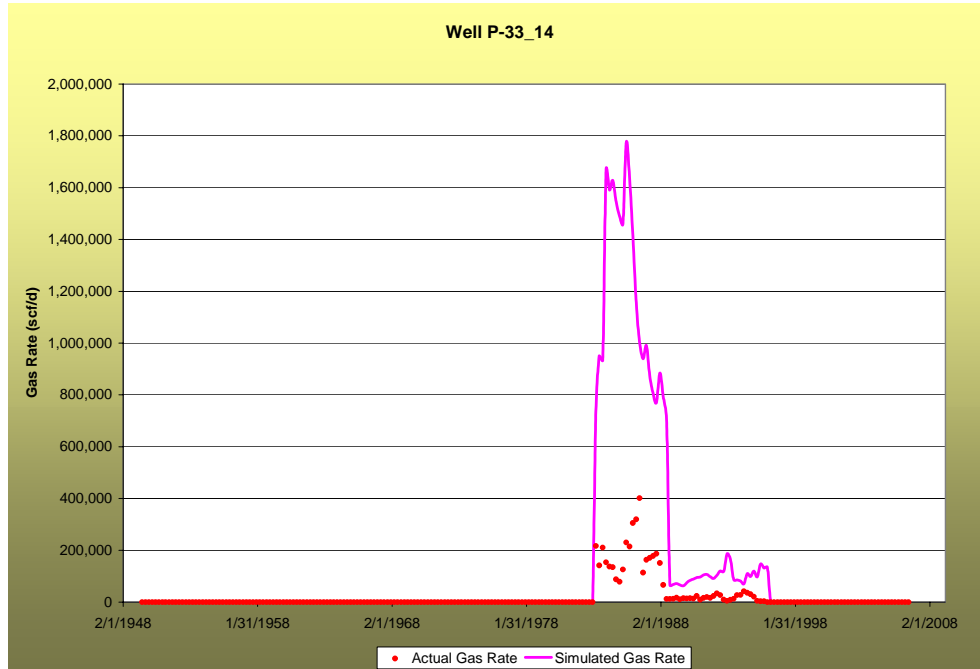**Figure A-4: History Match of Oil and Water Rates, Well P-33-11**

A-2

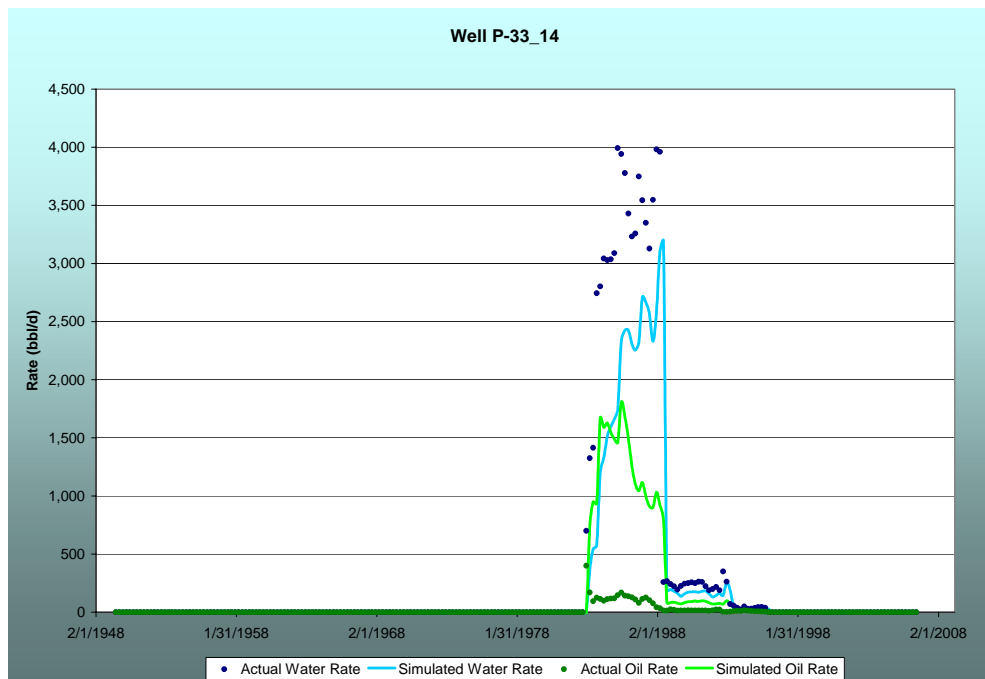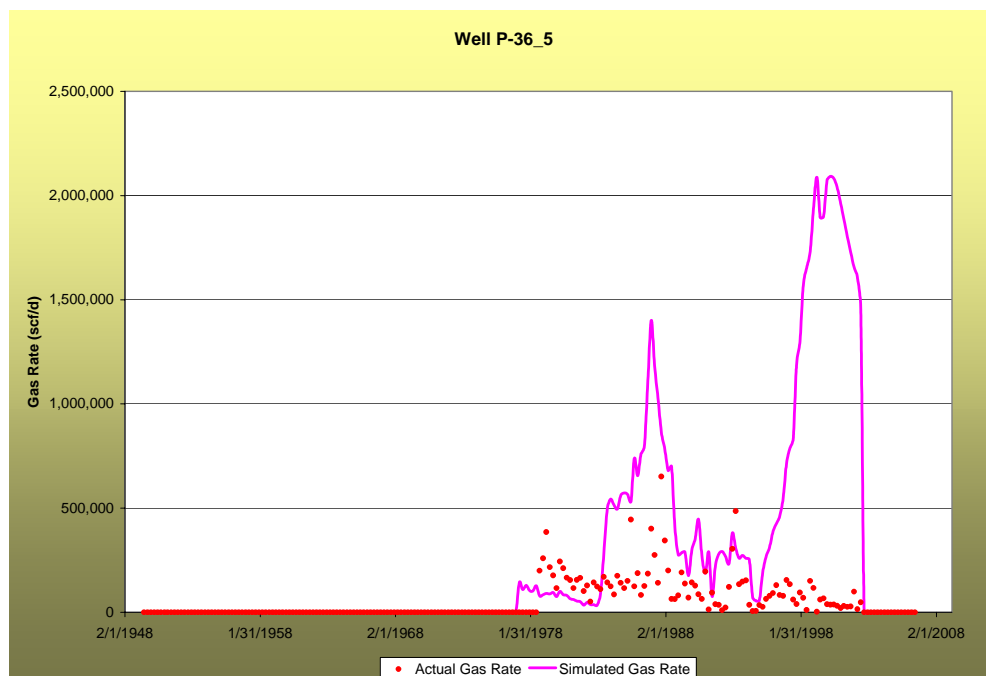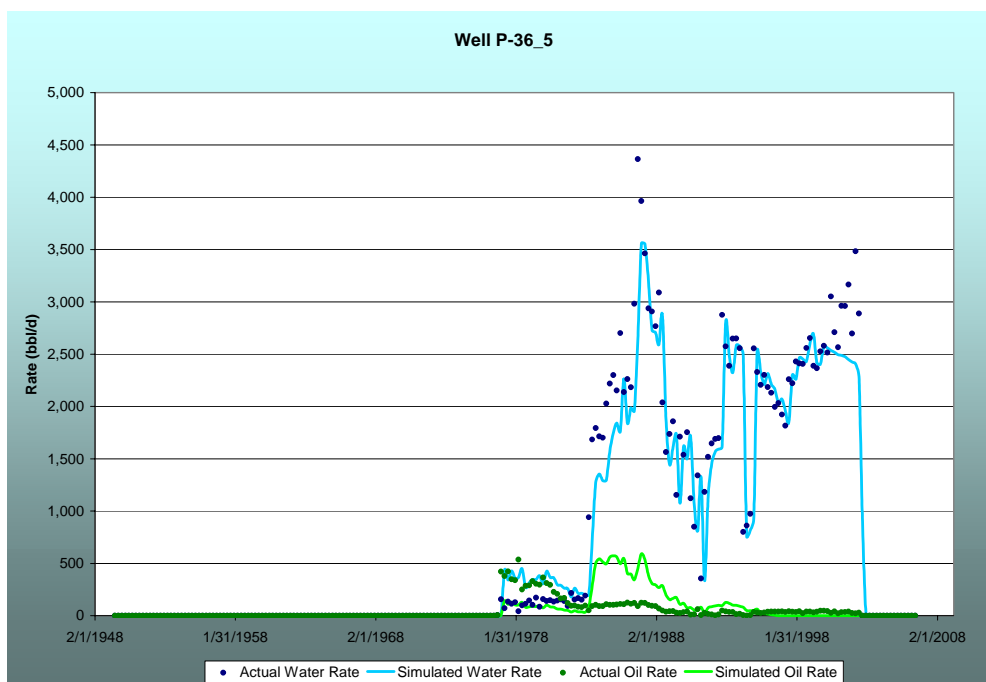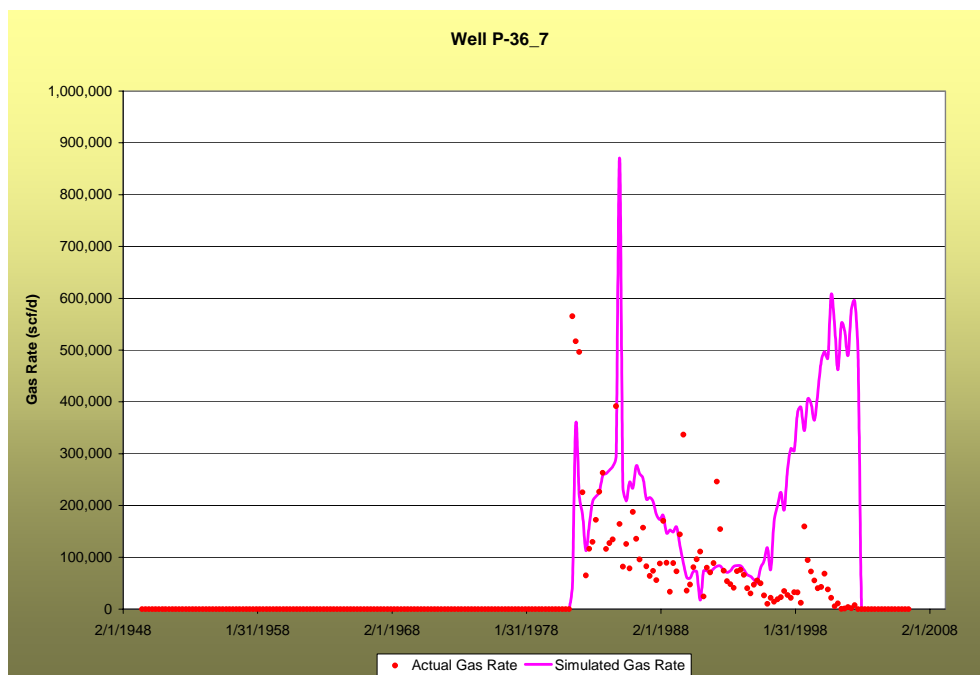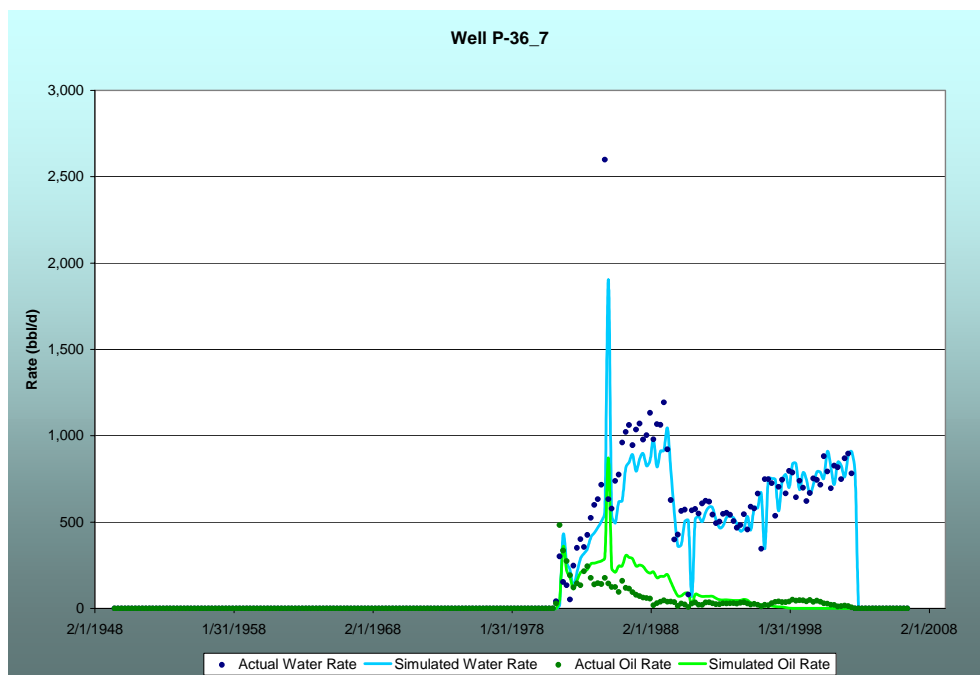**Figure A-5: History Match of Gas Rate, Well P-33-14**

Figure A-6: History Match of Oil and Water Rates, Well P-33-14

A-3

Figure A-7: History Match of Gas Rate, Well P-36-5
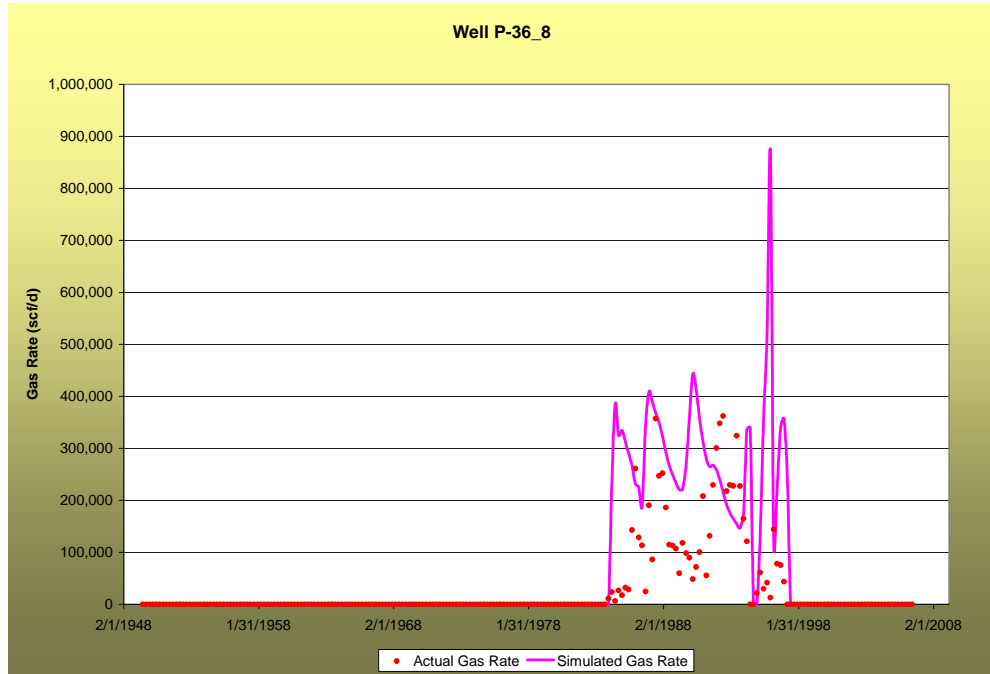

Figure A-8: History Match of Oil and Water Rates, Well P-36-5
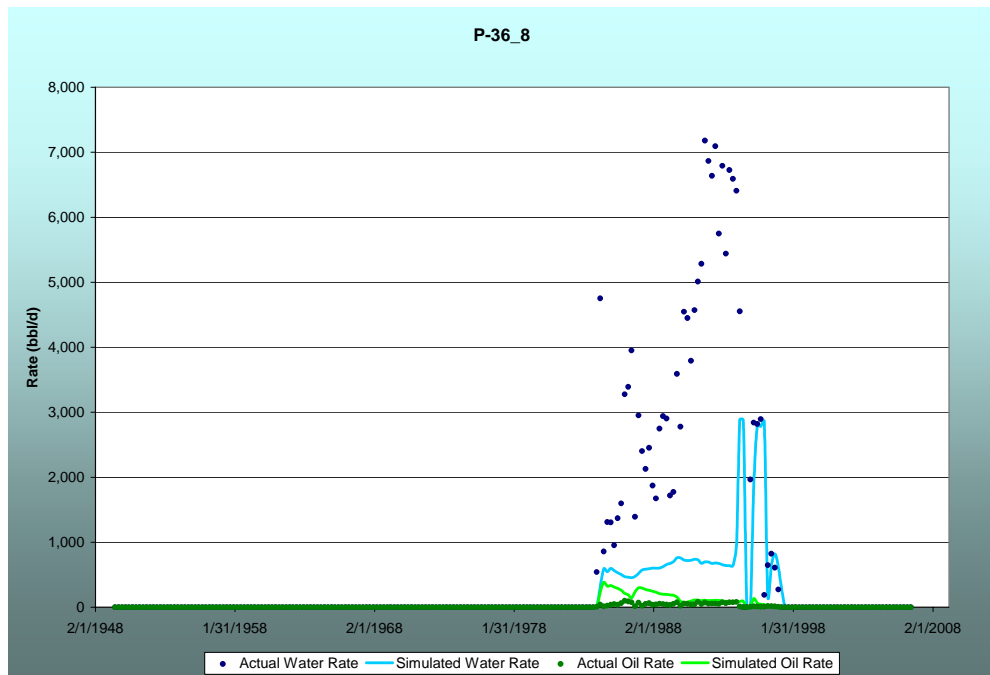
A-4

Figure A-9: History Match of Gas Rate, Well P-36-7

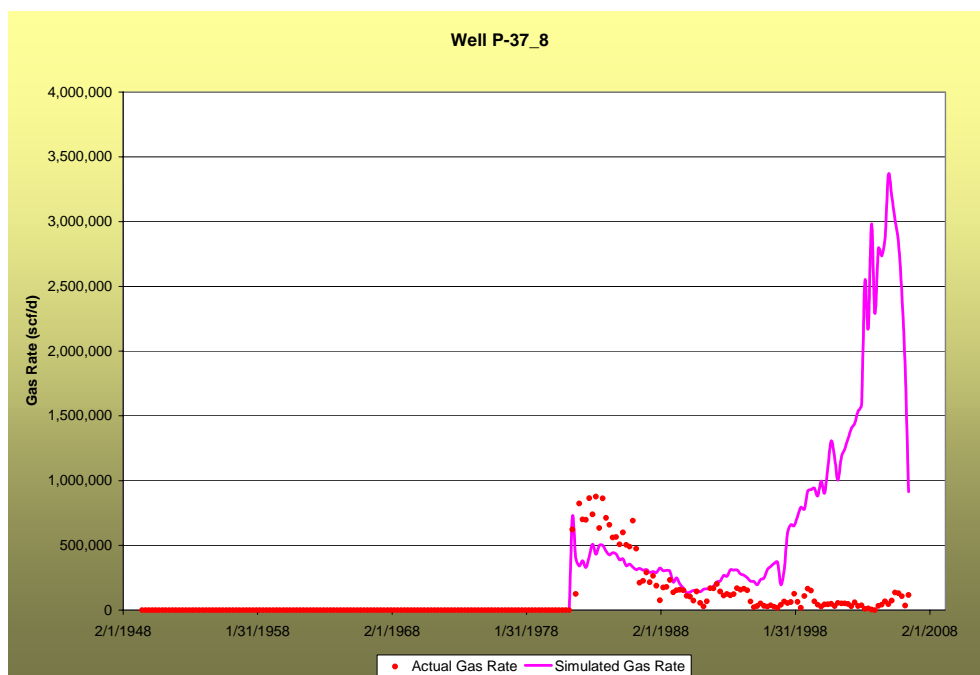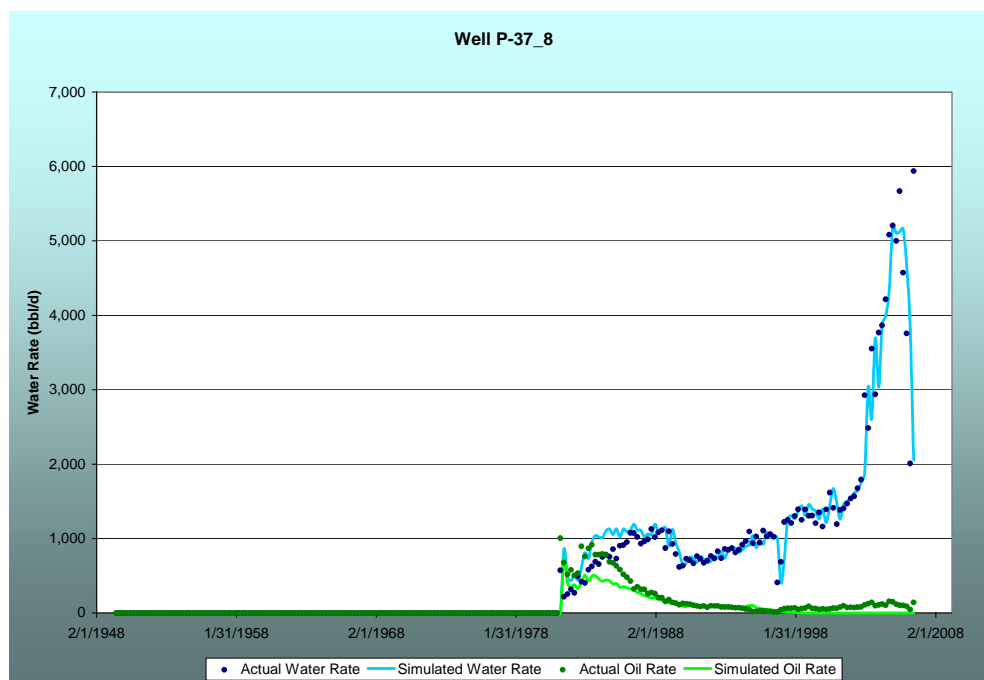**Figure A-10: History Match of Oil and Water Rates, Well P-36-7**

A-5

SACROC Simulation KS080807

Figure A-11: History Match of Gas Rate, Well P-36-8

Figure A-12: History Match of Oil and Water Rates, Well P-36-8

A-6

SACROC Simulation KS080807

Figure A-13: History Match of Gas Rate, Well P-37-8

Figure A-14: History Match of Oil and Water Rates, Well P-37-8

A-7
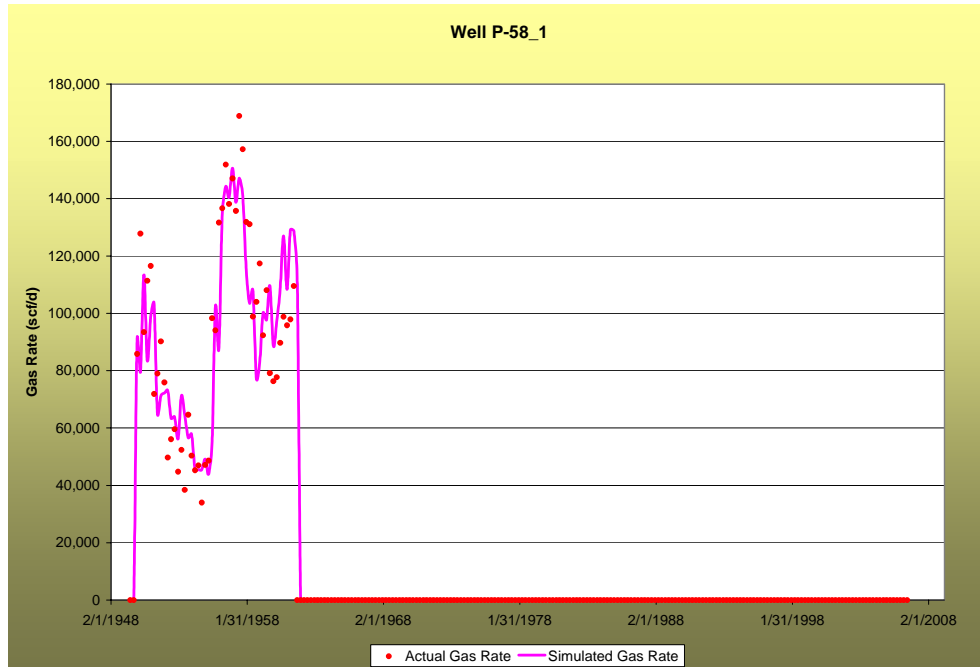
SACROC Simulation KS080807

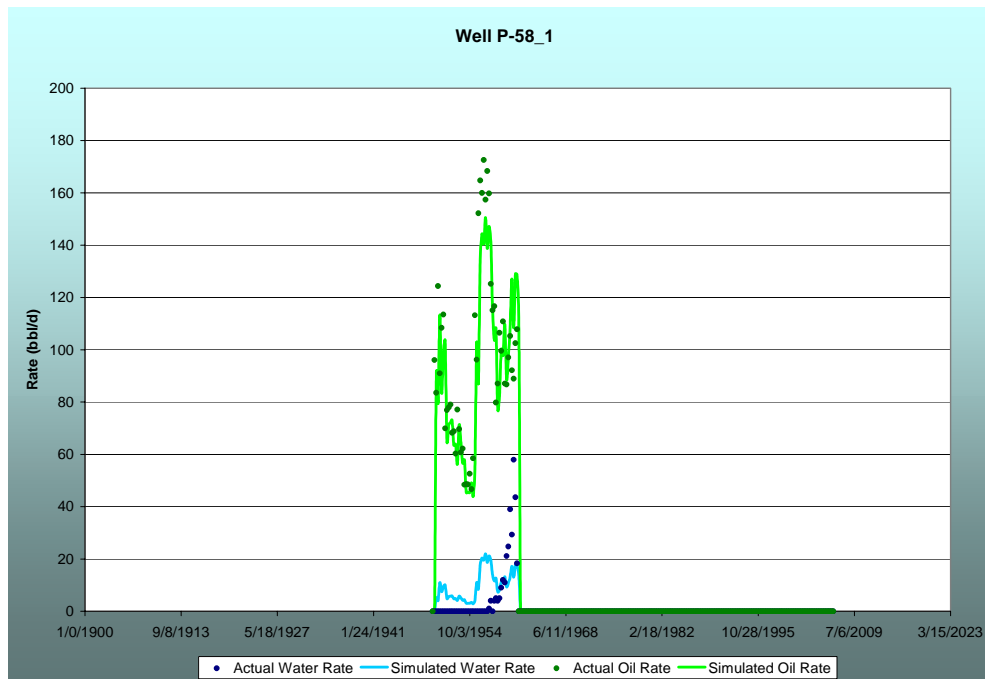**Figure A-15: History Match of Gas Rate, Well P-58-1**

Figure A-16: History Match of Oil and Water Rates, Well P-58-1

A-8

SACROC Simulation KS080807